

MSc. Thesis

Multi-level optimisation and global sensitivity analysis
of the probabilistic damage stability method for single
hold ships

Bas Milatz

MSc. Thesis

Multi-level optimisation and global sensitivity analysis of the probabilistic damage stability method for single hold ships

by

Bas Milatz

to obtain the degree of Master of Science
at the Delft University of Technology.

Student number: 4955218
Project number: MT.21/22.036.M
Project duration: November 19, 2021 – July 26, 2022
Thesis committee: Dr. A.A. Kana, TU Delft, supervisor and chairman
Ir. J.J. Zwaginga, TU Delft, committee member
Dr. ing. C.H. Thill TU Delft, committee member
Dr. M. Yang TU Delft, committee member
Bsc. J.D.J. van de Ridder, C-Job Naval architects, supervisor
Bsc. M. van Engeland, DELFTship maritime software, supervisor

An electronic version of this thesis is available at <http://repository.tudelft.nl/>.

Abstract

The probabilistic damage stability method offers great design freedom when used as a base of design. However, due to the complexity of the calculation and amount of parameters that influence the attained index, much of this freedom is not being harnessed by designers. This research tries to give the designer more insight in where to look when trying to comply with the regulations, by providing an initial subdivision design and create an overview of the influence of the parameters on the attained index. Many parameters have been found that either direct or indirect influence the damage stability calculation. A selection of parameters is chosen from this list as a starting point that are commonly used in the subdivision of large single hold vessels. A parameterised base ship has been made in the DELFTship program that is used for the execution of the optimisation and sensitivity analysis. The exploration for a suitable optimisation method and sensitivity analysis is based on the properties of these methods and method requirements that apply to this specific research. The most important requirement for both methods is the number of iterations needed to obtain a reasonable result, as the damage stability calculation can take up to 15 minutes. This resulted in the choice for the SACOBRA optimisation algorithm. To guarantee the effectiveness of the design, a second level to the optimisation is added where, the number of bulkheads is optimised, while simultaneously optimising the steel weight. During the research, the cargo hold volume was added as this proved to be an effective objective to ensure the efficiency of the design. This resulted in the change to the SAMO-COBRA algorithm, where the single objective SACOBRA algorithm was still used as a verification method and to investigate if it could be used for experimenting with certain design choices. For the sensitivity analysis the Morris method was chosen, mainly for its low number of sample points needed to converge. This method can be applied to a broad range of models and is characterised by its simplicity. However, this simplicity resulted in a relatively low amount of insight generated regarding the influence of the parameters on both the objectives as well as each other. A correlation matrix was added to further provide knowledge and insight. A sensitivity analysis by hand was performed to verify the results of both analysis methods.

The first optimisation stage showed to be a relatively fast way to determine the amount of bulkheads compared to the attained index that can be expected. However, a relatively large margin of error is observed in this stage and more information is needed to be able to make a decision on how many bulkheads is used to further optimise. The use of the SAMO-COBRA method in the second optimisation stage proved to be effective at providing the naval architect with a range of design proposals, where the probabilistic damage stability regulations were used as a base of design. Furthermore, it is shown that for single hold ships in general, the priority of the algorithm followed the influence of the parameters on the distance they were able to create between the cargo hold and the outer hull. The influence of the parameters, resulting from the sensitivity analyses endorse these claims. The Morris method showed the high non-linear and non-monotonic behaviour of the parameters that were investigated. This made it difficult to distinguish the level of influence between the parameters. The combination of the Morris method, Pearson correlation matrix and the sensitivity by hand proved to be sufficient for determining the behaviour of the probabilistic damage stability calculation. In the end, this research proposes a new foundation of designing a ship with the probabilistic damage stability regulations as a base of design. After the initial design from the two stage optimisation all other design requirements are implemented in the design. If the ship then fails to comply with the regulations, the knowledge and insight from this research can be used to increase the survivability of the ship in order for it to comply again.

Preface

The research that comprises the content of this master thesis is a result of nine months of dedicated work and continuous self improvement. The significance of performing a research, such as the master thesis, became all the more apparent the further I progressed. It is not only a method to assess the knowledge of the student, but more so to teach the student to approach a project or research in a structural and organised fashion and to prepare them for their future careers. I was particularly interested in this subject as the use of an optimisation algorithm and sensitivity analysis was fairly new to me, as well as designing a ship using the damage stability requirements as a base of design. The freedom and potential of this subject still continues to surprise me, even though my research has come to an end. Although the master thesis is considered and defined by the TU Delft as an individual in-depth research, it certainly did not feel individual at any stage these past nine months. I therefore want to thank my thesis committee and in particular my supervisors A. Kana, J.D.J. van de Ridder and M. van Engeland, for their continuous guidance and support. The insight, positive criticism and reassurance you provided me with, motivated me every step of the way. I also want to thank A. van den Ing and R. de Winter for taking an interest in my research and your preparedness to help. Next, I want to thank my family, friends and roommates for their mental support and providing the opportunity to take my mind of the research when I needed to. Lastly, I want to thank my girlfriend for putting up with me during this period and providing a sympathetic ear to my seemingly endless struggles and developments. The knowledge and confidence I gained from everyone involved is the reason I was able to accomplish my goals for this research and feel positive about my contribution to the scientific community and maritime industry.

*Bas Milatz
Delft, July 2022*

Contents

Abstract	iii
1 Introduction	1
1.1 Background	1
1.2 Introduction of Involved Companies	2
1.2.1 C-Job Naval Architects	2
1.2.2 DELFTship Maritime Software	3
1.3 Societal Relevance	3
1.3.1 Loss of Ships	3
1.3.2 Safety of Crew and Passengers	4
1.3.3 Environmental Impact	5
1.3.4 Efficiency	5
1.4 Previous Work and Knowledge Gap.	6
1.5 Research Goal	7
1.6 Thesis Structure	8
2 Probabilistic Damage Stability Method	9
2.1 Introduction Damage Stability	9
2.1.1 Two Methods for Finding the Ship Condition After Flooding	9
2.1.2 Deterministic Damage Stability Method	10
2.1.3 Probabilistic Damage Stability Method	11
2.2 Calculation Method Probabilistic Indices	12
2.2.1 Required Subdivision Index R	13
2.2.2 Attained Subdivision Index A	14
2.2.3 Factor p_i	15
2.2.4 Factor s_i	20
2.2.5 Factor v_m	23
2.3 Conclusion	24
3 Method Exploration	25
3.1 Base Ship Particulars	25
3.2 Parameters Considered	26
3.3 Properties of Different Optimisation Algorithms.	27
3.3.1 Local vs Global Solutions	27
3.3.2 Single- vs Multi-Objective	28
3.3.3 Constrained vs Unconstrained.	28
3.3.4 Single- vs Multi-Thread.	29
3.3.5 Type of Variables	30
3.3.6 Genetic- vs Non-Genetic.	30
3.3.7 Conclusion	31
3.4 Properties of Different Sensitivity Analysis Methods	31
3.4.1 Classifying Sensitivity Methods	31
3.4.2 Design of Experiments	33
3.4.3 Conclusion	34
3.5 Method Requirements	34
3.5.1 Optimization Method	34
3.5.2 Sensitivity Analysis	35

3.6	Choice of Methods	36
3.6.1	Single-Objective Method SACOBRA	36
3.6.2	Multi-Objective Method SAMO-COBRA	37
3.6.3	Sensitivity Analysis	37
3.7	Conclusion	39
4	Methodology	41
4.1	Creating a Parametric Model	41
4.1.1	Focused Section	42
4.1.2	Computing Damage Cases	42
4.1.3	Categorising the Variables	43
4.1.4	Other Parametric Measures	45
4.2	Set up of the First Stage	45
4.3	Setup of the Second Stage	46
4.3.1	Objective Function Single-Objective Optimiser (SACOBRA)	47
4.3.2	Objective Function Multi-Objective Optimiser (SAMO-COBRA)	47
4.3.3	Variables	48
4.3.4	Constraint Handling	50
4.3.5	Initial Optimisation Parameters	52
4.4	Setup of the Global Sensitivity Analysis	53
5	Analysis and Discussion	55
5.1	Results From the First Optimisation Stage	55
5.2	Results From the Second Optimisation Stage (SAMO-COBRA)	59
5.2.1	Convergence	59
5.2.2	Results For the First Design	62
5.2.3	Results For the Second Design	66
5.2.4	Conclusion	69
5.3	Single-Objective Optimisation (SACOBRA)	70
5.3.1	Convergence	70
5.3.2	Experiment 1 - Maximum Attained Index	71
5.3.3	Experiment 2 - Minimum Cargo Hold Volume	72
5.3.4	Experiment 3 - Cargo Hold Container Cutout	73
5.3.5	Experiment 4 - Change of Permeability	75
5.3.6	Conclusion	76
5.4	Results From the Sensitivity Analysis	76
5.4.1	Morris Sensitivity Analysis Method	76
5.4.2	Pearson Correlation Matrix	78
5.4.3	Verification by Hand	83
5.4.4	Conclusion	85
5.5	Design Process Implementation	86
6	Validation	89
6.1	Theoretical Structural Validity	89
6.2	Empirical Structural Validity	90
6.3	Empirical Performance Validity	91
6.4	Theoretical Performance Validity	91
7	Discussion, Recommendations and Conclusion	93
7.1	Discussion of the Main/Sub-question(s)	93
7.2	Recommendations	95
7.3	Conclusion - Main Research Question	96
7.4	Personal Reflection	96
A	Multi-Objective Optimisation Results	105
A.1	Constraint Function Results	105
A.2	Parallel Coordinate Plots	107

B	Single-Objective Optimisation Results	111
B.0.1	Cargo Hold Cutout	111
B.0.2	Change in Permeability	112
C	Sensitivity Analysis Results	113
C.1	Morris Method Results	113
C.2	Correlation Matrix.	116
D	Interview Design Process Implementation	119

List of Figures

1.1	Evolution of the damage stability regulations	2
1.2	Causes of total loss ships from 2011 to 2020 [12]	3
1.3	Total losses by ship type (left) and cause (right) January 1, 2020 to December 31, 2020 [12]	4
1.4	Wreck of the cruise ship Costa Concordia with the rock that caused the ship to flood [18]	4
1.5	X-press pearl after the engine room flooded as a result of a fire [22]	5
2.1	Subdivision length for the probabilistic damage stability method [43].	13
2.2	Three loading conditions for calculation of the attained index [41]	14
2.3	Longitudinal limits of damage zones [41]	15
2.4	Example of single and multiple zone damages in pure longitudinal direction [41]	15
2.5	Distribution density for the non-dimensional damage length [40]	16
2.6	Density distribution for the non-dimensional damage length [40]	16
2.7	Damage conditions for calculating $p(x_1, x_2)$ in condition 1,2 and 3 respectively	19
2.8	Non-dimensional penetration [40]	19
2.9	Density distribution for the non-dimensional penetration [40]	19
2.10	Calculation of the penetration depth b according to SOLAS Resolution MSC.281(85) [46]	19
2.11	Example of a GZ curve based on [28]	21
2.12	Example of a GZ curve for submerged openings based on [28]	21
2.13	Definition of the vertical extent of a damage [28].	23
2.14	Cumulative damage height [40].	23
3.1	Hypothetical ship model made in the DELFTship program	25
3.2	Simplified working principle of an optimisation method as can be applied to this research.	27
3.3	Example of search space with global and local maxima [49].	27
3.4	Constraint surfaces in a hypothetical two-dimensional design space [53].	29
3.5	Contours of the objective function with respect to the constraint surfaces [53].	29
3.6	Types of variables applicable to optimisation problems [55]	30
3.7	Structure of a genetic algorithm based on figure from [59]	31
3.8	Simplified working principle of a sensitivity analysis	31
3.9	Different sampling methods for the use of a DOE [67].	33
3.10	Coarse classification of main global SA methods in terms of required number of model evaluations and model complexity [65]	35
3.11	SACOBRA flowchart. The SACOBRA extensions compared to the COBRA-R algorithm are displayed in the grey boxes. [72]	36
3.12	SACOBRA performance comparison with the algorithms COBRA (with Rescale), Differential Evolution (DE) and COBYLA (Constrained Optimisation By Linear Approximation) on optimising on test problems called G-problems. [72]	37
3.13	An example of a single trajectory constructed for the three-dimensional space of input parameters. The trajectory is built with four points: one randomly chosen (a) and three points created as a result of changing one value at each step (b–d) [80]	38
3.14	Classification of parameters according to the mean of their elementary effects and their dispersion (standard deviation of the series of elementary effects)[83]	39
3.15	General setup of the methodology for this research	39
4.1	Flowchart of the parametric model set-up	42
4.2	Parametric model with, blue square indicating the optimisation region	42
4.3	Schematic example of non-regular compartment lay-out [85].	43
4.4	Side view of the parametric model showing the subdivision used for the PDS calculation	43

4.5	Correctly defined tank	43
4.6	Incorrectly defined tank due to overtaking BH	43
4.7	Illustration of the types of variables	44
4.8	New base ship without any of the water ballast bulkheads	45
4.9	Flowchart of the bi-level multi-objective optimisation	46
4.10	Number of constraint violations per option.	48
4.11	Variable reaching its upper boundary	49
4.12	Variable well within its boundaries	49
4.13	Halton sequence applied to the first, middle and last variable respectively	52
4.14	Flowchart of the Morris method set-up	53
5.1	Results from the first optimisation stage	55
5.2	SFAC diagram for two bulkheads in partial service draught	56
5.3	SFAC diagram for three bulkheads in partial service draught	56
5.4	Resulting design for two bulkheads	58
5.5	Resulting design for five bulkheads	58
5.6	Schematic example of the hypervolume [99].	60
5.7	Hypervolume progress of the SAMO-COBRA optimiser for 400 iterations and two WB bulkheads	60
5.8	Hypervolume progress of the SAMO-COBRA optimiser for 400 iterations and five WB bulkheads	60
5.9	Scatter plot and Pareto front for 400 iterations and two WB BH.	61
5.10	Scatter plot and Pareto front for 400 iterations and five WB BH.	61
5.11	Design corresponding with the lowest attained index on the Pareto front and the highest cargo hold volume for two water ballast bulkheads	62
5.12	Design corresponding with the highest attained index on the Pareto front with a maximum cargo hold volume for two water ballast bulkheads	62
5.13	Pareto front for two bulkheads and 200 iterations	63
5.14	Location trans. BHs for A-index.	63
5.15	Location long. BHs for A-index.	63
5.16	Location vert. BHs for A-index.	63
5.17	Penetration depth overview showing the distance of the cargo hold to the side shell at the aft and forward bulkheads	64
5.18	Damaged waterline (blue/white line) and location of openings at position zero for different cross section locations.	65
5.19	Influence of openings beyond their respective boundaries	65
5.20	Zone of influence according to chapter 2.2.4	65
5.21	Damaged waterline (blue/white line) over the length of the ship.	66
5.22	Pareto front for 200 iterations and five WB BH	66
5.23	Design corresponding with the lowest attained index on the Pareto front and the highest cargo hold volume for five water ballast bulkheads	67
5.24	Comparison between the new Pareto front with the old front.	67
5.25	Design corresponding with the highest attained index on the Pareto front with a maximum cargo hold volume for five water ballast bulkheads	68
5.26	Location transverse BHs for A-index.	68
5.27	Location water ballast BHs for A-index.	68
5.28	Location longitudinal BHs for A-index.	68
5.29	Location vertical BHs for A-index.	68
5.30	Comparison of the Pareto front for the two respective designs.	69
5.31	Attained index plot for 150 iterations	71
5.32	Best design for two bulkheads, after 150 iterations.	71
5.33	Single objective FO tanks result	72
5.34	Multi objective FO tanks result	72
5.35	Layout of the design for which a minimum cargo hold volume of $10,000m^3$ was introduced as a constraint.	72
5.36	Cargo hold without cutout sections.	74

5.37	Added cargo hold cutout section	74
5.38	Pump room size with no cutout.	74
5.39	Pump room size with cutout.	74
5.40	Resulting layout of the pump room after the change of permeability as shown in 5.7.	75
5.41	Results of the Morris method for N=20 and 100 respectively	77
5.42	Bootstrap confidence interval where situation A is not desired and situation B is desired.	77
5.43	Results of the Morris sensitivity analysis method of the second optimisation stage for five bulkheads.	78
5.44	Partitioning correlation coefficient matrix [103]	79
5.45	Matrix containing all Pearson correlation coefficients for the objectives, constraints and the five most influential parameters according to the Morris method.	79
5.46	Improved correlation matrix that combines a random sampling with the optimiser to show the correct correlation coefficients for both the parameters as well as the objectives and constraints.	81
5.47	Sensitivity in the normalised range of the transverse bulkheads with respect to the attained index A.	84
5.48	Sensitivity in the normalised range of the longitudinal bulkheads with respect to the attained index A.	84
5.49	Sensitivity in the normalised range of the decks and openings with respect to the attained index A.	85
5.50	Flowchart showing the use of the research results as a base of design	86
6.1	Validation square by Peterson et al. [34]	89
A.1	Constraint plot volume Aft FO tank	105
A.2	Constraint plot volume Fwd FO tank	105
A.3	Constraint plot volume pump room	106
A.4	Constraint plot R-A	106
A.5	Constraint plot volume Aft FO tank	106
A.6	Constraint plot volume Fwd FO tank	106
A.7	Constraint plot volume pump room	106
A.8	Constraint plot R-A	106
A.9	These figures show the parallel coordinate plots for the two WB BH design.	108
A.10	These figures show the parallel coordinate plots for the five WB BH design.	109
B.1	Converged layout for a minimum cargo hold volume of $8500m^3$ and maximum attained index.	111
B.2	Converged layout for a minimum cargo hold volume of $8500m^3$, a maximum attained index and fitted with the cargo hold cutouts	111
B.3	Pump room bulkhead location without cargo hold cutout	112
B.4	Pump room bulkhead location with cargo hold cutout	112
B.5	Converged layout for a minimum cargo hold volume of $8500m^3$, a maximum attained index and a change in permeability for the pump room and FO tanks.	112
B.6	Pump room volume without change in permeability	112
B.7	Pump room volume with change in permeability	112
C.1	Classification of the Morris method results	115
C.2	Correlation matrix for only the initial design points for all parameters	116
C.3	Correlation matrix for 200 iterations and all parameters	117

List of Tables

1.1	Comparison of previous work regarding parameter studies for the probabilistic damage stability method	7
2.1	Comparison between the added weight and lost buoyancy methods on a rectangular block [37]	10
2.2	IMO instruments containing deterministic damage stability [35]	11
2.3	Additional deterministic requirements for passenger ships [35]	11
2.4	Probabilistic ground rules and their application to the damages stability method	12
2.5	Non-dimensional constants for calculating $p(x_1, x_2)$ [45]	17
2.6	Optimisation parameters resulting from the probabilistic damage stability calculations	24
3.1	Main particulars hypothetical ship model	26
3.2	Optimisation method requirements with their respective priority and source	35
3.3	Sensitivity analysis requirements with their respective priority and source	35
4.1	Boundaries of all independent variables used for optimisation of the middle section with two bulkheads added, where WF is the web frame distance of 0.55m	49
4.2	Input data for all semi dependent variables, where WF is the web frame distance of 0.55m	49
5.1	Comparison between two pairs of designs, comparing the partial attained indices	56
5.2	Comparison between two pairs of designs, comparing for the partial draught	57
5.3	Comparison between two and five bulkheads in the ballast water tanks	57
5.4	Boundaries of all variables used for optimisation of the middle section with two bulkheads added, where WF is the web frame distance of 0.55m	58
5.5	Boundaries of all variables used for optimisation of the middle section with five bulkheads added, where WF is the web frame distance of 0.55m	58
5.6	Comparison between the infill points for the single and multi-objective optimisers for both their maximum attained index design and with a minimum cargo hold volume of 10,000m ³	73
5.7	Changes in permeability for experiment 4	75
5.8	Permeability of each general compartment according to SOLAS part B-1 regulation 7-3 [102]	75
5.9	Total size of the confidence interval when compared to the total size of the largest parameter w.r.t. the elementary effect	76
5.10	Difference between Morris and Pearson sensitivity analyses	80
5.11	Difference between Morris and Pearson sensitivity analyses for the improved correlation matrix	82
5.12	Summation of the lead time of all processes required to use the framework proposed in this thesis	87
C.1	Results Morris method for N=20 trajectories	114
C.2	Results Morris method for N=60 trajectories	114
C.3	Results Morris method for N=100 trajectories	114
C.4	Results Morris method for N=20 trajectories for five water ballast bulkheads	115

Nomenclature

Δ	Intact displacement
$\Delta_{i/d}$	Intact/damaged displacement
μ_j^*	Mean absolute value of the j^{th} parameter
Σ_j	Standard deviation of the elementary effect
θ	Maximum heeling angle; 15° for passenger ships, otherwise 30°
θ_e	Equilibrium heeling angle after damage
θ_{min}	minimum heeling angle; 7° for passenger ships, otherwise 25°
A	Attained subdivision index
A	Projected lateral wind area above waterline
A_c	Attained subdivision index for a specific loading condition
B	Maximum ship beam at draught
b	Penetration depth
b	mean transverse distance measured at right angles to the centreline at the deepest part of the subdivision draught between the shell and an assumed vertical plane extended between the longitudinal limits used in calculating the factor p_i
B^*	Final path matrix
B_s	Subdivision beam
d	Draught of the ship
D^*	k-dimensional diagonal matrix, each element is 1 or -1 with equal probability
d_l	Light service draught for which the estimated service trim must be used
d_p	Partial subdivision draught for which a level trim may be used
d_s	Deepest subdivision draught for which a level trim may be used
$EE_{i,j}$	Element effect for each path and variable
GZ_{max}	Maximum value of GZ
$H_{j,n,m-1}$	The least height above baseline, in metres, within the longitudinal range of $x_{1(j)} \dots x_{2(j+n-1)}$ of the $(m-1)^{th}$ horizontal boundary which is assumed to limit the vertical extent of flooding for the damaged compartments under consideration
$H_{j,n,m}$	The least height above the baseline, in metres, within the longitudinal range of $x_{1(j)} \dots x_{2(j+n-1)}$ of the m^{th} horizontal boundary which is assumed to limit the vertical extent of flooding for the damaged compartments under consideration
J	Non-dimensional damage length
j	Aftmost damage zone number involved in the damage, starting with number one at the stern

$J_{k+1,1}$	$k + 1$ by 1 dimensional matrix and vector of 1's
$J_{k+1,k}$	$k + 1$ by k dimensional matrix and vector of 1's
J_{kn}	Knuckle point in the distribution
J_k	Knuckle point between $b_1(J)$ and $b_2(J)$
J_{max}	Overall normalised max damage length
J_m	Maximum non-dimensional damage length
k	Number of particular bulkheads as a barrier for any transverse penetration in a damage zone counted from shell towards centre
KG_i	Vertical centre of gravity of intact ship
L	Ships length
l	Damaged compartment length
L^*	Length where normalised distribution ends
l_{max}	Maximum absolute damage length
L_{pp}	Length between perpendiculars
L_s	Subdivision length
m	Represents each horizontal boundary counted upwards from the waterline under consideration
M_{heel}	Maximum heeling moment
N	Number of persons, $N_1 + N_2$
n	Amount of zones that damage is inflicted upon
n	Number of all possible events
N_1	Number of persons for whom lifeboats are provided
N_2	Number of persons in excess of N_1 , including officers and crew
N_p	Maximum number of passengers permitted to be on board
P	Wind force for calculating M_{wind} , $120N/M^2$
P^*	k -by- k random permutation matrix, with in every column only one 1 element
p_i	Probability of a specific damage occurring
p_i	Probability that a specific damage condition occurs
p_k	Cumulative probability at J_{kn}
R	Required subdivision index
r	Factor accounting for the transverse extent of the damage
R_0	R value for cargo ships with a length above 100 meters
<i>Range</i>	Range with positive righting arm
s_{final}	Probability to survive in the final equilibrium stage of flooding
$s_{intermediate}$	Probability to survive all intermediate flooding stages until the final equilibrium
s_i	Survivability for a specific damage condition

s_{mom}	Probability to survive heeling moments
T	Respective draught (d_s, d_p or d_l)
$T_{i/d}$	Intact/damaged draft
v_m	Vertical extent of damage
x_1	Distance from the aft of the ship to the aft end of the zone
x_2	Distance from the aft of the ship to the forward end of the zone
$x_{1/2}$	Terminals of the compartment or group of compartments
Z	Distance from centre to lateral projected wind area to $T/2$

Acronyms

- ANOVA** Analysis of Variance. 33
- AWS** Amazon Web Services. 46
- BBO** Blackbox Optimisation . 47
- BH** Bulkhead. xii, 43, 63, 68
- CAPEX** Capital Expenses. 2, 28, 39
- CH** Cargo Hold. 77, 78
- COBRA** Constrained optimisation By Radial Basis Function Approximation. xi, 36, 37, 50, 52
- COBRA-R** Constrained optimisation By Radial Basis Function Approximation with Rescale. xi, 36
- COBYLA** Constrained Optimisation By Linear Approximation. xi, 37, 52
- CPU** Central Process Unit. 45
- DE** Differential Evolution. xi, 37
- DH** Double Hull. 77, 78
- DOE** Design Of Experiments. 33, 34
- ECHT** Ensemble of Constraint Handling Techniques. 29
- EE** Elementary Effect. 38, 80, 82
- EEDI** Energy Efficiency Design Index. 5
- FO** Fuel Oil. xiii, 44, 51, 62, 64, 69, 71–75, 77, 78, 82, 83, 85, 86, 94, 111, 112
- FORM** First Order Reliability Model. 33
- GHG** Greenhouse Gas. 5
- HARDER** Harmonisation of Rules and Design Rationale. 1, 13, 16, 19, 20, 23, 24
- HV** HyperVolume. 37
- IMO** International Maritime Organisation. xv, 1, 4, 9, 11, 20
- ISRES** Improved Stochastic Ranking Evolution Strategy. 37
- LB** Lower Boundary. 49, 58
- LHS** Latin Hypercube Sampling. 33, 116
- MARPOL** Prevention of Pollution from Ships. 5
- MOGA** Multiple Objective Genetic Algorithm. 6

- MV** Motor Vessel. 5
- NAPA** Naval Architectural PAcage. 90
- NeRF** Netherlands Regulatory Framework. 12
- O** Openings. 77, 78
- OAT** One-At-A-Time method. 37
- OPEX** Operational Expenses. 2, 28
- PDS** Probabilistic Damage Stability. xi, 1, 2, 6–9, 11, 12, 16, 19, 25, 26, 29, 31, 32, 34, 35, 41–43, 45, 47, 55, 56, 59, 64, 65, 69, 70, 76, 78, 85, 86, 90, 91, 93, 94, 96, 97
- PR** Pumproom. 77, 78
- PT** Pipetunnel. 77, 78
- RBF** Radial Basis Function. 36, 37, 48, 52
- SACOBRA** Self Adjusting Constrained Optimisation By Radial Basis Function Approximation. xi, 36, 37, 91, 93, 95
- SALib** Sensitivity Analysis Library in Python. 53, 54
- SAMO-COBRA** Self-Adaptive algorithm for Multi-Objective Constrained Optimisation by using Radial Basis Function Approximations. xii, 36, 59, 60, 91, 93–95
- SFAC** s_i factor diagram. 56
- SLF** Sub-Committee on Stability and Load Lines and on Fishing Vessels Safety. 1, 11
- SOLAS** Safety of Life at Sea. 1, 2, 10, 12, 16, 23
- SORM** Second Order Reliability Model. 33
- TD** Tweendeck. 77
- TT** Tanktop. 77, 78
- UB** Upper Boundary. 49, 58
- UNCLOS** United Nations Convention on the Law of the Sea. 5
- UTA** Utility Additive. 6
- VCG** Vertical Centre of Gravity. 10
- WB** Waterballast. 77, 78

Introduction

The idea behind (almost) every design method is to create a framework from which the designer can make the right design choices, whether it is in the initial or later stages of a design. A suitable design method can be chosen on the base of previous experience, the composition of the team that is involved and the type of design that is considered. Regardless of the method that is chosen, the desired design requirements remain the same. A ship is regarded to as a complex problem that requires a great deal of technical knowledge and experience across many disciplines. This thesis will focus on the damage stability of the ship, that is part of the design requirements for over 70 years now and will be for many years to come.

1.1. Background

The SOLAS Convention in 1914, resulting from the loss of Titanic in 1912, was the first of many conventions that slowly but steadily amended ship damage stability regulations over the years. These amendments resulted from new ship losses and following a more or less 'trial and error', semi-empirical procedure. Even though the safety level of passenger ships was continuously improved, since the late eighties and particularly after the spectacular sinking of the British ferry 'Herald of Free Enterprise' in 1987, the regulations regarding the stability of passenger ships was analyzed for any loopholes and further improvement. Notably, there were no specific damage stability criteria or subdivision requirements for cargo ships until the early nineties, when SOLAS 74 was amended to cater for dry cargo ships' damage stability by use of the probabilistic concept [1].

Since then, great progress has been made on improving the survivability of all ships that comply with the IMO regulations. Before the implementation of the SOLAS 2009 convention, the deterministic damage stability method dominated for damage stability calculations. The probabilistic method was already described by Kurt Wendel in the late sixties, when he published an article with the title "Subdivision of Ships" as an alternative to the SOLAS 60 deterministic requirements [2]. The first regulations for using the probabilistic method where introduced during the 1974 SOLAS convention. Following the 1992 SOLAS part B-1 developments, probabilistic standards for cargo ships where introduced, which consisted of the same principles as the 1974 probabilistic method. This was also called the "Harmonisation of Damage Stability Provisions in SOLAS based on the Probabilistic Concept of Survival". After the adoption of the enhanced deterministic requirements following the disaster of the Estonia in 1994, the IMO committees shifted their attention back to the harmonisation of the damage stability rules [3].

During this research period to determine the future direction, a team of European industries, classification societies, universities and research establishments, administrations and others proposed to the European Commission and received funding for the research project, 'Harmonisation of Rules and Design Rationale' (HARDER). This project's main objective was to generate knowledge in the general field of ships' damage stability. During the HARDER project, the new harmonised damage stability, probabilistic concept, known as the SLF42 proposal, under development at IMO, was systematically evaluated and an improved proposal was introduced for discussion at IMO, known as the HARDER-SLF46 proposal. After multiple revisions, the MSC80 revision was finally adopted. It is noted that the finally adopted MSC80 probabilistic damage stability (PDS) assessment concept was to apply to all new dry cargo and passenger ships constructed after 1 January 2009 [3].

Figure 1.1 shows a timeline of the evolution of the damage stability regulations.

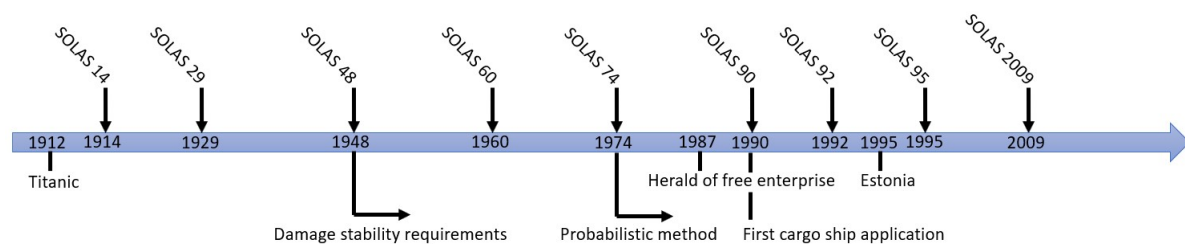


Figure 1.1: Evolution of the damage stability regulations

One of the advantages of the probabilistic method over the deterministic method is that, as ships with the same attained index (Attained index explained in chapter 2) are considered as equally safe regardless of their subdivision, the probabilistic method offers a lot more design freedom. This is a result from the designer is not being bound to follow the damage extents set by the deterministic method. This freedom also comes with a cost. Due to the many aspects of the design, many iterations are expected during a project. These iterations are time consuming, not only in the initial stages of the design, but even more so in later stages. This imposes a risk of not meeting the subdivision and damage stability requirements set by SOLAS chapter II-1 and therefore delaying the project significantly.

When looking at the classic design spiral by Evans [4], the damage stability aspect of the design is one of the last requirements to take into account. Although the spiral is mainly used to illustrate a method of approaching ship design and most of the time not literally followed, it still imposes the problem that the PDS method is not used as a base of design and therefore to its full extent. This results in the designer losing the freedom potential that this method has to offer. Nowadays, companies use design methods that aims to take more requirements into consideration simultaneously, e.g. more holistic design approaches. The Accelerated Concept Design method [5] of C-Job Naval Architects is an example of such a method. With this method, the traditional design spiral is also followed. However, the interrelationships of all variables on the spiral are already taken into account for every calculation. This is already a great improvement. However, if the PDS method can not be used to its full extent, it is still difficult to use as a base of design. There are many variables that can be used as input (either directly or indirectly) for the PDS calculation, but there is only one output variable: The Attained index "A". The coherence of many of the design parameters results in difficulty understanding the behaviour of the survival index, especially in the preliminary design phase [6, 7, 8].

1.2. Introduction of Involved Companies

This research is done in coöperation with C-Job Naval Architects and DELFTship maritime software.

1.2.1. C-Job Naval Architects

C-Job Naval Architects, from here on named C-Job, is an engineering firm whose aim is to help clients build better ships, become 100% sustainable, and run better because of it. The portfolio of services, designs and programs guarantee better OPEX and CAPEX for new ships, as well as existing ones [9].

Currently, in many designs, a first estimate of the subdivision (the division of a hull into a series of watertight compartments) is made by calculating the damage stability for two or three damaged compartments and calculating if the deck remains above the waterline. This method is entirely based on the knowledge and experience of the naval architect. This means that potentially a significant part of the attained index is lost when using this method. There is therefore a demand for a clear overview of what parameters have the most influence on the attained index regarding the PDS method and to give an initial design which the designer can use as a base of design.

1.2.2. DELFTship Maritime Software

DELFTship maritime software, from here on named DELFTship, is a visual hull modeling and stability analysis program that allows for the derivation of all data needed for calculations from the model itself. The aim of the DELFTship program is to work smarter, faster and with user-driven software that is built on years of product development in real life environments [10]. The software has multiple extensions regarding the damage stability calculations (both deterministic and probabilistic), as well as intact stability, bending moments and shear forces and other vital extensions that provide the data that is needed for designing a ship.

1.3. Societal Relevance

The quest for safer ships has always been of interest to any party involved and affected by the shipping industry. This interest can be sparked by financial motivation, but also from concerns about the safety of passengers and crew and the impact on the environment and marine life. The catalyst for regulation changes have often been series of maritime disasters that highlighted increasing risks [11]. Examples of this are discussed in chapter 1.1 and show the societal pressure that causes government agencies to respond with extensive investigations and regulation changes.

1.3.1. Loss of Ships

A report by Allianz [12] identifies loss trends and highlights a number of risk challenges in the maritime sector. Although this report shows a 50% drop of total losses over a decade, 2020 was the first time in five years that losses have not continued to decline. Figure 1.2 below, shows the causes of the total losses of ships between 2011 and 2020. Both actual and constructive total losses were taken into account in the report. An actual total loss is defined in the Marine Insurance Act 1906 [13] as: 'Where the subject-matter insured is destroyed, or so damaged as to cease to be a thing of the kind insured, or where the assured is irretrievably deprived thereof, there is an actual total loss.' the constructive total loss is defined as: 'There is a constructive total loss where the subject-matter insured is reasonably abandoned on account of its actual total loss appearing to be unavoidable, or because it could not be preserved from actual total loss without an expenditure which would exceed its value when the expenditure had been incurred.'

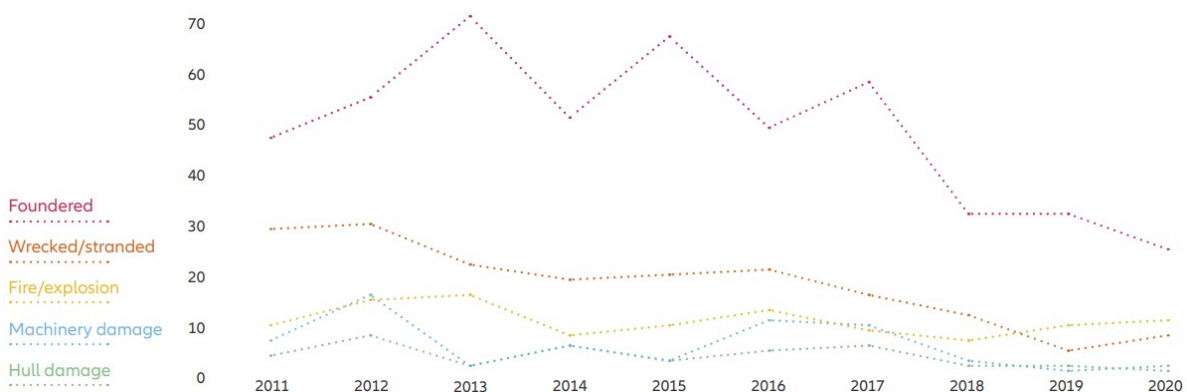


Figure 1.2: Causes of total loss ships from 2011 to 2020 [12]

The total loss as a result from foundered and wrecked/stranded ships dominated the causes of total ship loss in the beginning of the recorded decade. Still, foundered ships are the main cause of total loss. Foundered includes the loss of ships due to heavy weather, leaks, breaking in two etc. [14]. In figure 1.3 below, the total losses by ship type and cause are shown from January 1, 2020 to December 31, 2020.

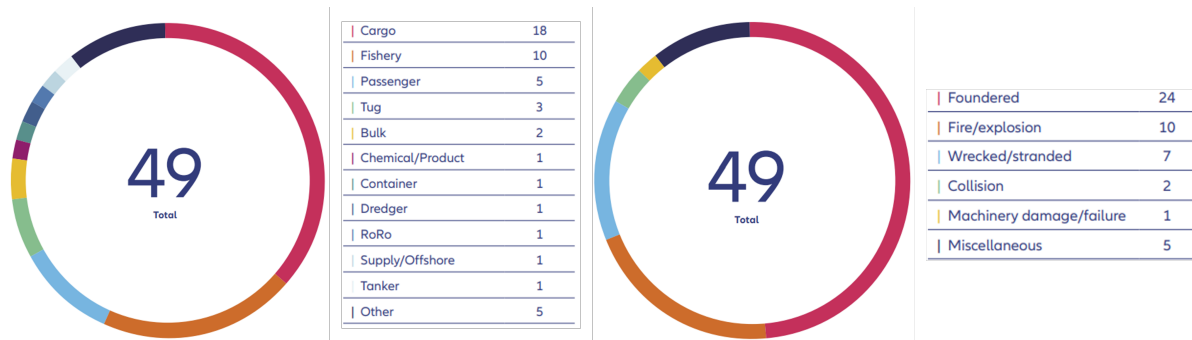


Figure 1.3: Total losses by ship type (left) and cause (right) January 1, 2020 to December 31, 2020 [12]

This shows more clearly that almost half of the ships are lost as they are foundered and wrecked/stranded. What is also remarkable is that according to the 2020 world merchant fleet statistics from Equasis [15] 13.7% of the world fleet consists of cargo ships, while 37% of all total losses occur for this ship type as can be seen in figure 1.3 above.

One can debate about the actual cause of this inconsistency. However, it seems that a significant margin of safety can be reached in the smarter subdivision of ships, as this reduces the chances of a total loss due to foundered and wrecked/stranded ships.

1.3.2. Safety of Crew and Passengers

The safety of crew and passengers is an important part in the design of ships. This can be seen in figure 1.1, where rigorous changes in damage stability were a result of a maritime disaster.

A recent example of a disaster that resulted in additional amendments regarding subdivision and damage stability by the IMO, is the Costa Concordia accident [16]. The Costa Concordia struck a reef and partially sank off the coast of Isola del Giglio with 4,299 people on board, killing 32 people [17].



Figure 1.4: Wreck of the cruise ship Costa Concordia with the rock that caused the ship to flood [18]

Today, the trend for safety regulations is to be more proactive and goal-based, instead of responding to incidents and describing how to prevent it in the future. This can be seen from recent proactive changes by the IMO that also promises more flexibility [19].

1.3.3. Environmental Impact

The last decade has seen a steadily growth in the world fleet [15]. This means that if no action is taken to improve the safety of ships, the probability of accidents will increase. This increases the chances of pollution as a result from these accidents. Today, the vast majority of ships still operate on (heavy) fuel oil. Petroleum spills remain among the highest publicised and environmentally damaging disasters worldwide [20]. There are many international legislations that focus on reducing environmental impacts of marine transportation, such as the International Convention for the Prevention of Pollution from Ships (MARPOL) introduced by the IMO, and the United Nations Convention on the Law of the Sea (UNCLOS). A recent example of a major spillage due to a fire is the sinking of the MV X-Press Pearl close by the coast of Sri Lanka. A report of the UN environmental advisory mission [21] showed the environmental impact by not only the fumes from the fire, but also the oil and chemical pollution as a result from the partial sinking of the ship. The partially sunken MV X-Press Pearl can be seen in figure 1.5 below.



Figure 1.5: X-press pearl after the engine room flooded as a result of a fire [22]

A day prior to the sinking of the ship, salvors already reported that the engine room was flooded and concerns were expressed over the stability of the ship. During one of the towing efforts, the ship began to sink, eventually leading to the stern settling on the bottom at a depth of approximately 70 feet [23]. These types of incidents spark public outrage, as was also the case after the grounding of MV Wakashio of the coast of Mauritius [24]. It is therefore important to continuously improve the survivability of ships resulting in less stress on the environment from these accidents.

Another objective is the reduction of the light weight of the ship. This not only reduces the raw material needed for construction, but also results in less fuel consumption and therefore emissions, due to either a more slender or more shallow design. According to a study by Lindstad et al. a slender design can over perform the EEDI standards [25]. By optimising the subdivision, a lighter ship can be designed.

1.3.4. Efficiency

A study by Buhaug et al. [26], shows that shipping has the lowest carbon footprint per unit of cargo transported. This efficiency is reached by the sheer amount of cargo a ship can carry compared to its fuel consumption per unit of distance. It is not only important to maintain this efficiency with regards to GHG emissions per unit of cargo transported, but also as ships need to maintain its economic viability. As an example, container ships have a relatively fluctuating average carrier operating margin. However, it rarely peaks above 5% according to a study by Notteboom et al. [27]. Therefore, it is vital for designers to not only design safe ships, but they also have to be economically viable. This is part of the holistic design problem the designer faces during the initial design of the ship.

1.4. Previous Work and Knowledge Gap

Ever since the introduction of the PDS regulations in 1974, research has been conducted to test the robustness of the probabilistic method and to give designers more insight in how to use this method in their advantage. What can be seen in the literature is that most of the research has been done around the implementation of the harmonised rules. The research gap is based on previous work that has been done regarding this subject. As a start, the following requirements for the research have been identified.

- Use of an optimisation algorithm to generate an initial design;
- Use of a sensitivity analysis to identify the influence of parameters on the attained index;
- Use of both discrete as well as continuous parameters for the optimisation;
- Focus on single hold ship.

In this chapter, the relevant research is first explained and then table 1.1 shows the research gap that results from this exercise.

Most of the damage stability regulation changes were a reaction on the loss of Ro-Ro/Ro-Pax vessels, as can be seen in figure 1.1. The majority of the literature found is centered around this type of vessel. Ro-Ro/Ro-Pax vessels are subjected to the 1996 Stockholm agreement, which imposes extra regulations regarding water on the watertight vehicle deck. One can argue that this can contribute to research focusing on this type of ship rather than other types.

Two master's theses have already been written about the effect of parameters on the attained index for offshore vessels. One by Ole Martin Djupvik in 2015 [28] and the other by Stian Royset Salen in 2016 [29]. Both investigated the effect of multiple design parameters on one or more hull designs. Djupvik focussed on the arrangement of U-tanks and the location of longitudinal bulkheads in the double bottom without U-tanks. Salen investigated the effect of wing ballast tanks above the U-tanks, by changing the height of the horizontal surface, and the effect of changing the intact stability on the attained index. The results were obtained from the NAPA stability software and processed by hand to show the effect of the parameter changes. The results of these theses are limited to the use of offshore ships due to the choice of parameters. Also, the comparison was not done by means of optimisation algorithms, which limits the ability to find the best solution in a large parameters space and apply the method to different situations.

A PhD thesis by Erik Sonne Ravn [30] has more similarities regarding the methodology of this research. For his research, optimisation algorithms were used to investigate the PDS of Ro-Ro ferries with regard to their subdivision based on the PDS concept. A multi-objective optimisation of the subdivision was performed as well as some simplifications and developments of the probabilistic method where made. The objective of the optimisation tool was to maximise the attained index and Ro-Ro deck area and minimise the ship's lightweight. The Multiple Objective Genetic Algorithm (MOGA) was used to seek and find the Pareto front (all solutions that are not dominated by any other solutions) of the optimisation problem. The Utility Additive (UTA) method was used as multi-criteria decision-making technique. The conclusion of this thesis was that the most important contributors to the attained index were the position of the Ro-Ro deck, the position of the KG, existence of side casings and to some extent the number of transverse bulkheads. This thesis is limited to Ro-Ro ferries and is not applicable to any other type of ship.

A paper from 2004 by Boulougouris, et al about the optimisation of arrangements of Ro-Ro passenger ships with genetic algorithms [31], also has some similarities with this research. The paper describes the use of genetic algorithms to optimise the attained index, while also optimising for vehicle lane length and steel weight. This research uses NAPA to create the macros for the generation of the ship's internal watertight arrangement. The input variables comprised the depth of the ship, minimum double bottom margin, minimum breadth of different holds, number of bulkheads in front of the engine room and heights of control points of the forward and aft bulkhead distribution curves. The computational time was still relatively large, which limits the applicability of this research for any commercial purpose. This also means that there is a significant margin to improve with state-of-the-art algorithms and perhaps the use of multi-threading (explained in chapter 3.3)

In a paper by Vassalos et al. [32], a sensitivity analysis is performed regarding the parameters that influence the attained index for a large RoPax vessel. Different configurations are used to change the subdivision of the design. The sensitivity analysis is performed by plotting the results for the different

ranges of input variables. These input variables comprised the longitudinal bulkhead configuration below the main vehicle deck, side casings on the main vehicle deck, position of the main vehicle deck and double bottom, the effect of water on deck and some operational parameters. This paper only looks at RoPax vessels, which limit the applicability of the research.

A paper from 2009 by Dracos Vassalos and Luis Guarin [33] attempts to give more insight and create more understanding of the probabilistic concept and its limitations and range of applicability. Different methods are evaluated regarding the approach of using the probabilistic method for designing a ship. A hypothetical cruise vessel is used on which time domain simulations with the PROTEU3 program are performed. A significant reduction in the probability of capsizing is achieved for different amount of compartment damages. A Monte Carlo simulation and a simpler (inference) model are used. For large amount of parameters, constraints and parameter spaces, the Monte Carlo simulation can be very inefficient and time consuming.

The knowledge gap this thesis aims to fill is determined by comparing previous relevant work and state-of-the-art methodologies, that are able to expand the knowledge obtained so far. Earlier research shows the testing of the robustness of the method, while later research focuses more on the influence of the parameters on the attained index and how to use the method as a base of design. In table 1.1, the most relevant research is compared to the goals of this thesis. As this table resulted partly from the findings during the literature study, some of the topics like discrete and continuous parameters are further explained in chapter 3.3.

Table 1.1: Comparison of previous work regarding parameter studies for the probabilistic damage stability method

Research	Discrete parameters	Continuous parameters	Single hold ships	Sensitivity analysis	Optimisation algorithm
Djupvik [28]	X	X		X	
Salen [29]		X		X	
Ravn [30]		X		X	X
Boulougouris [31]	X	X			X
Vassalos and Guarin [33]	X	X			X
Simopoulos et al. [32]	X			X	

What can be seen in table 1.1, is that although similar research has already been performed, no research has been done that combines the use of an optimisation algorithm together with a global sensitivity analysis that is applicable to single hold ships in general. These two methods can provide new insight as they explore the entire parameter space. It could be very beneficial for designers to understand, during the design, what steps can be taken in order to comply with the PDS regulations. Another improvement is the calculation time and accuracy of the obtained results as state-of-the-art algorithms allow for this. This makes the research more applicable and relevant for current commercial purposes.

1.5. Research Goal

The problem that is addressed in this thesis is that during initial stages of the design, it is still unclear for the designer what parameters, regarding the PDS method, have the most impact on the attained index. This thesis aims to create a framework to study and optimise the parameter space influencing the attained index during initial stages of the design of ships with a single hold, while maintaining the effectiveness of the design. To test this framework, a sensitivity study will be performed and validated.

To put this into a research question, the following can be formulated:

- To what extent can a design framework study and optimise the parameter space influencing the attained index during initial stages of the design for ships with a single hold, while maintaining the effectiveness of the design?

Five sub questions remain after establishing the knowledge gap determined in chapter 1.4:

- What parameters influence the attained index based on the PDS calculation?
- What are the properties and requirements for an optimisation algorithm and sensitivity analysis and which methods are most suitable for this research?
- How can the base ship model be parameterised in order to be subjected to different optimisation and analysis methods?
- To what extent is it possible to provide a preliminary design by the use of an optimisation algorithm?
- What set of parameters has the most influence on the attained index?

The framework aims to give the designer a base from which he/she can find the most optimum design regarding the PDS regulations. This framework can also be used during later stages, when the design, due to the many iterations, fails to comply with the regulations and the attained index needs to be increased. In the end, the goal of this thesis is to contribute to the design of safer ships, not only from an economical standpoint, but especially from a safety and environmental point of view. New insight needs to be aimed for, where the designer can confidently aim for a safer and more efficient ship design.

1.6. Thesis Structure

This research is centered around the PDS method, all optimisations, calculations and models are build around these regulations. The first step in this research is therefore to understand the origin of the damage stability regulations and a thorough understanding of the calculation method. In chapter two, an introduction of both the deterministic and probabilistic method is presented, after which only the calculation method for the probabilistic method is further investigated. A generic ship model is built in the DELFTship software, which will be used as a base ship for testing the sensitivity analysis and optimisation algorithm. In order to make a generic model, it was decided to use one base ship with many different parameters instead of multiple ships with fewer parameters, as it is difficult to compare multiple ships within the same model. It is therefore important to use a base ship that is able to represent a wide variety of other ship designs. Instead of the specific ship types that have already been investigated by others, a hypothetical general cargo ship will be used. In chapter three, the methods for both the sensitivity study and multi-objective optimisation are presented, which will eventually decide the methods that are used for this research. First, the method requirements are determined and the relevant methods are selected based on these requirements. Then, a decision can be made which methods are most suitable for this research problem. The methods are applied to the DELFTship program and PDS calculations in chapter four. The set up of the models is described in detail, as well as the verification methods and how the results can be obtained from the DELFTship program. Any uncertainties and limitations of the models are discussed and it is determined in what degree this influences the robustness of and confidence in the model. The results from both the optimisation and sensitivity analysis is discussed and analysed in chapter five. The results from this chapter determines the validity of this research and whether the research is sufficient to contribute to the design process. Chapter six presents the validation with the help of the validation square by Pedersen et al. [34]. Finally, chapter seven provides the conclusion, discussion, recommendations and a personal reflection.

2

Probabilistic Damage Stability Method

This chapter aims to give an understanding of the damage stability methods and the probabilistic method in particular and answers the sub question, *What parameters influence the attained index based on the PDS calculation?* This is done by introducing multiple methods of determining the survivability of the design. The PDS calculations are covered in detail in order to find the limitations of this method and to find the parameters that are applicable to this research.

2.1. Introduction Damage Stability

Damage stability is an important factor of a ship to determine how safe the ship is. The design must comply with international regulations set by the IMO and aim to increase the survivability of the ship in case damage occurs that leads to the flooding of a single or multiple compartments. Some of the common events that can lead to the flooding of compartments are [35]:

- Collision; defined as ship to ship collision
- Grounding; ship hits the ground
- Contact; collision with a fixed object
- Fire/explosion
- Structural failure

The methods for calculating the survivability of the ship in case any damage occurs from these events do not take the type of event into account, but rather only incorporate the location and size of the damage that results from it. The two methods of calculating the effect of flooding after a damage is described in this chapter as well as the two methods that describe the size and location of the damages and survivability of the ship as a consequence of these damages. The focus is on the PDS method rather than the deterministic method, as this is the focus of this thesis.

2.1.1. Two Methods for Finding the Ship Condition After Flooding

The two ways of calculating the effect of flooding after a damage has occurred are known as the method of lost buoyancy and the method of added weight. The book *Ship hydrostatics and stability* by Biran [36], gives a clear explanation of these two methods and is used to describe them in this chapter.

The lost buoyancy method is based on the principle that a flooded compartment does not contribute to the buoyancy anymore. If the damaged compartment has an open connection to the surrounding water and the water pressure inside the compartment equals that of the external water, the compartment is regarded as flooded. The lost buoyancy method states that the volume of the flooded compartment does not belong to the ship anymore, while the weight of its structures still contributes to the displacement of the ship. A new equilibrium is established with the buoyancy of the 'remaining' ship. The displacement as well as the position of the centre of gravity remains constant for this method. The water that floods the compartments does not contribute to the free-surface effect as it does not belong to the ship.

The method of added weight does consider the water entering a damaged compartment as belonging to the ship. The mass of the water is added to the displacement. Hence, the total displacement

of the ship in this damaged condition is sum of the intact displacement and the mass of the water that entered the damaged compartments. This results in a new position of the centre of gravity which is obtained from the sum of the moments on the intact ship and the water that entered the damaged compartments. In this method, the free-surface effect of the flooding water must be calculated and considered in all equations.

Table 2.1: Comparison between the added weight and lost buoyancy methods on a rectangular block [37]

	Lost buoyancy	Added weight
Draft	$T_d = T_i \cdot \frac{L}{L-l}$	Idem
Displacement	$\delta_i = L \cdot B \cdot T_i$	$\delta_d = L \cdot B \cdot T_d$
VCG	KG_i	$KG_d = KG_i + \frac{T_d}{2-KG_i}$
KM	$= \frac{T_d}{2} + \frac{B^2}{12T_d} - KG_i$	$= \frac{T_d}{2} + \frac{\frac{1}{12} \cdot L \cdot B^3}{L \cdot B \cdot T_d}$
Free surface	Nil	$= \frac{\frac{1}{12} \cdot L \cdot B^3}{L \cdot B \cdot T_d}$
GM	$= \frac{T_d}{2} + \frac{B^2}{12T_d} - KG_i$	$= \frac{T_d}{2} + \frac{B^2(L-l)}{12T_d \cdot L} - KG_i \frac{(L-l)}{L} - \frac{T_d}{2} \cdot \frac{l}{L}$
Righting moment	$\delta_i \cdot GM(\text{lost buoyancy})$	$\delta_d \cdot GM(\text{added weight})$ $= \frac{L}{L-l} \cdot \delta_i \cdot \frac{L-l}{L} GM(\text{lost buoyancy})$

Where:

- L = ship length
- B = Breadth
- l = Damaged compartment length
- $T_{i/d}$ = Intact/damaged draft
- $\Delta_{i/d}$ = Intact/damaged displacement
- KG_i = VCG of intact ship

The equations in table 2.1 show the difference between the two damage stability methods. In this case, the equations are based on a rectangular box ship floating in fresh water. It can be shown that for the added weight method, the displacement is calculated by increasing the intact displacement by the ratio $\frac{L}{L-l}$ whilst the GM in this case is that of the lost buoyancy method reduced by the ratio $\frac{L-l}{L}$. This gives, as would be expected, identical righting moments for the two methods. For both the deterministic and probabilistic damage stability calculations, the lost buoyancy method is most often used [37].

2.1.2. Deterministic Damage Stability Method

A deterministic system can best be described as a system in which there is no randomness or variation. This means that for a certain initial state, the system will always produce the same results. According to the Wärtsilä encyclopedia of ship technology [14], the deterministic approach to damage stability is based on a set of damage assumptions. The damage assumptions consist of the damage length, transverse extent, vertical extent and its location. Whether the survivability of the design complies with the required compartment status depends on the ship type, number of passengers or potential risk to the environment by the cargo carried. The deterministic stability requirements and calculations are clearly explained in the SOLAS 66 convention [38].

As the requirements for the deterministic damage stability depend among other things on the number of passengers and cargo, the requirements can be achieved relatively easy in the case of passenger ships. The difference in "cargo" for each loading condition is relatively small, so only a small range of draughts need to be considered. When considering tankers or general cargo ships, or any other ship

with a large variety of cargo weight and density, complying with the regulations for as many allowed loading conditions as possible requires an extensive analysis and systematic approach. Despite this, the advantage of the deterministic method is that it does not require advanced damage stability calculations, and the method gives a rapid impression of the ship's damage stability capabilities. However, the method gives little flexibility in the design and the deterministic rules cannot be used as a quantification of risk [39].

While the deterministic method is not the prominent damage stability method anymore, it is still relevant to many different aspects of ship design. In table 2.2, the relevance of the deterministic method can be seen.

Table 2.2: IMO instruments containing deterministic damage stability [35]

Regulatory framework	Application area
ICCL-66	Cargo ships and tankers with reduced freeboard
MARPOL 73/79	Tankers carrying cargo oil
IBC code	Ships carrying dangerous chemicals in bulk
IGC code	Ships carrying liquefied gases in bulk
HSC code	High-speed craft

In the harmonised regulations, the IMO SLF realised that the probabilistic method for passenger ships would not be sufficient without including a deterministic analysis of the so called "minor damages". The reason for this conservative chapter in the new harmonised regulations is the possibility of a ship design that is vulnerable to a small local damage that could have a catastrophic outcome (a single compartment damage due to grounding that would result in the loss of the ship for example). This would be unacceptable, even if the ships attained index is sufficient and the probability of this small damage occurring is practically zero. In addition, some deterministic side damages have to be assumed for passenger ships [35]:

Table 2.3: Additional deterministic requirements for passenger ships [35]

Number of persons (N)	Vertical extent	Penetration	Damage length	Location
$N \geq 400$	$d_s + 12,5$ m	0,1B but not less than 0,75m	0,03Ls but not less than 3 m	Anywhere in the ship's length
36 <N<400	$d_s + 12,5$ m	Linear interpolation	Linear interpolation	Between effective transverse watertight bulkheads (>3m)
36	$d_s + 12,5$ m	0,05B but not less than 0,75 m	0,015Ls but not less than 3 m	Between effective transverse watertight bulkheads

2.1.3. Probabilistic Damage Stability Method

In contrast to a deterministic system, the outcome of a probabilistic system is not determined by the initial state. The PDS method is based on the concept that two different ship designs with the same attained index are considered as equally safe.

The size and location of a damage is randomly generated. The probability of flooding of a compartment can be determined if the probability of a damage in that compartment is calculated. Hence, the probability of flooding is equal to the probability of occurrence of all such damages that create a direct entrance to the surrounding water. The open compartments are assumed as flooded, after which the survivability of the ship is calculated through the geometry and various ship characteristics, like GM

initial draught and permeability of the damaged compartments. Most of these factors are random within their set boundaries. [40]

The method is divided in two parts. A required subdivision index, which depends on the ship length and number of passengers, and an attained subdivision index, which is a summation of all the probabilities of occurrence and probabilities of survival. In table 2.4 below, the probabilistic ground rules are given and translated to the damage stability situation.

Table 2.4: Probabilistic ground rules and their application to the damages stability method

Mathematical	Damage stability	Explanation
$0 \leq P(A) \leq 1$		Probability range
$P(\text{not}A) = 1 - P(A)$	$P = 1 - p_i$	The complement rule: The probability that an event will not occur
$P(A \text{ and } B) = P(A) \times P(B)$	$P = p_i s_i$	Compound probability: The probability that two independent events will occur at the same time
$P(A) = \sum_n P(A \cap B_n)$	$P = p_1 s_1 + p_2 s_2 + \dots + p_n s_n$	The total probability is the sum of all compound probabilities for all events

Where:

- p_i = Probability of a damage i occurring;
- s_i = Survivability for the given damage i ;
- n = The number of all possible events.

As explained in chapter 1.1, while the probabilistic method gives the designer much more freedom in their design to reach the required index, it is in reality difficult to use the method as a design tool instead of just a stability criterion that has to be met. In order to comply with the PDS method, the attained index (A) should be higher or equal to the required index (R), as can be seen in equation 2.1. Where the attained index is the residual stability of the ship when considering all possible damages.

$$A \geq R \quad (2.1)$$

It is however, not necessary to take every damage scenario into account in order to satisfy equation 2.1. Hence, only the damage scenarios that contribute to the residual stability of the ship are added to the attained index. This means that if it becomes apparent that a part of the ship will not contribute to the attained index, it can be left out of the calculation method to reduce calculation time. This counter intuitive decision is also where the flexibility of the probabilistic method originates from. It is possible to obtain a high enough attained index by only focusing on specific parameters, leaving out other parameters that do have to be taken into account with the deterministic method.

2.2. Calculation Method Probabilistic Indices

The calculations addressed in this chapter are based on SOLAS Ch. II-1, Part B-1, the explanatory notes published by the Netherlands Regulatory Framework (NeRF) [41] and some of the results from a PhD thesis written by Lützen [40]. A masters thesis by Ole Martin Djupvik [28] and a paper by Olufsen and Hjort [35] are used to further explain different parts of the calculations.

A fundamental parameter for the use of the PDS method is the subdivision length. This length differs from the subdivision length used in the deterministic method. The length is used for the calculation of the required index and the p and r factor and is defined by SOLAS 74 Ch II-1, regulation 2 [42] as follows: "Subdivision length (L_s) of the ship is the greatest projected moulded length of that part of the ship at or below deck or decks limiting the vertical extent of flooding with the ship at the deepest

subdivision draught.” The buoyant hull represents the volume of the enclosed ship below the waterline, denoted as d_s . The $d_s + 12.5$ line represents the maximum vertical damage line which is the same for every ship. In figure 2.1 below, three different scenarios are shown for different ship designs and their subdivision length as used in the probabilistic method.

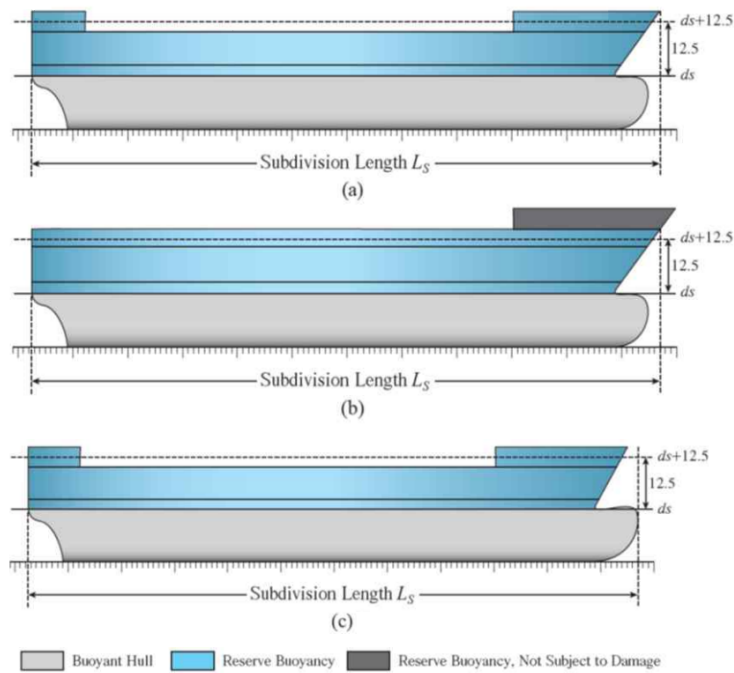


Figure 2.1: Subdivision length for the probabilistic damage stability method [43].

- (a) The damage length is governed by the upper compartments of the ship;
- (b) The upper compartment does not influence the subdivision length as it does not intersect with the maximum vertical extent of flooding;
- (c) The damage length is determined by the bulbous bow in this case as it extends further than any other compartment that influences the subdivision length.

In short, the subdivision length is the length comprised by all sections of the ship that are subjected to any damage in the probabilistic method.

2.2.1. Required Subdivision Index R

The required subdivision index R for passenger ships was established through the work of the HARDER project [44]. The empirical equations for calculating the R index were based on calculation results for sample ships. It can be seen in equation 2.2 that for passenger ships, the length of the ship hardly contributes to the required index when comparing it to the significance of the number of persons on board [35].

The required subdivision index for passenger ships can be calculated as follows:

$$R = \frac{5000}{L_s + 2.5N + 15225} \quad (2.2)$$

Where:

- L_s = Subdivision length;
- N_1 = Number of persons for whom lifeboats are provided
- N_2 = Number of persons in excess of N_1 , including officers and crew
- $N = N_1 + N_2$

For cargo ships above 100 meters the calculation is as follows:

$$R_0 = 1 - \frac{128}{L_s + 152} \quad (2.3)$$

For cargo ships not less than 80 meters, but not greater than 100 meters, equation 2.4 is used, with R_0 being the result of equation 2.3.

$$R = \left[1 / \left(1 + \frac{L_s}{100} \times \frac{R_0}{1 - R_0} \right) \right] \quad (2.4)$$

In contrast to equation 2.2 where the ships length and amount of passengers determine the required index, for cargo ships the index is purely a function of the ships length [45].

2.2.2. Attained Subdivision Index A

In principle, the attained index is made up of three partial factors that determine the residual stability of the ship after sustaining damage. The probability that each damage can be expected is measured in terms of the factor p . The factor s is used to measure the survivability of the ship after a damage has occurred. As the vertical extent of the damage is not covered by either s or p , a third factor v (equation 2.6) is used to complete the calculation. This factor provides the probability that the vertical deck above the waterline remains intact after the damage.

$$A = 0.4A_s + 0.4A_p + 0.2A_l \quad (2.5)$$

The three partial indices A_s , A_p and A_l are obtained by applying the three different loading conditions, d_s , d_p and d_l respectively [45].

Where:

- d_s is the deepest subdivision draught for which a level trim may be used.
- d_p is the partial subdivision draught for which a level trim may be used.
- d_l is the light service draught for which the estimated service trim must be used.

The three loading conditions as described above are illustrated in figure 2.2 below:

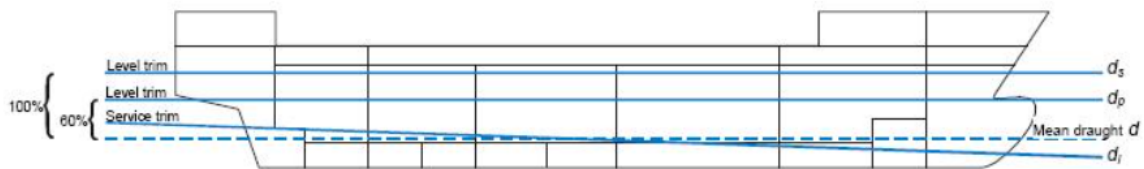


Figure 2.2: Three loading conditions for calculation of the attained index [41]

As the attained index per draught is the summation of the probability of the damages multiplied by the survivability and vertical extent of the damage, the equation becomes [45]:

$$A_c = \sum_{i=1}^{i=t} p_i [s_i v_m] \quad (2.6)$$

Where c is the index representing the three loading conditions, the index i represents each investigated damage or group of damages under consideration, m represents each horizontal boundary counted upwards from the waterline under consideration and t is the number of damages to be investigated in order to calculate A_c . The value of each partial attained index should be larger than $0.9R$ for passenger ships and $0.5R$ for cargo ships.

2.2.3. Factor p_i

The factor p_i is only dependent on the geometry of the watertight arrangement of the ship. It represents the probability of sustaining a specific damage. To explain the p_i factor, first a calculation for single and multiple zone damages is shown for pure longitudinal subdivision. Figure 2.4 illustrates the single, dual and triple zone damages as calculated below respectively.

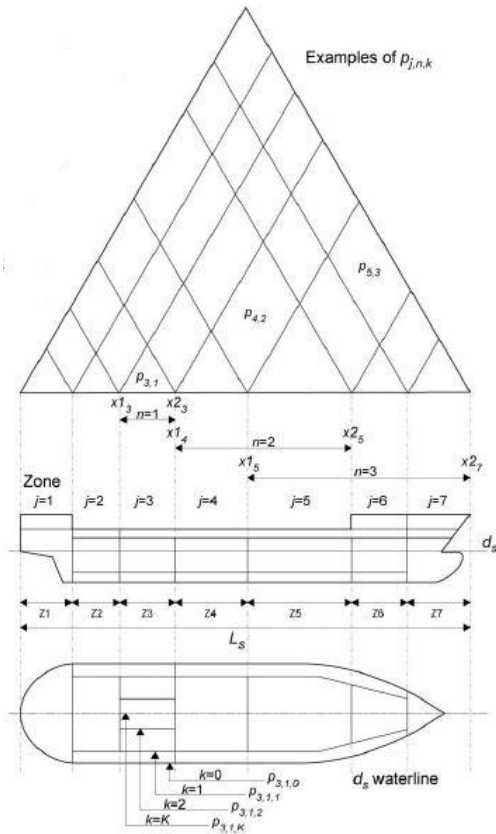


Figure 2.3: Longitudinal limits of damage zones [41]

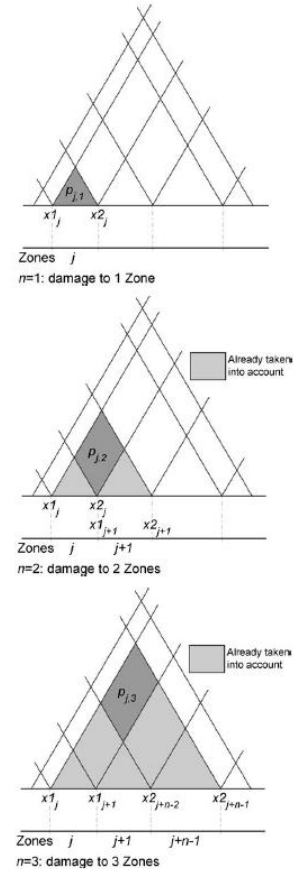


Figure 2.4: Example of single and multiple zone damages in pure longitudinal direction [41]

A single zone damage is calculated as follows [45]:

$$p_{j,1} = (x1_j, x2_j) \tag{2.7}$$

For two adjacent zones:

$$p_{j,2} = (x1_j, x2_{j+1}) - (x1_j, x2_j) - (x1_{j+1}, x2_{j+1}) \tag{2.8}$$

For three or more adjacent zones:

$$p_{j,1}(x1_j, x2_{j+n-2}) - p(x1_j, x2_{j+n-2}) - p(x1_{j+1}, x2_{j+n-1}) + p(x1_{j+1}, x2_{j+n-2}) \tag{2.9}$$

Where:

- j = The aftmost damage zone number involved in the damage, starting with number one at the stern;
- $x1$ = Distance from the aft of the ship to the aft end of the zone;
- $x2$ = Distance from the aft of the ship to the forward end of the zone;
- p = Factor accounting for the longitudinal extent of the damage;
- n = Amount of zones that damage is inflicted upon.

The subdivision in longitudinal direction of the subdivision length L_s consists of a number of water-tight compartments which is used to define the damage zones of the ship. The division is not bound by any rigid rules. By disregarding some of the transverse bulkheads, a number of small compartments are disregarded, so their contribution to the attained index will be disregarded as well. An advantage of this is that this results in fewer zones to calculate. The transverse subdivision cannot be disregarded this way. Here, the p-factor is to be adjusted for the probability that any longitudinal subdivision will not be breached [35]. This results in the r-factor, which results in the following p_i in case of a single zone damage:

$$p_i = p(x_{1j}, x_{2j}) \cdot [r(x_{1j}, x_{2j}, b_k) - r(x_{1j}, x_{2j}, b_{k-1})] \quad (2.10)$$

Where:

- k = Number of particular bulkheads as a barrier for any transverse penetration in a damage zone counted from shell towards centre;
- b = mean transverse distance measured at right angles to the centreline at the deepest part of the subdivision draught between the shell and an assumed vertical plane extended between the longitudinal limits used in calculating the factor p_i ;
- r = Factor accounting for the transverse extent of the damage.

The equations for two or more adjacent zones, or multi-zone damages follow the same principle as equation 2.10, but then combined with equations 2.8 and 2.9. Due to the complexity of these equations, they are not shown in this report [45].

During the HARDER project, the deterministic method was compared to the results obtained for that project and a new function was composed to be used for the PDS calculation of the longitudinal damage extent. In the PhD thesis by Marie Lützen, new datapoints are compared to the old database and the SOLAS B1 function. It can be seen in figure 2.5 that the SOLAS B1 function does not describe both the old and new database results well. Therefore a new bi-linear function was proposed and eventually adopted in the SOLAS regulations which can be seen in figure 2.6. The bi-linear function can be described as follows [40]:

$$b(J) = \begin{cases} b_1(J) = b_{11} \cdot J + b_{12} & \text{if } J \leq J_k \\ b_2(J) = b_{21} \cdot J + b_{22} & \text{if } J \geq J_k \end{cases} \quad (2.11)$$

Where:

- J = Non-dimensional damage length;
- J_k = Knuckle point between $b_1(J)$ and $b_2(J)$

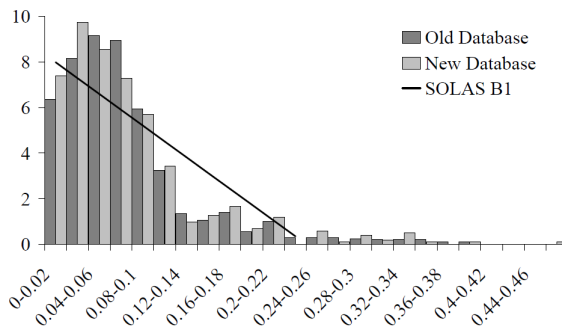


Figure 2.5: Distribution density for the non-dimensional damage length [40]

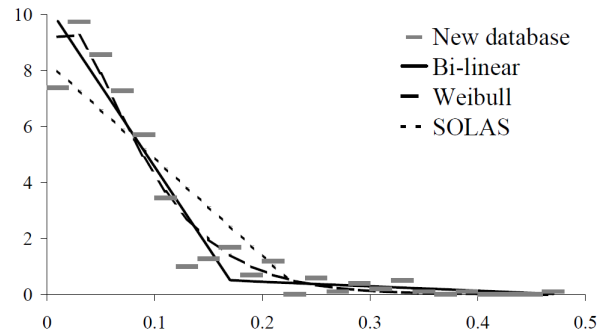


Figure 2.6: Density distribution for the non-dimensional damage length [40]

The factor $p(x_1, x_2)$ can be calculated according to the SOLAS Chapter II-1, Part B-1, Reg. 7-1, with the constants given in table 2.5

Table 2.5: Non-dimensional constants for calculating p(x1,x2) [45]

Overall normalised max damage length	$J_{max} = 10/33$
Knuckle point in the distribution	$J_{kn} = 5/33$
Cumulative probability at J_{kn}	$p_k = 11/12$
Maximum absolute damage length	$l_{max} = 60m$
Length where normalised distribution ends	$L^* = 260m$

From equation 2.11 and the statistics on non-dimensional damage length, the following coefficients are derived and implemented. [28, 45].

$$b_{11} = 4 \frac{1 - p_k}{(J_m - J_k)^2 - 2 \frac{p_k}{J^2 k}} \quad (2.12)$$

$$b_{21} = -2 \frac{1 - p_k}{(J_m - J - k)^2} \quad (2.13)$$

$$b_{22} = -b_{21} J_m \quad (2.14)$$

$$b_{12} = \text{dependent on ships length} \quad (2.15)$$

Where:

- J_m = Maximum non-dimensional damage length;
- J_k = Knuckle point in the distribution;
- J_k, J_k and b_{12} = Knuckle point in the distribution;

For cases in which the ships subdivision length is less than the length where the normalised distribution ends, the coefficients are calculated as follows:

When $L_s \leq L^*$:

$$J_m = \min \left\{ J_{max}, \frac{l_{max}}{L_s} \right\} \quad (2.16)$$

$$J_k = \frac{J_m}{2} + \frac{1 - \sqrt{1 + (1 - 2p_k)b_0 J_m + \frac{1}{4} b_0^2 J_m^2}}{b_0} \quad (2.17)$$

$$b_{12} = b_0 \quad (2.18)$$

According to equation 2.16, for a subdivision length of 198 meters, J_{max} will be the least value and subsequently used for J_m . This results in J_k being constant for a subdivision length below 198m. For a subdivision length of 260 meters or more ($L_s \geq L^*$), far fewer information is available about damage extents in the databases used. The factors J_m^* and J_k^* are introduced for splitting up the functions for J_m and J_k , as the data on ships with a subdivision less than 260 meters is different from ships with a subdivision larger than 260 meters [28, 45].

When $L_s \geq L^*$:

$$J_m^* = \min \left\{ J_{max}, \frac{l_{max}}{L_s} \right\} \rightarrow J_m = \frac{J_m^* \cdot L^*}{L_s} \quad (2.19)$$

$$J_k^* = \frac{J_m^*}{2} + \frac{1 - \sqrt{1 + (1 - 2p_k)b_0 J_m^* + \frac{1}{4} b_0^2 J_m^{*2}}}{b_0} \rightarrow J_k = \frac{J_k^* \cdot L^*}{L_s} \quad (2.20)$$

$$b_{12} = 2 \left(\frac{p_k}{J_k} - \frac{1 - p_k}{J_m - J_k} \right) \quad (2.21)$$

The non-dimensional damage length and normalised damaged length are described by equations 2.22 and 2.23 respectively.

$$J = \frac{x_2 - x_1}{L_s} \quad (2.22)$$

$$J_n = \min(J, J_m) \quad (2.23)$$

When $J = 0$ the probability density becomes:

$$b_0 = \left(\frac{p_k}{J_{kn}} - \frac{1 - p_k}{J_{max} - J_{kn}} \right) \quad (2.24)$$

Now the $p(x_1, x_2)$ factor can be calculated using the non-dimensional damage length and normalised damage length. There are three different cases which determine the calculation needed to obtain $p(x_1, x_2)$. In figure 2.7, the three different cases are illustrated for clarification [45].

1. *Where neither limits of the compartment or group of compartments under consideration coincides with the aft or forward terminals [45]:*

$$J \leq J_k :$$

$$p(x_1, x_2) = p_1 = \frac{1}{6} J^2 (b_{11} J + 3b_{12}) \quad (2.25)$$

$$J > J_k :$$

$$p(x_1, x_2) = p_2 = -\frac{1}{3} b_{11} J_k^3 + \frac{1}{2} (b_{11} J - b_{12}) J_k^2 + b_{12} J J_k - \frac{1}{3} b_{21} (J_n^3 - J_k^3) + \frac{1}{2} (b_{12} J - b_{22}) (J_n^2 - J_k^2) + b_{22} J (J_n - J_k) \quad (2.26)$$

2. *Where the aft limit of the compartment or group of compartments under consideration coincides with the aft terminal or the forward limit of the compartment or group of compartments under consideration coincides with the forward terminal [45]:*

$$J \leq J_k :$$

$$p(x_1, x_2) = p_1 = \frac{1}{2} (p_1 + J) \quad (2.27)$$

$$J > J_k :$$

$$p(x_1, x_2) = p_2 = \frac{1}{2} (p_2 + J) \quad (2.28)$$

3. *Where the compartment or groups of compartments considered extends over the entire subdivision length (L_s) [45]:*

$$p(x_1, x_2) = 1$$

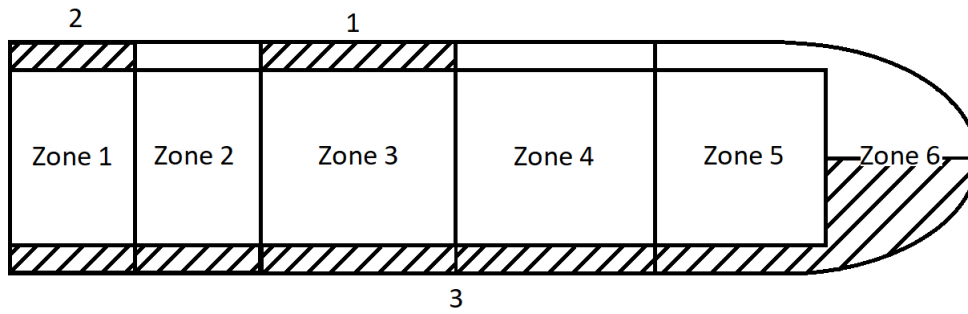


Figure 2.7: Damage conditions for calculating $p(x1,x2)$ in condition 1,2 and 3 respectively

The $r(x1,x2,b)$ factor represents the probability of penetration that is less than a given transverse breadth. Figure 2.8 shows the data obtained in the HARDER project and for the PhD thesis of Marie Lützen. Figure 2.9 addresses a linear function as proposed by Lützen to be implemented in the PDS calculations. As less than 5% of the damage penetrations exceed $B/2$, the maximum damage penetration is kept at $B/2$. This is a significant difference as opposed to the deterministic method where $B/5$ was taken as the maximum damage penetration. [40]

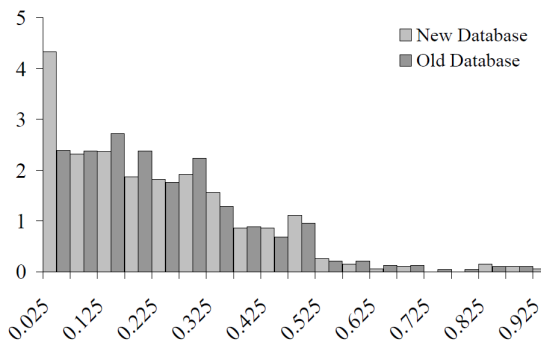


Figure 2.8: Non-dimensional penetration [40]

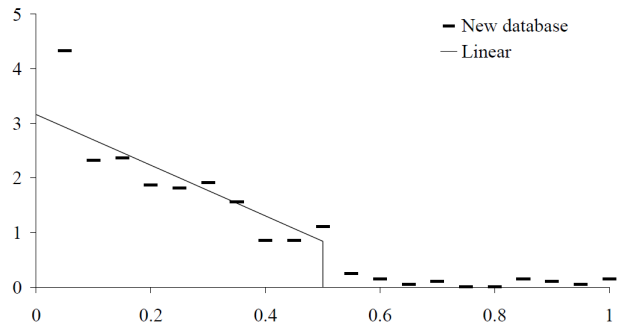


Figure 2.9: Density distribution for the non-dimensional penetration [40]

The calculations that represent the linear line in figure 2.9 can be seen in equations 2.29 till 2.32 [45].

$$r(x1, x2, b) = 1 - (1 - C) \cdot \left[1 - \frac{G}{p(x1, x2)} \right] \tag{2.29}$$

Where:

- $C = 12 \cdot J_b(-45J_b + 4)$;
- $J_b = b/15B$;
- $b =$ Penetration depth;
- $B =$ Maximum ship beam at draught.

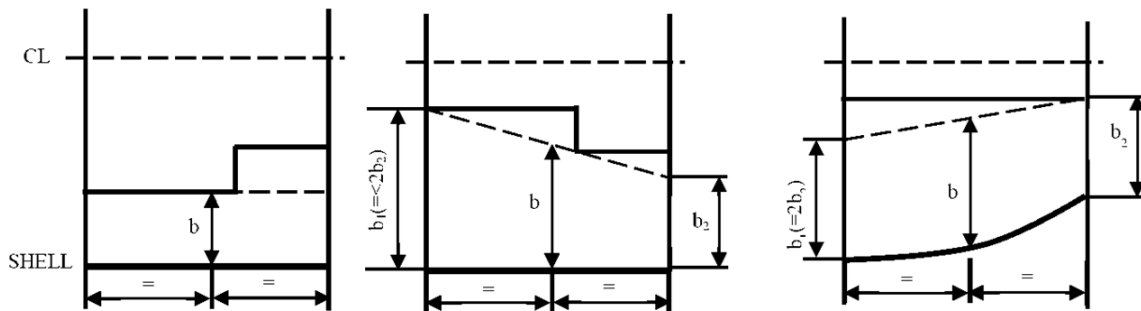


Figure 2.10: Calculation of the penetration depth b according to SOLAS Resolution MSC.281(85) [46]

1. Where the compartment or groups of compartments considered extends over the entire subdivision length (L_s) [45]:

$$G = G_1 = \frac{1}{2}b_{11}J_b^2 + b_{12}J_b \quad (2.30)$$

2. Where neither limits of the compartment or group of compartments under consideration coincides with the aft or forward terminals [45]:

$$G = G_2 = -\frac{1}{3}b_{11}J_0^3 + \frac{1}{2}(b_{11}J - b_{12}J_0^2 + b_{12}J \cdot J_0) \text{ Where } J_0 = \min(J, J_b) \quad (2.31)$$

3. Where the aft limit of the compartment or group of compartments under consideration coincides with the aft terminal or the forward limit of the compartment or group of compartments under consideration coincides with the forward terminal [45]:

$$G = \frac{1}{2} \cdot (G_1 + G_2 \cdot J) \quad (2.32)$$

2.2.4. Factor s_i

The factor s_i is dependent on the calculated survivability of the ship after the considered damage for a specific initial condition. With the initial condition being the three loading conditions, d_i, d_p and d_l .

The survivability of the ship is rather difficult to calculate due to the number of consideration which are included in the respective regulations. The survivability in its current form is the residual static stability, or the probability of survival by means of the righting lever (GZ) curve. The HARDER project concluded that 90% of collisions occurred in sea states with significant wave heights of 2 meters or less while 99% occurred when the significant wave height was 4.5 meters or less. Therefore, the HARDER project suggested that the GZ-curve based criteria within the 0 to 4 meter sea state range would be reasonable to accurately predict the ship's survivability. The survivability of the ship is calculated by taking the lesser value of the predicted survivability factor in intermediate and final stages, as well as by the effect of the heeling moment [35].

$$s_i = \min [s_{intermediate,i}, (s_{final} \cdot s_{mom,i})] \quad (2.33)$$

Where:

- $s_{intermediate}$ = Probability to survive all intermediate flooding stages until the final equilibrium;
- s_{final} = Probability to survive in the final equilibrium stage of flooding;
- s_{mom} = Probability to survive heeling moments

For calculating the survivability coefficients, the GZ_{max} and range should be obtained first. The GZ_{max} is the maximum righting lever (in metres) within the range given in equations 2.36, 2.34 and 2.37 in this chapter. The range is understood as the range of positive righting levers beyond the angle of equilibrium for which the boundary conditions are also set by the respective equations. The boundaries were modified during the by the IMO in 2009, influenced by the HARDER project. [47] In the graphs below, an example is shown where the GZ_{max} curve is lower than the actual GZ_{max} for the ship. This is due to an opening being submerged when the heeling reaches θ_v . The GZ_{max} curve is cut at this point and the corresponding value will be used for further calculations [28].

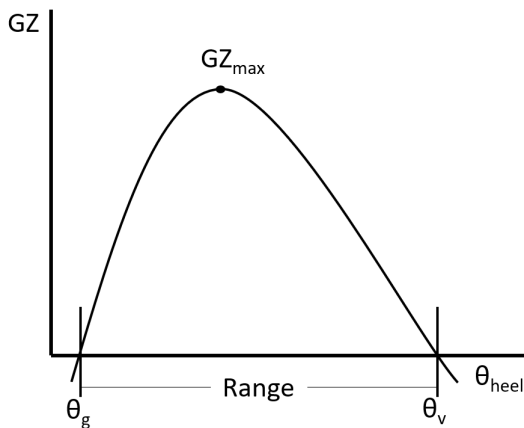


Figure 2.11: Example of a GZ curve based on [28]

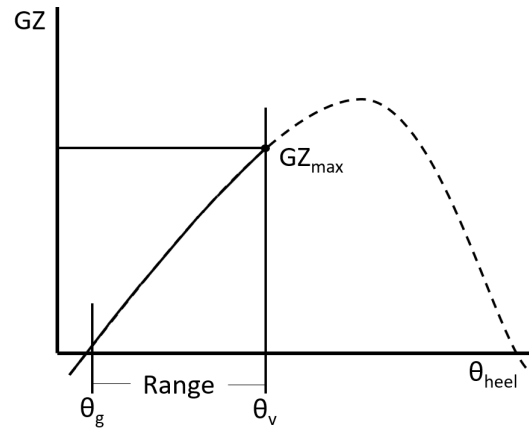


Figure 2.12: Example of a GZ curve for submerged openings based on [28]

Many of the calculations of SOLAS Ch. II-1, Part B-1, Reg. 7-2 appear to be of a deterministic kind. However, the probabilistic method shows itself with the probability of a successful evacuation, which increases with a low static heeling angle and the requirement that the evacuation route is not flooded with water.

$$s_{final,i} = K \times \left[\frac{GZ_{max}}{TGZ_{max}} \times \frac{Range}{TRange} \right]^{\frac{1}{4}} \quad (2.34)$$

Where:

- TGZ_{max} = 0.12 m, in every other damage case than Ro-Ro passenger spaces
- GZ_{max} = Not to be taken as more than TGZ_{max}
- $TRange$ = 16° , in every other damage case than Ro-Ro- passenger spaces
- $Range$ = Range with positive righting arm. Not to be taken as more than $TRange$

With:

$$K = \begin{cases} \sqrt{\frac{\theta_{max} - \theta_e}{\theta_{max} - \theta_{min}}}, & \text{if } \theta_{min} \leq \theta_e \leq \theta_{max} \\ 1, & \text{if } \theta_e \leq \theta_{min} \\ 0, & \text{if } \theta_e \geq \theta_{max} \end{cases} \quad (2.35)$$

Where:

- θ_{max} = maximum heeling angle, 15° for passenger ships, otherwise 30° ;
- θ_{min} = minimum heeling angle; 7° for passenger ships, otherwise 25° ;
- θ_e = Equilibrium heeling angle after damage;

The K factor is based on the heeling angle of the ship. Its purpose is to give acceptable heeling angles for different types of ships. For passenger ships, the maximum heeling angle is 15 degrees and for cargo ships 30 degrees. If the heeling angle exceeds these values, the K factor will be zero which will translate to s_{final} being zero as well. This means that if the ship is designed such that a damage case results in a larger heeling angle than θ_{max} , the damage conditions will not contribute to the attained index [28, 45].

Cargo ships have no requirements regarding the intermediate stages of stability, so $s_{intermediate}$ is set to 1 and therefore not interfering with equation 2.33.

$$s_{intermediate,i} = \left[\frac{GZ_{max}}{0.05} \times \frac{Range}{7} \right]^{\frac{1}{4}} \quad (2.36)$$

Where:

- GZ_{max} = Not to be taken as more than 0.05;
- Range = Not to be taken as more than 7°;
- $s_{intermediate}$ = 0 if heeling angle exceeds 15° for passenger ships and 30° for cargo ships.

The probability to withstand the heeling moment from passengers, wind and survival crafts is determined using equation 2.37. This s-coefficient is also not applicable to cargo ships and therefore set to 1.

$$s_{mom,i} = \frac{(GZ_{max} - 0.04) \times \Delta}{M_{heel}} \quad (2.37)$$

Where:

- Δ = Intact displacement at the respective draught (d_s, dp or dl);
- $M_{heel} = \max(M_{passenger}, M_{wind}, M_{survivalcraft})$;
- $s_{mom,1} \leq 1$

$M_{passenger}$ is used to describe the movement of all passengers to one side of the ship. As can be derived from equation 2.38, the weight assumed for each passenger is 75 kg and the centre of gravity of all passengers is placed on $0.45B$ from the centreline.

$$M_{passenger} = (0.075 \times N_p) \times (0.45 \times B) \quad (2.38)$$

Where:

- N_p = Maximum number of passengers permitted to be on board;
- B = Breadth of the ship

The moment due to the wind effect is assumed to result from a wind force of $120N/M^2$ projected on the lateral wind area above the waterline. The arm that is used depends on the respective draughts used in this probabilistic method.

$$M_{wind} = \frac{P \times A \times Z}{9.806} \quad (2.39)$$

Where:

- $P = 120N/M^2$;
- A = Projected lateral wind area above waterline;
- Z = Distance from centre of lateral projected wind area to $T/2$;
- T = Respective draught (d_s, dp or dl)

$M_{survivalcraft}$ is the maximum heeling moment caused when fully-loaded davit-launched survival craft are launched on one side of the ship. This moment is calculated based on the five assumptions given in SOLAS Ch. II-1, Part B-1, Reg. 7-2 rather than equations like with the other moments [45].

Another important part of the probabilistic method is the symmetrical flooding of compartments to minimise heel due to any damages. Tanks and compartments that take part in equalisation by symmetrical flooding should have sufficient openings in order to effectively flood any of the other compartments. The removal of the margin line concept resulted in the implementation of a penalty on the attained index. The s-factor is set to zero is one of the following features occurred [35]:

- Progressive flooding through unprotected openings occur;
- Evacuation along the bulkhead deck will be impeded in water;
- Vertical (emergency) escape hatches become immersed;
- Local controls for operation of watertight doors and other means of closure becomes inaccessible or inoperable due to immersion;
- Progressive flooding through damaging piping, ducts etc located in the damage zone will occur.

2.2.5. Factor v_m

The factor v_m is dependent on the geometry of the watertight arrangement (decks) of the ship and the draught of the initial loading condition. It represents the probability that the spaces above the horizontal subdivision will not be flooded. This can be translated to the probability that the bow of the ramming ship will be higher than the deck in question of the rammed ship. This factor is multiplied with the p_i and s_i factor in determining the total attained index and can be calculated using equation [45]:

$$v_m = v(H_{j,n,m}, d) - v(H_{j,n,m-1}, d) \tag{2.40}$$

Where:

- $H_{j,n,m}$ = The least height above the baseline, in metres, within the longitudinal range of $x_{1(j)} \dots x_{2(j+n-1)}$ of the m^{th} horizontal boundary which is assumed to limit the vertical extent of flooding for the damaged compartments under consideration;
- $H_{j,n,m-1}$ is the least height above the baseline, in metres, within the longitudinal range of $x_{1(j)} \dots x_{2(j+n-1)}$ of the $(m - 1)^{th}$ horizontal boundary which is assumed to limit the vertical extent of flooding for the damaged compartments under consideration;
- j = Signifies the aft terminal of the damaged compartments under consideration
- m = Represents each horizontal boundary counted upwards from the waterline under consideration
- d = Draught of the ship
- $x_{1/2}$ = Terminals of the compartment or group of compartments

$$v(H, d) = \begin{cases} 0.8 \frac{H-d}{7.8}, & \text{if } (H - d) \leq 7.8 \\ 0.8 + 0.2 \frac{(H-d)-7.8}{4.7}, & \text{if } (H - d) > 7.8 \end{cases} \tag{2.41}$$

Where:

- $v(H_{m,d}) = 1$ if H_m coincides with the uppermost watertight boundary of the ship within the range of the damage in longitudinal direction
- $v(H_{0,d}) = 0$

In figure 2.13 below, the heights used in the calculations for the vertical extent of the damages are illustrated.

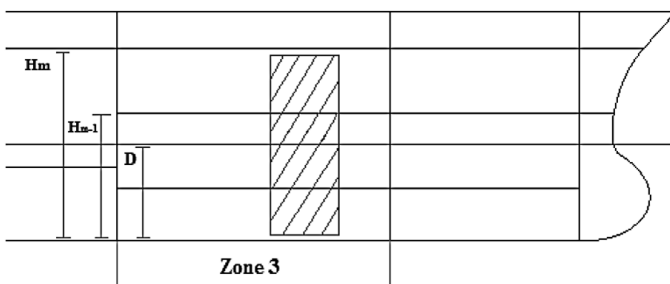


Figure 2.13: Definition of the vertical extent of a damage [28].

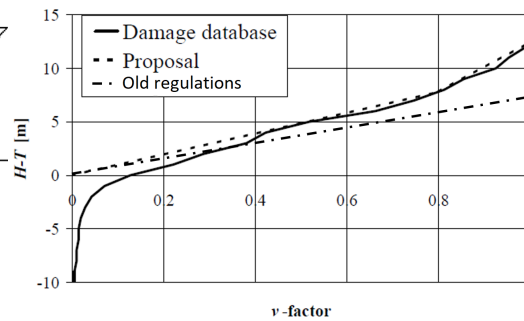


Figure 2.14: Cumulative damage height [40].

For the deterministic damage stability calculations, a length dependent formula was created as the data at the time showed a tendency that many ships were hit by ships their own size. As significantly more data was collected by the HARDER project, it was observed that there were a significant number of damages that extended higher than the 7 meters set by the deterministic method. In figure 2.14 above, the difference between the deterministic regulations and the results from the HARDER project can be seen. The new maximum damage height was set to 12.5 meters above the waterline. In SOLAS Ch. II-1, Part B-1, Reg. 7-2, the vertical extent is directly taken into account in the calculation of the survivability factor v_i because of the dependency of the GZ curve and the assumed buoyancy above the waterline. [35].

2.3. Conclusion

Based on the calculation method explained in this chapter, the parameters that influence the attained index for the survivability of the ship can be derived. These parameters can be obtained by looking at the variables used in equations 2.29 till 2.41 that directly influence the attained index, but also by looking at variables that are indirectly linked to these calculations. The parameters that are found and considered as possible parameters to use for this research are shown in table 2.6 below. They are divided in two categories, parameters that influence the design of the ship and parameters that influence the settings of the calculation.

Table 2.6: Optimisation parameters resulting from the probabilistic damage stability calculations

Parameters	Design/settings
Main parameters	Design
Number of bulkheads	Design
Position longitudinal bulkheads	Design
Position transverse bulkheads	Design
Height of decks	Design
Location superstructure	Design
Height of cargo hold coaming	Design
Intact freeboard	Design
Cross flooding arrangements	Design
Distance GM	Design
Location openings/hatches/vents	Design
Location superstructure	Design
Location staircase	Design
Permeability of tanks and spaces	Design
Heeling angles	Settings
Compartments considered	Settings
Number of subdivision zones	Settings

The limitations of the probabilistic method can be found in the combination of the complexity of the calculations and the use of the database obtained from the HARDER project. The design freedom offered by this method is difficult to capitalise on, when no framework is present that shows the designer what parameters influence the attained index the most and what decisions need to be made in order to reach the required index.

3

Method Exploration

In this chapter, the methods for both the sensitivity analyses and optimisation algorithms are investigated and eventually presented. This aims to answer the sub question, *What are the properties and requirements for an optimisation algorithm and sensitivity analysis and which methods are most suitable for this research?* First, the base ship particulars and parameters considered are discussed. This is what eventually determines the type of methods that can be used for this research. Next, the method requirements determine what methods are most suitable for this research. This chapter is the last chapter that is part of the literature study and definition stage of this research. At the end of this chapter, a clear plan of the methodology for the execution part of this research is presented.

3.1. Base Ship Particulars

A hypothetical ship model built in the DELFTship program is used as a base ship for this research. A standard hull provided by the DELFTship program is used and the subdivision of the ship is based on an actual ship designed by C-Job. This is to ensure that the design of the ship is realistic and applicable to real life problems. Due to confidentiality matters and because it has no added value to this research, the name of the example ship is not presented.

A ship with a single large cargo hold was chosen as this type of ship is particularly interesting regarding the PDS calculation. The design of cargo ships with a single cargo hold like this, dredgers, Ro-Ro ships and other ships with a single large compartment in the centre, can experience difficulty complying with the PDS. This happens when single compartment damages next to the cargo hold penetrate as far as this hold, resulting in a significant loss of attained index due to the loss of buoyancy and the free surface moment effect.

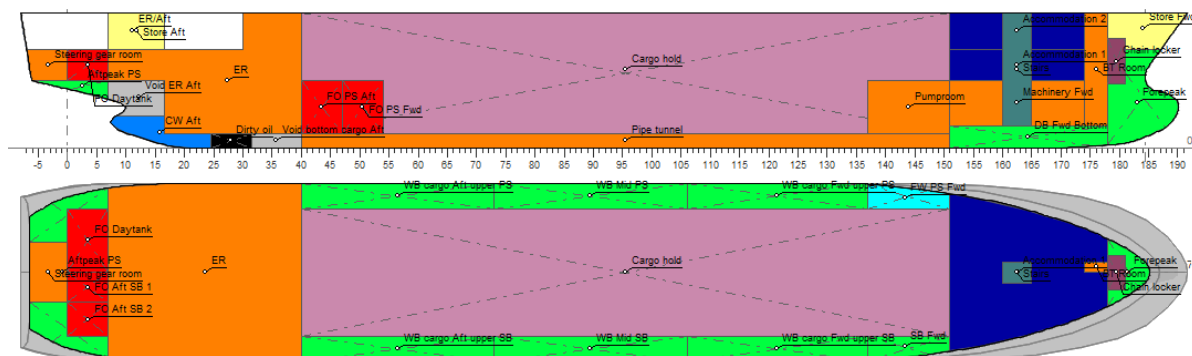


Figure 3.1: Hypothetical ship model made in the DELFTship program

The setup of the base ship model is designed such that the parameters that influence the attained index can be incorporated in an optimisation model as efficiently as possible. To illustrate this, all compartments are linked to transverse/longitudinal bulkheads and decks in order to keep all compartments

connected and maintain a similar internal and external geometry. In figure 3.1 on the previous page, a side view of the parameterised ship is shown. The base ship is fully designed regarding the PDS calculations. Critical points such as openings, watertight doors, escape routes, deck lines and tank connections from the example ship are added to the base ship, to try and create a realistic model that is suitable for this research.

Table 3.1: Main particulars hypothetical ship model

Main particulars base ship			
Ship type		General cargo ship	
Subdivision length	L_s	109,76	[m]
Length between perpendiculars	L_{pp}	101,42	[m]
Subdivision beam	B_s	16,80	[m]
Moulded Depth	D	9,30	[m]
Light service draught	d_l	3,44	[m]
Partial subdivision draught	d_p	4,94	[m]
Deepest subdivision draught	d_s	5,94	[m]
Displacement	Δ	7882,28	[t]

3.2. Parameters Considered

In chapter 2.3, the distinction between the design parameters and settings parameters is already made. This distinction does not influence the type of algorithm that can be used, but by making this distinction, it becomes clear what influence the settings have over the influence of changes in the design. It could be of interest to the designer to know when a part of the attained index is lost in setting up the calculation rather than in their actual design. By optimising the settings of the calculation for every design, unnecessary loss of attained index can be minimised. By trying to optimise the settings of the model however, no real improvements are made towards the safety of the design. It is possible that by trying to find as many parameters as possible that result in a higher attained index by changing settings rather than by the actual design of the ship, the flaws of the method will result in unsafe ships still being considered as safe. It is decided to focus on the subdivision of the design before more subtle design parameters are used to optimise the attained index. This results in the following parameters:

- Number of transverse bulkheads
- Position longitudinal bulkheads
- Position transverse bulkheads
- Deck height
- Location openings/hatches/vents

As can be seen in the list of parameters above, the number of bulkheads is the only discrete parameter. Why this difference is important and why they are difficult to combine is explained in section 3.3.5. It is however, important to take this parameter into account as it is vital to the way ships are subdivided and allow for a multi-objective method to be used.

3.3. Properties of Different Optimisation Algorithms

Optimisation algorithms are designed to solve specific optimisation problems. The variables, constraints and objectives determine the characteristics of the algorithm. In this chapter, the properties of algorithms are investigated, after which relevant methods can be chosen and compared by means of their performance and how well they fit the set of requirements that apply to this research. Figure 3.2 shows a simplified working principle of an optimisation method.

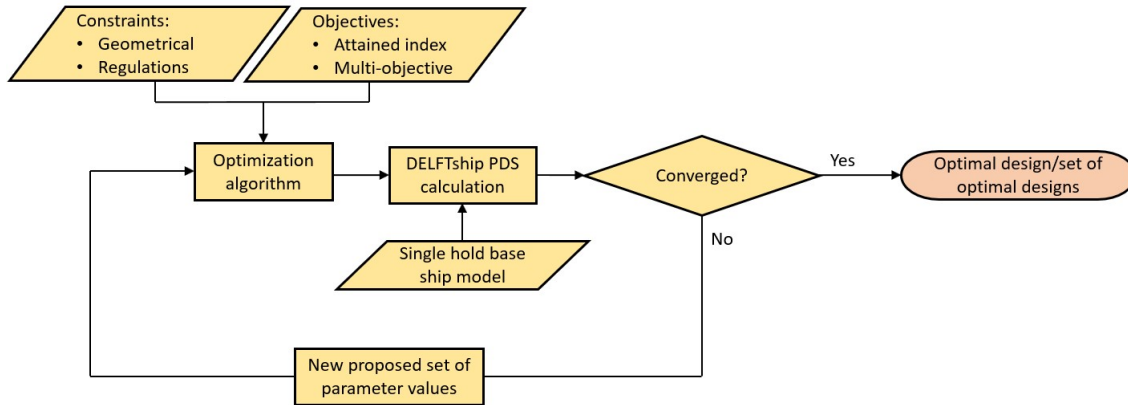


Figure 3.2: Simplified working principle of an optimisation method as can be applied to this research.

The DELFTship program is used as the simulation model for this research, where the base ship is the initial input for the model. As a base for choosing relevant algorithms, the following characteristics frequently found in literature are used to determine the usefulness of an algorithm:

- Local/global solutions
- Single/multi-objective
- Constrained/unconstrained
- Single/multi core
- Type of variables
- Genetic/non genetic

3.3.1. Local vs Global Solutions

One of the common problems with optimisation algorithms is that they get stuck on a local optimum. This is for instance the case with algorithms that use hill climbing. Hill climbing is a heuristic search method that tries to find a sufficiently good solution to the optimisation problem. The obtained solution may not be the global optimal maximum [48]. Hill climbing uses an initial guess, after which it starts moving until a peak is reached. For hill climbing to work, the search area must be smooth and the initial value must be located near the optimal solution. In figure 3.3, an example shows the local and global maxima for two design variables. As the parameter space is highly likely to have local optima, a global optimisation method is aimed for in this research.

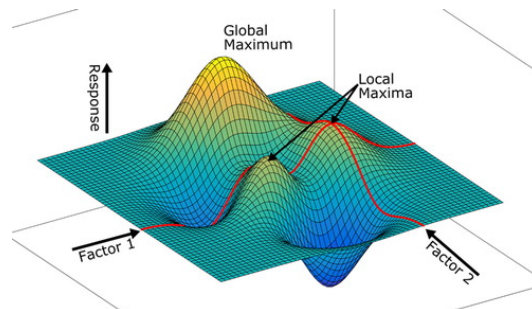


Figure 3.3: Example of search space with global and local maxima [49].

3.3.2. Single- vs Multi-Objective

Most real world problems require multi-objective optimisation solutions. When optimising multiple objectives that are non-commensurable and no clear preference of the objectives relative to each other, a minimisation multi-objective optimisation is defined as follows: Given an n -dimensional decision variable vector $x = \{x_1, \dots, x_n\}$ in a solution space X , find a vector x^* that minimises a given set of K objective functions $z(x^* = \{z_1(x^*), \dots, z_k(x^*)\}$. The solution space X is generally restricted by a series of constraints, such as $g_j(x^*) = b_j$, for $j = 1, \dots, m$, and bounds on the decision variables. The objectives under consideration conflict with each other in many real world problems. This means that when optimising for only one objective, often an unacceptable result with respect to other objectives is reached. This implies that when designing for multiple objectives, a perfect multi-objective solution is impossible to find. This point is also called the utopia point. Therefore a reasonable solution would be to investigate a set of solutions which satisfy the objectives at an acceptable level without being dominated by any other solution [50]. When working with multi-objective optimisations for example, the opposing objectives can be used to keep the objectives from diverging, resulting in the need for less stringent constraints.

The use of less stringent constraints for the model can be very beneficial, as by widening the parameter space, a larger space for finding a global optimum can be used. Some of the other objectives that can be used for the optimisation are listed below. It must first be determined whether or not these objectives are influenced by the parameters listed in chapter 3.2.

- Minimising CAPEX
- Minimising OPEX
- Cargo carrying capacity

The above mentioned objectives can all be considered financial objectives. The reason they are listed that way is because the efficiency of the ship mainly results from the production costs as well as the financial returns during its operational lifetime. The financial objectives are translated to geometrical objectives as these can be better implemented in this research:

Geometrical objectives:

- Minimising steel weight
- Maximizing cargo hold volume

The CAPEX of a ship consists of many types of expenses. For this research, the most relevant expense with the biggest contribution is the steel weight of the ship. This parameter also influences the cargo capacity, hydrostatics and GM of the ship design. This would be a good objective to use for the multi-objective optimisation. However, most of the parameters from chapter 3.2 do not influence the steel weight of the ship enough to be of any significance to the optimisation problem. It is therefore difficult to incorporate this objective together with the parameters into one optimisation algorithm.

The OPEX are mainly influenced by the design of the hull as fuel consumption is the biggest contributor to the OPEX. In this research the main parameters of the hull are not taken into account, therefore the OPEX is not a viable objective to use for a multi-objective optimisation.

Cargo capacity can also be maximised by expanding the volume of the cargo hold. This does not result in the ability of the ship to carry more cargo by weight, but by volume. However, by expanding the volume of the cargo hold, the volume of other compartments is reduced, instead of their dimensions scaled differently. This means that by trying to maximise this objective, the cargo capacity by weight and hydrostatics of the ship can be negatively influenced. This influence is considered as part of the more holistic design problem and therefore is not taken into account in this research. Therefore, the cargo hold volume is considered as a viable second objective.

The weight is in this case determined by the number of bulkheads and can be optimised without most of the negative aspects that other objectives can introduce. This could be used as a starting point for optimising the design for multiple objectives, ensuring an effective ship design.

3.3.3. Constrained vs Unconstrained

Whether an optimisation is required to be fitted with constraints depends on the characteristics of the problem and how the optimisation algorithm is set up. Most real world problems are bound by physical, regulatory or safety constraints. Most of these constraints are used as actual constraints in the model.

However, some real world constraints are not applicable to some models. Hypothetical constraints can therefore be used to mimic the behavior of the real world constraints. This ensures an efficient model that is designed according to the boundaries of the program that is used. A constrained optimisation problem with n parameters that is to be optimised is usually written as a nonlinear problem of the following form [51]:

$$\begin{aligned} \text{Minimise : } & f(X), & X = (x_1, x_2, \dots, x_n) \text{ and } X \in S \\ \text{Subject to : } & g_i(X) \leq 0, & i = 1, \dots, p \\ & h_j(X) = 0, & j = p + 1, \dots, m. \end{aligned} \quad (3.1)$$

For this research, many real world, regulatory and safety constraints are present in the process of designing a ship. Most of the parameters described in chapter 2.3 are subjected to these constraints. Therefore, the optimisation method will most definitely have to be able to handle constraints. For both single and multi-objective optimisation, constraints are needed. For single-objective optimisation however, the constraints are critical to remain an efficient design as there are no other objectives to keep the model from diverging. There are different constraint handling techniques. A study by Mallipeddi et al. [52], proposes an ensemble of these constraint handling techniques (ECHT).

Constraint can be very helpful when applied correctly. However, in the case of an over-constrained model, the optimisation method is unable to fully explore the parameter space. Figures 3.4 and 3.5 show the constraint surfaces and contours of the objective function to these constraint surfaces respectively. This shows that the most optimum solution might not be reachable when using certain constraints. An example of the misuse of constraints, is when a designer implements stringent constraints due to a certain bias, resulting in only feasible designs that resemble for instance previous designs of the designer. Also, when using relatively stringent constraints there is a chance the designer "steers" the optimisation to a certain design. The goal of this research is to try and explore as much of the design space as possible and find different possibilities of handling the cargo hold space.

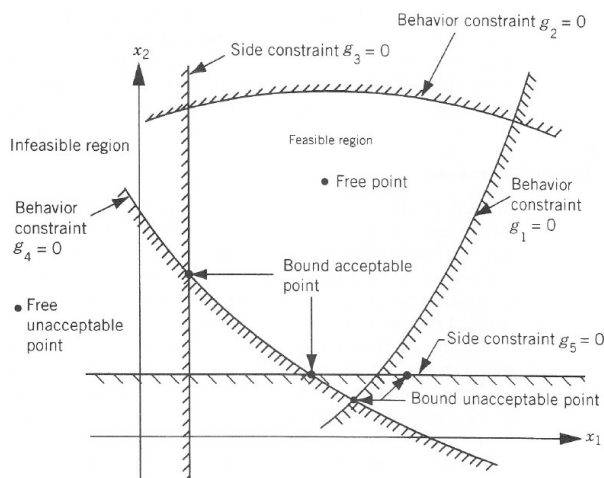


Figure 3.4: Constraint surfaces in a hypothetical two-dimensional design space [53].

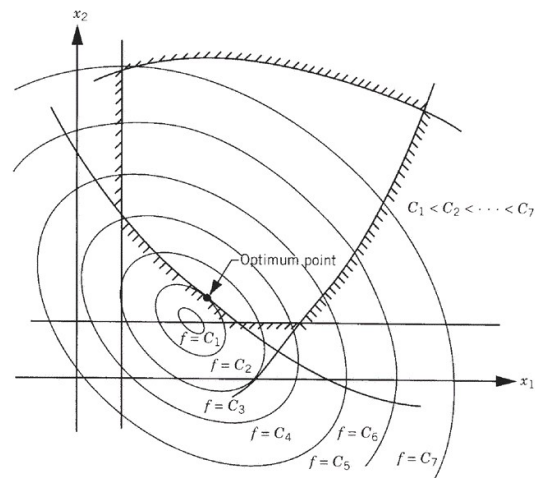


Figure 3.5: Contours of the objective function with respect to the constraint surfaces [53].

3.3.4. Single- vs Multi-Thread

Two ways to increase the speed of an optimisation are to reduce the execution times of individual applications or to run multiple independent applications (or threads of a single application) on a correspondingly number of cores. This defines the difference between optimising the processor's single and multi-threaded performance respectively. Although it may be reasoned that a multi-threaded approach is faster and more power efficient than a single-threaded approach, its utility is limited to specific parallel applications [54].

It could be very beneficial to optimise using an algorithm that supports multi-threaded optimisation. Some of the parameters listed in table 2.6, allow for a multi-threaded optimisation, while others are not independent enough. The DELFTship program already uses multi-threading by utilising all available cores for the PDS calculation. It is possible to run multiple instances of the DELFTship program parallel.

However, when running X instances of the program parallel, the number of cores per instance is also reduced by X , increasing the calculation time per instance by again, that same factor X . By running multiple instances of the program, each on different computers via cloud computing, the calculation time per instance remains the same, resulting in a significantly faster optimisation.

3.3.5. Type of Variables

A variable can describe either a quantitative or qualitative characteristic of a ships design. Quantitative variables only describe some quantity about the ships design and are often measured. Qualitative or categorical variables describe a quality or attribute to the design of the ship. Both quantitative and qualitative variables can be divided in two more variables that are regarded as the basic types of variables that are investigated in this research. In figure 3.6 below, the basic types of variables are shown.

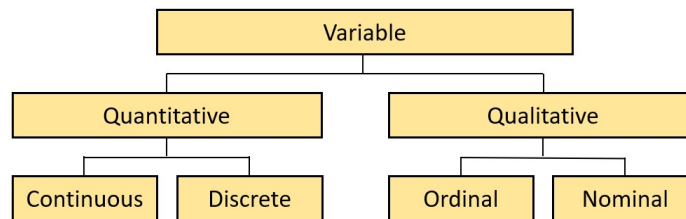


Figure 3.6: Types of variables applicable to optimisation problems [55]

Continuous variables can take any value in an interval and are only limited by the precision of the measuring instrument. Examples of continuous variables are a ships main dimensions (length, breadth, height), speed and propeller rpm. A discrete variable can only take specific numerical values as long as they have a clear quantitative interpretation. Examples of discrete variables are number of bulkheads, number of engines and number of damages. For these examples, only positive integers are possible as a values. Ordinal variables have a specific order while nominal values have not. Examples of nominal variables are small/medium/large, less than/between/over. Examples of ordinal values are the location of the superstructure, having a bulbous bow yes or no and applying cross flooding devices between tanks or voids yes or no [55].

Most of the parameters described in this research regarding the design of the ship are continuous variables. There are also some discrete and nominal variables. A possibility to cope with different types of variables is to create a bi-level or nested optimisation, as was described in a paper by Barg et al. [56], where the lower level is only able to process the continuous variables and the upper level consists of the discrete and nominal variables.

3.3.6. Genetic- vs Non-Genetic

Genetic algorithms are inspired by the evolutionist theory explaining the origin of species through natural selection. Weak and unfit species are faced with extinction by natural selection. The stronger species have a higher chance of passing on their genes to the next generation. Over many generations, the species that carry the correct combination in their genes become dominant in their environment. As this algorithm also possesses a certain randomness, random changes in genes may occur. If these changes provide additional advantages to the survivability, new species evolve from the old ones. Whereas unsuccessful changes in genetics are eliminated by natural selection [50].

For this research, the use of genetic algorithms is not a necessity, but could be of interest if it adds to the effectiveness of the optimisation. In the book Introduction to genetic algorithms by S.N. Sivanandam and S.N. Deepa, the advantages and disadvantages of using genetic algorithms are clearly summarised. The biggest advantage of using genetic algorithms according to the book is its ability to be parallelised and the use of recombination operators which enables the algorithm to mix good characteristics from different solutions [57]. One of the common problems with genetic algorithms is premature convergence. This occurs when the offspring of the population of chromosomes no longer outperforms their parents and the crossovers only regenerate the current parents [58].

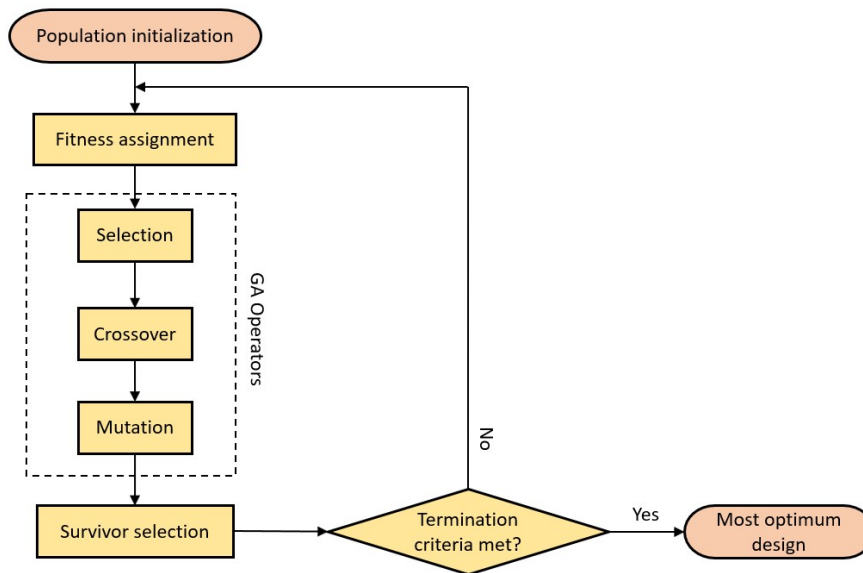


Figure 3.7: Structure of a genetic algorithm based on figure from [59]

3.3.7. Conclusion

A conclusion can be drawn from this chapter as to what properties the optimisation method should possess in order to be applied to this research and to produce satisfactory results. A global optimisation method is aimed for as this provides the designer with the best result of the entire parameter space. As the parameter space is constrained by different real world constraints and regulations, the optimiser should be able to handle this as well. Both a multi and single objective optimiser are used to determine the most efficient design (multi-objective) and to show the behaviour of the PDS calculation (single-objective). The DELFTship program already uses multi-threading to calculate the PDS on all available cores. If the algorithm allows it, multi-threading can be implemented to speed up the optimisation process. Most of the parameters are of the continuous kind, therefore an algorithm needs to be chosen that is able to handle these types of parameters. At last, it is possible to use genetic algorithms for this research. However, genetic algorithms are not specifically aimed for.

3.4. Properties of Different Sensitivity Analysis Methods

To determine which sensitivity analysis method is applicable to this research, the properties of the methods are first investigated. This is the same motivation as for the optimisation method property exploration explain in chapter 3.3. In the flowchart in figure 3.8 below, the simplified working principle of a generic sensitivity analysis is shown. This helps understanding the steps required to assemble the sensitivity analysis method which will be used for this research.

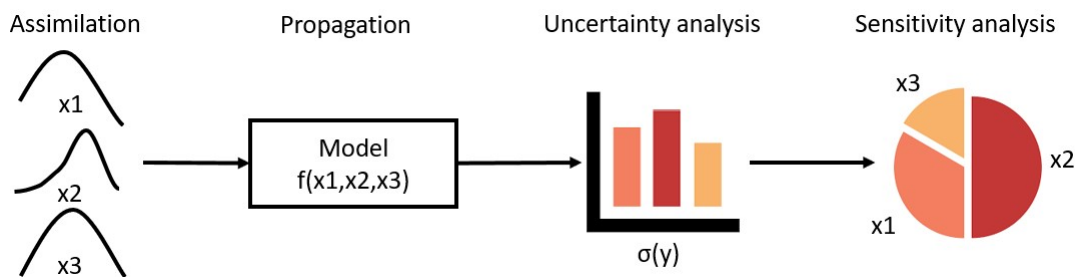


Figure 3.8: Simplified working principle of a sensitivity analysis

3.4.1. Classifying Sensitivity Methods

There are many types of methods for performing a sensitivity analysis. In the literature, different approaches are used to classify the different sensitivity methods that can be used. Some useful ap-

proaches are described in this chapter in order to set a base for choosing the most suitable method. Some common sensitivity analysis methods are identified in a paper by H. Christopher Frey and Sumeet R. Patil [60]. The methods are classified as:

- Mathematical methods
- Statistical methods
- Graphical methods

As explained in the paper by Frey and Patil, mathematical methods use the range of variation of an input to assess the sensitivity of the model output. As these models work mainly with input instead of output, they are very suitable for deterministic models as the variance in input can be linked to a certain variance in output where this is not possible for probabilistic methods.

The paper further explains that statistical methods are used to identify the effect of interactions among multiple inputs. Depending on the method used, a single or multiple inputs are varied at a time. A variety of techniques can be used to propagate the range and relative likelihood of inputs. When looking at the different types of statistical methods, it can be seen that they are not applicable to deterministic methods where the same input results in the same output.

Scatter plots give a visual representation of the inputs. The interpretation of such a plot can be qualitative and may rely on judgement. It cannot always be judged from a scatter plot if two inputs differ significantly from each other. In the paper of H. Christopher Frey and Sumeet R. Patil, table 2 shows a list of sensitivity analyses and their properties [60]. The paper originates from 2002. However, the methods are still very much applicable to this day, therefore it can be used as a base to decide the method on.

The PDS uses, as its name suggests, a set of stochastic variables and therefore involves some level of uncertainty. This means that, even though the exact same input results in the same attained index every time, the influence of these random variables is different for different ship characteristics [46]. Therefore the damage stability model is of a probabilistic kind and mathematical methods for sensitivity analyses are not applicable to this research and statistical methods are a better fit.

Saltelli classified the different sensitivity analysis methods as follows [61]:

- Local methods - one parameter varies at a time, where the other one is set.
- Global methods - influence is quantified on the whole variation range to determine their impact and ordering the parameters by their level of importance.
- Screening methods - determining the most influential inputs covering all the whole input space with few simulations.

Local methods only focus on the impact of the input parameters on a specific target area of the input space, where global methods give more accurate results and cover the whole variation range. The disadvantage of a global method is that it requires a large number of simulations. Screening methods are therefore often used to provide a qualitative analysis of the input parameters and to determine their influence [62].

One more classification method is discussed before the properties of a suitable analysis can be concluded. A study by Rivalin et al. compares sensitivity analysis methods based on the classification by Saltelli [61] and identifies the following methods [62]:

- Screening methods
- Approximation methods
- Sampling methods
- Metamodels

An example of one of the most used screening methods is the use of the Morris method. This is the most used screening method for sensitivity analyses [63]. The advantages are the small number of sampling methods, its simplicity and the fact that it only requires $2M$ experiments, with M being the number of parameters studied. The Morris method is however not able to analyse the interaction between different parameters [64, 65].

There are three families of approximation methods [62]:

- Quadratic combination - both the moments and sensitivity are given
- The first and second order reliability model (FORM and SORM) - sets the failure probability and sensitivity analysis around the threshold.
- Regression methods - provide input correlation information and sensitivity.

The advantage of quadratic combination is that it can provide importance factors with only $2M$ simulations, where M is the number of parameters. The disadvantages are that it may need a relatively large time to calculate and that the non-regularity of the model must not be of any significance. FORM and SORM methods have a relatively short calculation time and is always the same regardless of the precision. However, the approximation is not always accurate and the method can not be applied when the model is not differentiable. Regression methods can only be applied to linear or non monotonous models. In other words, the complexity or irregularity of a model can not be too high for this method to work [62].

A common sampling method is the Latin Hypercube Sampling method (LHS) [66]. This type of random sampling method uses the principle that each row and column contains exactly one point. In figure 3.9, the difference between random sampling, stratified sampling (dividing a population into smaller groups based on their characteristics) and LHS is shown.

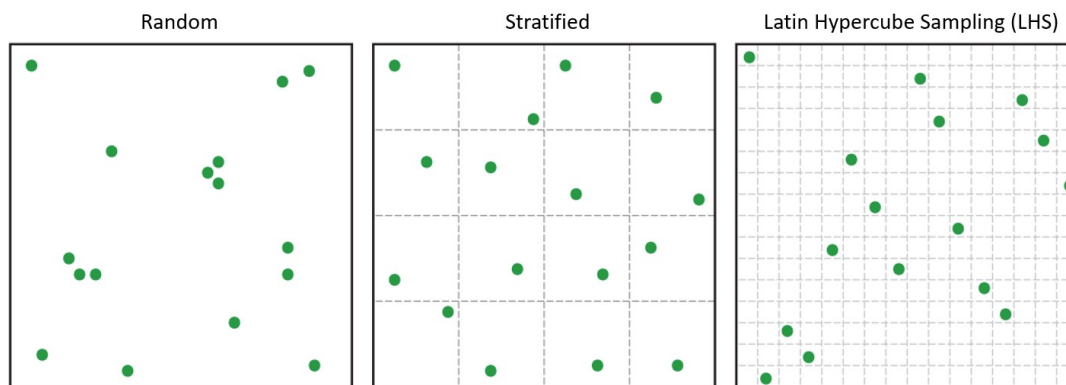


Figure 3.9: Different sampling methods for the use of a DOE [67].

The advantage of sampling methods is that it is space-filling, which means that the entire parameter space is used. A disadvantage of the sampling methods is that they need a relatively high sampling size. For instance, a convergence analysis for LHS showed a minimum number of realizations of 600 and 1300 for a 2D and 3D autocovariance function respectively [68].

3.4.2. Design of Experiments

Aside from the classification of sensitivity analysis, a tool can be used that encompasses the use sensitivity analyses. This is the design of experiments (DOE) and serves as a tool that helps in deciding which factor combinations to examine. The DOE was first introduced by Fisher [69] and can be helpful when performing a sensitivity analysis on a model with many parameters. For models with long calculation times, limiting the number of parameters to be studied is very important, especially in practical real world applications.

First a design method is chosen, which can be a Morris method or a sampling method for example. Next, a method for analysing the results of the design can be applied. There are several methods available, depending on the design and goal. Examples are an analysis of variance (ANOVA) for a full or fractional factorial design or a Gaussian process that not only estimates the importance of individual parameters, but also the influence of parameters on the outcome of a model [64]. This shows the broad applicability and capability of a DOE and that it can be further be expanded to perform other tasks that relate the parameters to the output. Other design types for a DOE are the following [70]:

- Comparison - One factor among multiple comparisons to select the best option that uses t-test, Z-test or F-test.
- Variable screening - Two-level factorial designs intended to select important factors among many that affect performances of a system.
- Transfer function identification - Relationship between important input variables and output variables is used for further performance exploration via a transfer function.
- System optimization - the transfer function can be used for optimization.
- Robust design - deals with reduction of variation in the system
- Practical conclusions and recommendations - this includes graphical representation of the results and validation.

3.4.3. Conclusion

Based on the literature described in this chapter, the properties of the sensitivity analysis that determine whether the method is applicable to this research can be listed. As explained before, mathematical methods are not applicable to this research and are therefore excluded. Scatter plots are a nice tool to visualise the behaviour of the variables, but as this requires the designer to determine the sensitivity of- and correlation between variables him/herself, it is not considered a desirable method. This leaves statistical methods as a best fit for this research.

The PDS calculation is an expansive calculation which suggests that global sensitivity analyses can potentially require too many function evaluation to be a realistic method for this research. In the next chapter, the difference in function evaluations between global and screening methods is investigated to determine the most suitable method. Local methods are excluded, these only show why a particular set of variables is the best as only one parameter varies at a time is being investigated and therefore not the entire parameter space is being investigated. Note that this is not the same as a global one a time method.

From the four different classes of sensitivity analysis by the study of Rivalin et al. [62], sampling methods are excluded due to their relatively large number of function evaluations. The difference in function evaluations between the other methods will be investigated to determine the best fit for this research.

It can be concluded that a statistical screening or approximation method or a meta model is to be used as a sensitivity analysis. As the DOE is a framework from which different kinds of sensitivity analyses can be performed, the available time schedule determines if a DOE is feasible or that it is better to focus on a single sensitivity analysis.

3.5. Method Requirements

The method requirements for both the optimisation algorithm and sensitivity analysis method are discussed in this chapter. This is the second and last step in determining the methods that will be used in this research. Relevant methods from the literature obtained from chapter 3.3 and 3.4 are compared with the help of the method requirements, which aims to provide the best option for this research.

3.5.1. Optimization Method

To determine which requirements are applicable to this research, the basic requirements of an algorithm in order to be considered useful are used and listed below [71]:

- Input: Inputs come from a specified set of elements, the amount and type are specified;
- Output: Clearly specify the output and how it is related to the input;
- Definiteness: Clearly defined and detailed steps;
- Effectiveness: Doable and effective steps;
- Finiteness: Must have a finite number of steps

The requirements for the optimisation algorithm can then be determined, after which integers are added to indicate the priority of the requirement from 1 to 6, where 1 is the most important requirement and 6 the least. The priority is determined by the focus of the research that result from the goal of the research, the knowledge gap and the preferences of the involved parties. Note that the applicability

is not included in this list as it is not necessary to compare methods that do not satisfy the required properties listed in chapter 3.3.7.

Table 3.2: Optimisation method requirements with their respective priority and source

Requirement	Priority	Source
Computation time	5	Based on standardised optimisation problems
Function evaluations	1	Convergence rate from standardised optimisation problems
Accuracy	2	Based on standardised optimisation problems
Knowledge support	3	Based on own experience
Interpretability	4	Based on literature
# of parameters	6	Based on algorithm properties

The number of function evaluations is the most important method requirement as the calculation time of the PDS method takes relatively long (approximately 10 minutes). This is called a computationally expensive optimisation problem, as the time it takes for one iteration to finish limits the number of function evaluations significantly, as it otherwise results in unacceptable computation times.

3.5.2. Sensitivity Analysis

The method requirements for the sensitivity analysis are listed below with their respective priorities which uses the same method as for the optimisation. The number of samples/iterations required to converge to a sufficient accuracy is the most important requirement for the same reason the function evaluations were most important for the optimisation algorithm.

Table 3.3: Sensitivity analysis requirements with their respective priority and source

Requirement	Priority	Source
# of samples required	1	Based on other applications
Size of the parameter space	2	Based on method properties
# of parameters	6	Based on method properties
Interpretability	4	Based on literature
Accuracy	3	Based on other applications
Knowledge support	5	Based on own experience

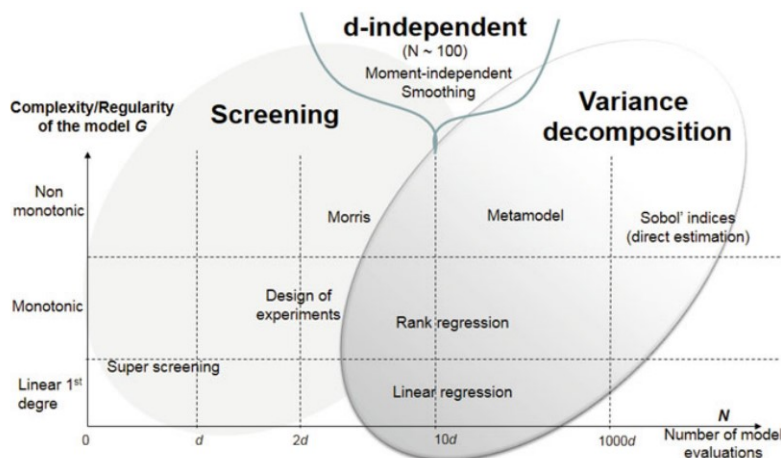


Figure 3.10: Coarse classification of main global SA methods in terms of required number of model evaluations and model complexity [65]

3.6. Choice of Methods

Based on the method properties and requirements, two methods are chosen. An optimisation method and a sensitivity analysis method. These are then used as main elements for the a larger method that should answer the research question stated in chapter 1.5.

3.6.1. Single-Objective Method SACOBRA

Different optimisation algorithms have been investigated in the literature using the properties mentioned in chapter 3.3 as a guideline. Many optimisation method surveys and independent papers have been used to find the best possible fit for this research. In the end the following state of the art algorithm has been found, that satisfies both the properties and the requirements mentioned in chapter 3.5.1: SACOBRA (Self Adjusting Constrained optimisation By Radial Basis Function Approximation) [72]. In this chapter, the choice of the algorithm is justified using the different properties that should satisfy the requirements set by the previous chapters. This algorithm was also used by C-Job employee R. de Winter to develop a multi-objective constrained optimisation method called SAMO-COBRA [73]. This kind of knowledge support is an advantage to this research as this increases the chance of using the full potential of the algorithm.

The SACOBRA algorithm is based on Regis' COBRA [74] algorithm. The SACOBRA algorithm uses surrogate models to deal with constraints, as these constraint functions may constitute highly conflicting goals and can be expensive to evaluate. The surrogate modeling technique used for this algorithm is radial basis function (RBF). Radial basis function methods are used to approximate multivariate functions. This method is especially well suited for the following cases when the functions to be approximated [75]:

- depend on many variables or parameters,
- are defined by possible very many data,
- the data are 'scattered' in their domain.

In figure 3.11, a flowchart of the SACOBRA algorithm can be seen, with the five extensions in comparison to the COBRA-R optimisation framework displayed in the grey boxes.

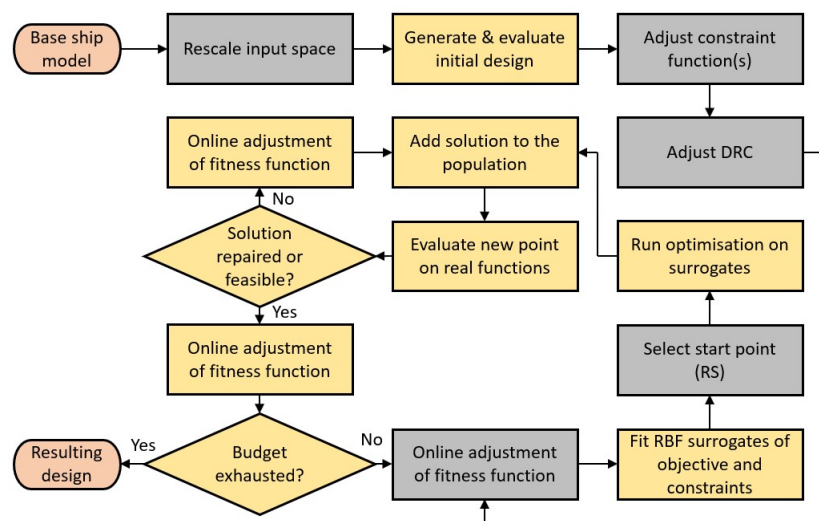


Figure 3.11: SACOBRA flowchart. The SACOBRA extensions compared to the COBRA-R algorithm are displayed in the grey boxes. [72]

The SACOBRA algorithm can be used for constrained single-objective optimisation problems with continuous variables and is well suited for optimisations under limited budget. Most of the parameters listed in chapter 3.2 can be optimised using this algorithm, except for the number of bulkheads. The number of bulkheads however, can still be optimised using a different method and is discussed in the conclusion of this chapter.

The SACOBRA algorithm is not only selected for the fact that it satisfies the properties listed in chapter 3.3, but it also performs according to the requirements set by chapter 3.5. The most important requirement is the number of function evaluations needed for the algorithm to converge. In the paper by Bagheri et al. [72], convergence plots for all G-problems show a clear improvement compared to the COBRA algorithm. The accuracy of the algorithm is compared to different state-of-the-art optimisers in table 4 of the paper which shows that the SACOBRA algorithm almost has the same solution quality as ISRES (Improved Stochastic Ranking Evolution Strategy) and DE (Differential Evolution) optimisers. These two optimisers can be considered as the best in terms of solutions quality [72]. Figure 3.12, the SACOBRA algorithm is compared to other well-known constraint optimisation solvers. What can be seen from this figure is that DE achieves very good results after many function evaluations ($\alpha \geq 800$). But the left plot shows that DE is not really competitive if very tight bounds are set on the budget. The full SACOBRA method also has no infeasible runs, which is an advantage over the rest of the methods that do have infeasible runs.

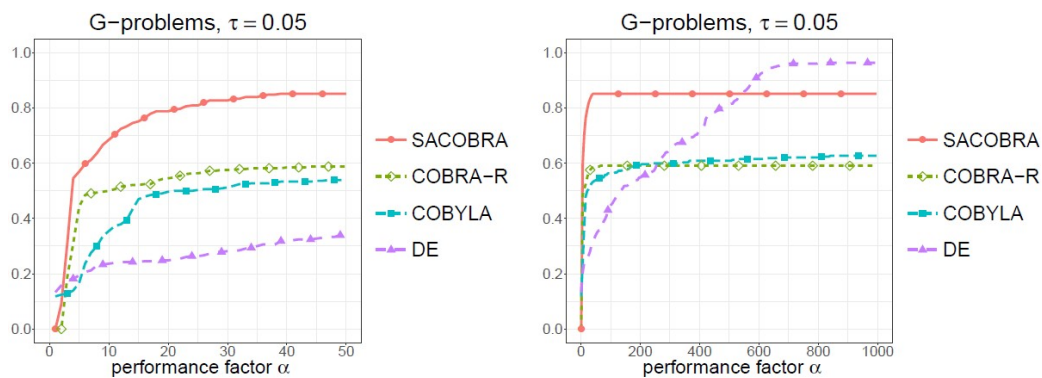


Figure 3.12: SACOBRA performance comparison with the algorithms COBRA (with Rescale), Differential Evolution (DE) and COBYLA (Constrained Optimisation By Linear Approximation) on optimising on test problems called G-problems. [72]

3.6.2. Multi-Objective Method SAMO-COBRA

A multi-objective version of the SACOBRA optimiser is used to compute the best feasible designs when optimising for not only the attained index, but also the cargo hold volume. A paper by de Winter et al. [73] describes the idea behind the SAMO-COBRA algorithm, stating that the algorithm seeks to find independently, for every iteration, each objective and for each constraint the best transformation and RBF kernel. The best fit from every iteration is then used to find new feasible Pareto efficient points that contribute the most to the hypervolume (HV). In the paper it is shown that the algorithm outperforms other relevant algorithms in terms of achieved HV after a fixed number of function evaluations. This method, just like the SACOBRA algorithm, possesses the properties discussed in chapter 3.3 and satisfies the requirements set in chapter 3.5.1. It can therefore be used for this research to obtain relevant results.

3.6.3. Sensitivity Analysis

Based on the sensitivity analysis properties from chapter 3.4 and requirements from chapter 3.5.2, the Morris method is chosen as the most suitable option for this research. Many different methods were compared based on their properties, Sobol indices [76], surrogate-based sensitivity analyses [77] and regression-based sensitivity analyses [78].

As explained in chapter 3.4, the Morris method is a screening method. The method is a specialized randomized one-at-a-time (OAT) method. A OAT sensitivity analysis changes all input variables in question by the same relative amount. The Morris method distinguishes itself from other OAT methods by changing a variable between two model simulations. The difference computed between the two model simulations is used to identify and rank the important variables [79].

The algorithm uses a randomly chosen starting point in the k -dimensional space. A path is then created through the whole k -dimensional variable space and is built with $k+1$ points. A standardised step Δ_i differs two adjacent points. The coordinates of every point of a single path are used as input values for the method [80]. A step-by-step construction of the single path for $k = 3$ parameters is presented in figure 3.13.

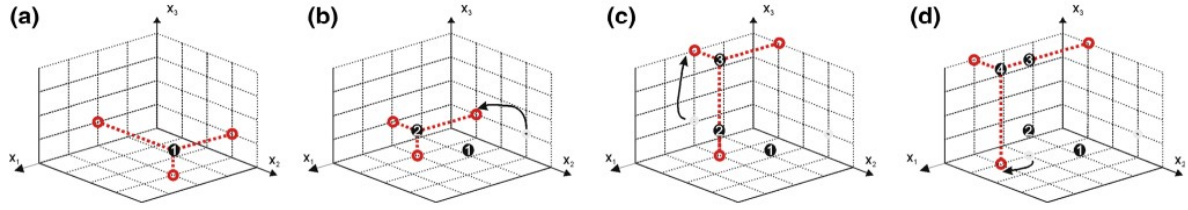


Figure 3.13: An example of a single trajectory constructed for the three-dimensional space of input parameters. The trajectory is built with four points: one randomly chosen (a) and three points created as a result of changing one value at each step (b–d) [80]

The single path consists of levels, which are discrete values taken by each input factor in the construction of the single path. These levels are chosen within the factor range of variation. The levels are denoted as p and are sampled each factor range evenly: $X_i = \{0, 1/(p-1), 2/(p-1), \dots, (p-2)/(p-1), 1\}$. p is typically taken as 4, 6 and 8. The space used for the sensitivity analysis is thus transformed in a k -dimensional p -level grid where the magnitude of the experiment step Δ is equal to a multiple of $1/(p-1)$ [80]. The final path matrix B^* is then computed as [79]:

$$B^* = \left(J_{k+1,1} X^* + \frac{\Delta}{2} [(2B - J_{k+1,k}) D^* + J_{k+1,k}] \right) P^* \quad (3.2)$$

Where:

- $J_{k+1,k}$ and $J_{k+1,1}$ = $k+1$ -by- k and $k+1$ -by-1 dimensional matrix and vector of 1's;
- B = $(k+1, k)$ -dimensional sampling matrix containing only 0's and 1's;
- D^* = k -dimensional diagonal matrix, each element is 1 or -1 with equal probability;
- P^* = k -by- k random permutation matrix, with in every column only one 1 element.

The sensitivity analysis is based on estimating the distribution of the elementary effect (EE). For each path and variable, the EE is calculated separately based on the output values for the two adjacent points in of the path [80]. The elementary effect is described as:

$$EE_{i,j} = \frac{Y(X_1, X_2, \dots, X_i + \Delta_i, \dots, X_k) - Y(X_1, X_2, \dots, X_i, \dots, X_k)}{\Delta_i} \quad (3.3)$$

The $EE_{i,j}$ values are used to compute the following two sensitivity measures [80]: The mean absolute value of the j^{th} parameter

$$\mu_j^* = \frac{1}{r} \sum_{n=1}^r |EE_{i,j}| \quad (3.4)$$

The standard deviation of the elementary effect

$$\sigma_j = \sqrt{\frac{1}{r} \sum_{n=1}^r \left(EE_{i,j} - \frac{1}{r} \sum_{n=1}^r (EE_{i,j}) \right)^2} \quad (3.5)$$

Three groups are created following the results from the mean absolute value and standard deviation:

- Inputs with negligible effects;
- Inputs with large linear effects without interactions;
- Inputs with large nonlinear or interaction effects.

The Morris method is mainly chosen for its low number of sampling points needed to converge [81, 82, 78]. This can also be seen in figure 3.10, where at the same time the ability to use the method for more complex/irregular models is shown. The method also uses the entire parameter space as is explained in chapter 3.4, which is a great advantage over local sensitivity methods. In figure 3.14, the resulting graph of the Morris method is shown.

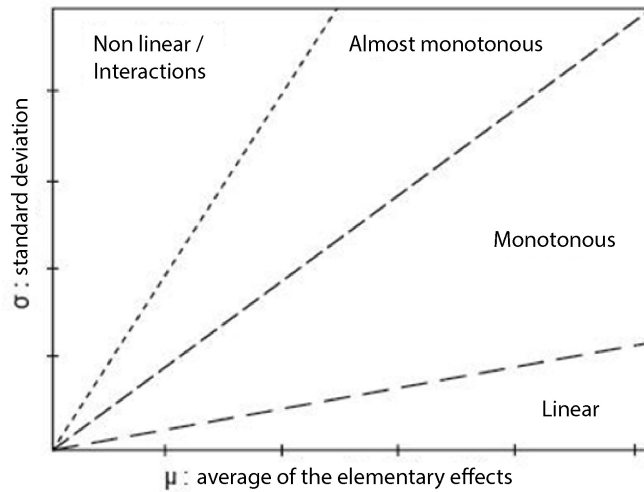


Figure 3.14: Classification of parameters according to the mean of their elementary effects and their dispersion (standard deviation of the series of elementary effects)[83]

3.7. Conclusion

It can be concluded from this literature study that creating an overview of what parameters influence the attained index the most and optimising the subdivision accordingly, is a complex task with many different types of factors at play. The choice of methodology for this research, in order to accomplish the goals set in chapter 1.5, are based on the information gathered about these factors. This conclusion provides a summary of all decisions that are made as a result from the findings of the literature study phase of this research. During the research, different aspects of the initial approach were changed due to new insight obtained during the execution of the methods. An example is the addition of the multi-objective optimiser, where first only the single objective optimiser was deemed as the best fit for this research.

A multi-level method is chosen to optimise the design parameters. This is due to the variety of parameters that are important for the designer and the objectives that guarantee the effectiveness of the design. In the figure below, the methodology setup is shown more clearly:

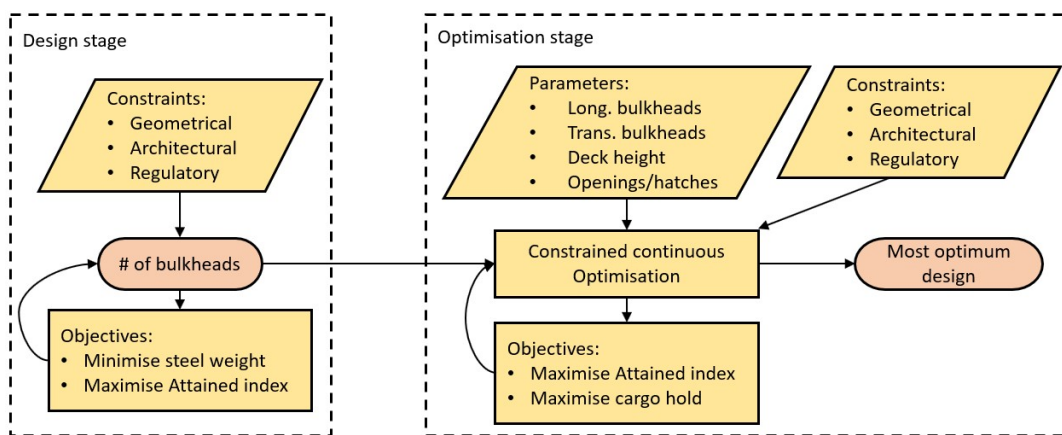


Figure 3.15: General setup of the methodology for this research

The first stage is the "design stage", where the amount of bulkheads is determined by means of placing the bulkheads with respect to architectural considerations and geometrical boundary conditions (e.g. no bulkheads in the cargo hold) and calculating the attained index for the different designs. The objectives are to maximise the attained index, to minimise steel weight and the size of the cargo hold. The steel weight should always be minimised as this has a positive influence on the CAPEX and cargo capacity of the ship. This also minimises the GM. By minimising the GM, the accelerations of the ship

are kept low, which is beneficial for forces resulting from sea conditions and cause less stress on the crew on board. For this case study, the steel weight is not actually minimised as the weight is not calculated due to the size of the scope. However, a framework is created from which the designer can choose the number of bulkheads based on the attained index and determine whether or not the increase in attained index outweighs the increase in steel weight by adding another bulkhead. The second stage is the "optimisation stage", where the continuous parameters are optimised for the amount of transverse bulkheads determined in the first stage. This is done by means of both a single and multi-objective optimiser. The constraints of the design and the boundaries of the parameters further guarantee the effectiveness of the design.

The sensitivity study should give a clear overview to the designer, where more margin in the attained index can be found to further optimise the design in case changes are made. As explained in chapter 3.6.3, the Morris method is used to perform the sensitivity analysis, where the main reason of choice is the limited time available due to practical applicability. This is done either before or after the optimisation method. An interesting application when using a sensitivity study and optimisation method at the same time, is the ability to first explore which parameters have the most influence on the attained index after which these parameters can be explained. Also, the other way around is an option, where the sensitivity of the already optimised parameters is studied. This can be helpful to correct the parameters after some changes have been made in the design that influence the attained index either directly or indirectly. For this research the latter option is used as the Morris method does not give the correlation between the variables. Therefore, when leaving out parameters due to a low influence, potential influential correlations can be overlooked.

4

Methodology

This chapter aims to explain the set-up of all methods used to answer the research questions. Specifically the research question *How can the base ship model be parameterised in order to be subjected to different optimisation and analysis methods?* The same as chapter three, this chapter consists of three sub sections describing the set-up of the parametric base ship model, the optimisation methods and the sensitivity analysis method. The set-up is described such that all decisions that influence the output are discussed and a clear overview of all methods is given. The methodology is a mix of quantitative and qualitative methods. All quantitative data obtained by the methods needs to be interpreted, in order to generate insight in the actual behaviour of the PDS method. The multi-objective optimiser will be used to generate an initial design, while the single-objective optimiser is used to run several specific experiments to better understand certain design choices. In the end, this chapter gives a step by step guide of the methodology.

4.1. Creating a Parametric Model

Parametric modelling is used to describe the changes in a model, or geometry in this case, when certain input changes. Optimisation algorithms, sensitivity analysis methods and other methods can be applied to parametric models with the aim to obtain valuable results from the changes in geometry. A parametric model has to satisfy a number of different characteristics. The model should be flexible and generic to be applicable to many different designs. Furthermore, it should be detailed enough to cover all essential characteristics of the design, while simultaneously be as simple as possible to avoid unnecessary complexities. These goals should all be reached, while also ensuring the models integrity, robustness and functionality [84]. In this chapter, all considerations regarding the setup of the parametric model are discussed. In figure 4.1 below, a flowchart of the parametric model is given.

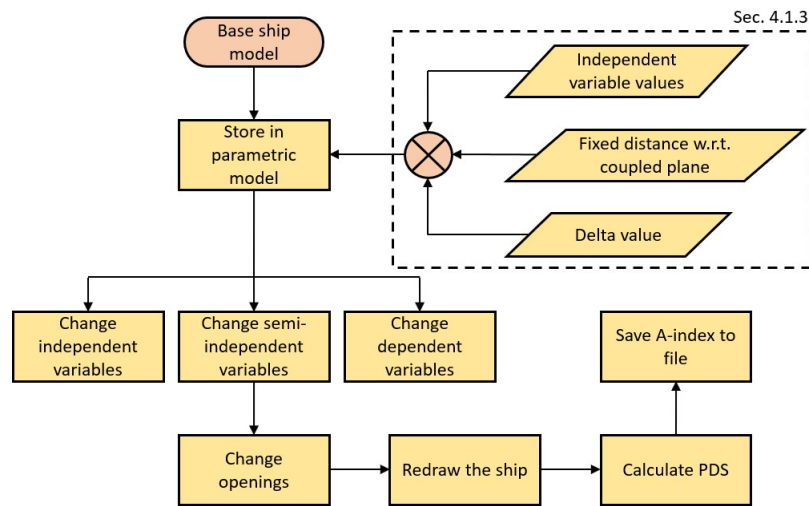


Figure 4.1: Flowchart of the parametric model set-up

4.1.1. Focused Section

The parametric model is built in the DELFTship software. The variable values, or infill points, proposed by the optimisation method are used as input for this model. The variables used for this research are located in the middle section of the ship. These variables all have lower and upper bounds to define the parameter space. Chapter 4.3.3 expands on these variables and also the choice of their boundary values. In table 3.1, the main particulars of the ship can be found. These remain constant throughout the optimisation, as the goal of this research is to optimise the attained index within a certain design.

The aim of this research is to generate results that are applicable to single large hold ships in general. Therefore, the parametrisation of the base ship should take into account design choices that can be applied to other case studies as well. The first choice made in order to reach this goal is by dividing the ship into three parts, an aft, middle and forward section, whereby only the middle section is focused on in this research. Although this could potentially impose some limitations on the results and insight of this research, it greatly reduces the number of design variables, eliminating the need for dimensionality reduction measures in that particular section, which in turn increases the insight in that section. This is vital for creating insight in how the single large hold reacts to different modifications. Also including the aft and forward section of the ship results in a more holistic problem that could potentially lead to a wrong interpretation of how the variables react due to the high complexity of the model. It is still possible to shift the cargo hold in longitudinal direction in its entirety, this allows for changing the size and location of the sections.

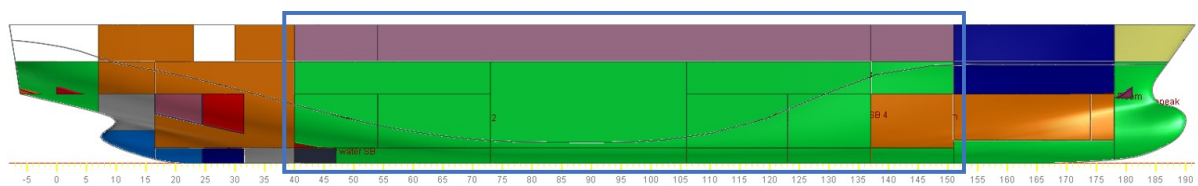


Figure 4.2: Parametric model with, blue square indicating the optimisation region

4.1.2. Computing Damage Cases

The PDS calculation of the initial base ship model generates 841 unique damage cases. The exact number of damage cases is based on the design of the ship and the location of the subdivision zones. A more complex subdivision, results in more subdivision zones, which means that more damage cases are created to define the single and multi zone damages. This is explained in section 2.2.3 in more detail. These zones represent a portion of the ship between two longitudinal boundaries (e.g. transverse bulkheads). The PDS method relies on a regular compartment layout, meaning that all transverse bulkheads extend over the entire length of the ship, and all decks and longitudinal bulkheads extend

from one transverse bulkhead to the next. In reality, this is not the case for many compartments of the design, therefore becoming non-regular and unable to be subjected to the PDS calculation. An irregular layout cannot be processed without fictitious subdivision in order to make it virtually regular. A schematic example is given in figure 4.3 below. It can be seen that compartment "D" is the most irregular area, where irregular compartments "A" and "C" are overlapping each other as well.

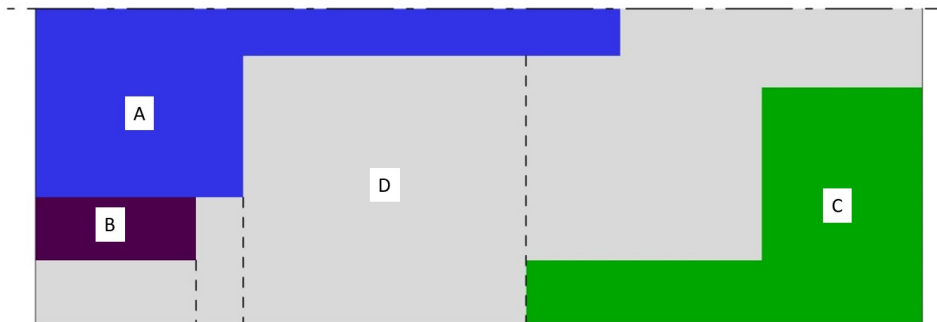


Figure 4.3: Schematic example of non-regular compartment lay-out [85].

The zonal concept forces the subdivision model into regularity, avoiding the above mentioned pitfall [85]. For every design, the layout of these zones should be determined and applied to the DELFTship model. DELFTship offers the possibility to automatically generate the subdivision zones based on tank boundaries. This comes in handy when subjecting the parametric model to an optimisation method. For every iteration, a new design is generated, and therefore creating the need for a new zonal subdivision. As it is not realistic to create a new zonal subdivision by hand between each iteration, the automatic subdivision is used. In figure 4.4 below, the lay-out of the initial subdivision zones is shown:

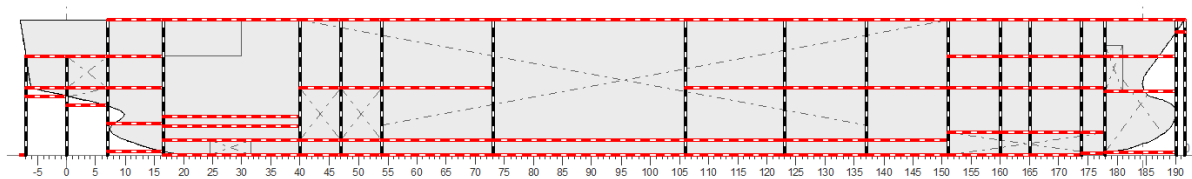


Figure 4.4: Side view of the parametric model showing the subdivision used for the PDS calculation

4.1.3. Categorising the Variables

One of the problems with using only independent variables is for example the pitfall that arises when the upper boundary of one transverse bulkhead is greater than the lower boundary of the transverse bulkhead in front and the aft bulkhead "overtakes" forward bulkhead.

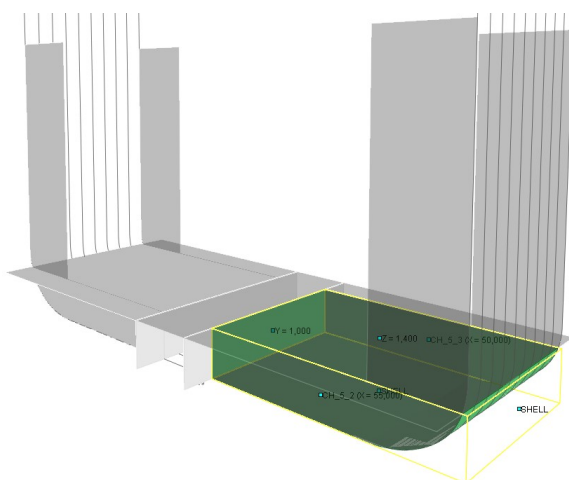


Figure 4.5: Correctly defined tank

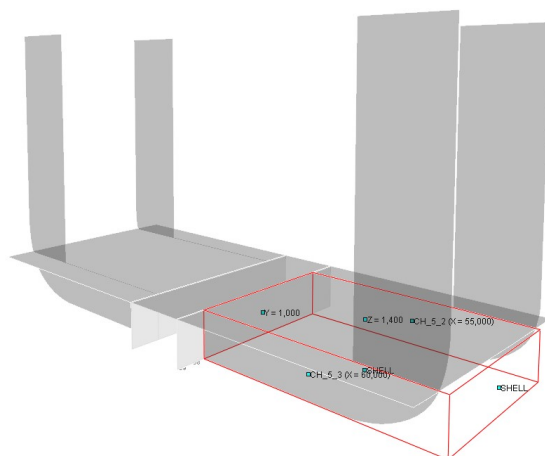


Figure 4.6: Incorrectly defined tank due to overtaking BH

Different solutions have been investigated for countering this pitfall. For example, when one bulkhead "overtakes" the other, the position values they acquire are switched. Another solution is when the forward bulkhead is "overtaken" it is placed at a small fixed distance in front of the aft bulkhead. These solutions may work for the parametric model. However, this change in position is then not relayed to the algorithm. The algorithm then receives the attained index for a different design than the design corresponding to the infill points it believes the results are from. Also from a parametric point of view, these solutions are not the most desirable solution. Eventually, the best method proved to be the subdivision of the variables into three categories.

The first category are the independent variables, the location of these variables is fully dependent on the value returned from the SACOBRA optimiser in its respective lower and upper boundary. The second type of variables are the dependent variables. These have a fixed distance from their assigned variables, which can be any type of variable. The last type of variables are the semi-dependent variables. Their position is determined by a fixed distance from another variable, after which a delta returned from the SACOBRA algorithm is added to this fixed distance. This results in the ability of tanks to have the same position relative to a certain bulkhead while still being able to vary their shape and size.

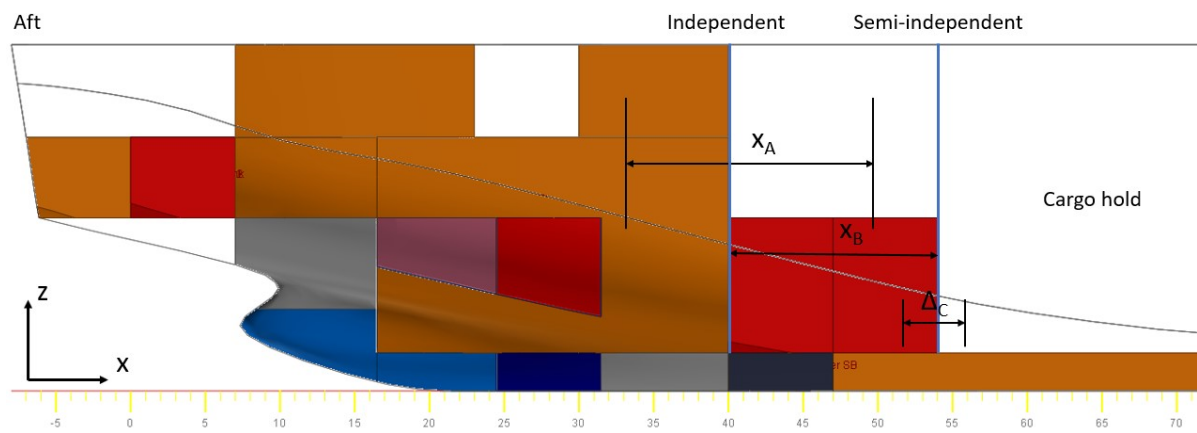


Figure 4.7: Illustration of the types of variables

Distance "A" in figure 4.7 is the independent variance of the aft cargo hold bulkhead. "B" indicates the fixed distance of the forward bulkhead of the FO tanks. This means that when the aft cargo hold bulkhead shifts forward, the FO tanks also shift forward with the same distance. Next, the FO tank bulkhead is reshaped as is indicated by distance "C". Fully dependent bulkheads do not have a distance "C", their location only relies of their coupled independent bulkhead and a fixed distance ("B"). In the form of an equation it looks like the following:

$$x_{semi-dependent} = x_A + x_B + \Delta_C \quad (4.1)$$

Where:

- $x_{semi-dependent}$ = Distance of the semi-dependent bulkhead from the origin;
- x_A = Distance of the independent bulkhead from the origin;
- x_B = Fixed distance from the independent bulkhead;
- Δ_C = Independent component of the semi-dependent bulkhead.

Direction is added to the variables by means of a vector, resulting in the following definition:

$$\mathbf{v}' = x_{semi-dependent} \cdot \begin{bmatrix} v_x \\ v_y \\ v_z \end{bmatrix} \quad (4.2)$$

By subdividing the ship in three sections and only optimising the middle section, problems in later stages of the design process may arise regarding stiffness for example. A result is that the position

of the inside of the double hull, the height of the tween deck and tank top do not connect to the same planes in the aft and forward section of the design anymore. A possibility is to take make an exception for these parameters in the other two sections, and make them connect at all times. However, this greatly influences the behaviour of the variables in the middle section where this research focuses on. The decision is made to keep these variables out of this optimisation and sensitivity analysis, but to remind the designer that this is something to keep in mind when interpreting the results from this research.

4.1.4. Other Parametric Measures

The permeability of tanks and spaces also influences the attained index as is indicated in table 2.6. Special attention is given to the behaviour of tanks and spaces with a different permeability. This parameter is however not used as a variable for every optimisation and sensitivity analysis in this research. However, the influence of changing the permeability of a tank can lead to some interesting new findings. Therefore, a small case study will be done to indicate the change in behaviour of the model when the permeability of a tank or space is changed. It should also be noted that according to a study by Cardinale et al. [86], the permeability values applied to tanks intended for liquids in cruise ships result in a very conservative approach in Attained index calculation. Although not the same, this could potentially have the same influence on the attained index for single large hold ships.

To increase the speed of the PDS calculation, the DELFTship calculation can be set on maximum processor (CPU) utilisation. For testing, the speed is increased by not taking into account the lesser vertical extents of the damages, reducing the time of the calculation by over five times. For some testing purposes it is also possible to only calculate the damages for one draught instead of three, significantly reducing the time even further. For the final optimisation, the full calculation needs to be executed, taking approximately 10 minutes per iteration.

4.2. Set up of the First Stage

The first stage, also referred to as the design stage, aims to determine the most optimum amount of bulkheads required. All bulkheads from the water ballast tanks are removed to create a new base ship that allows the first stage of the optimisation to determine the number of bulkheads required. The new base ship can be seen in figure 4.8 below.

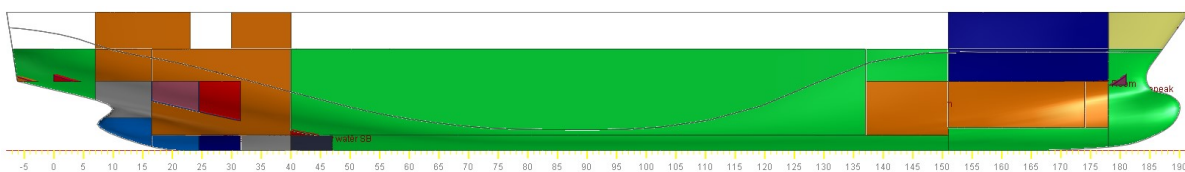


Figure 4.8: New base ship without any of the water ballast bulkheads

In figure 4.9 a flowchart of the first stage and second stage can be seen. The first stage consists of five steps that are repeated until the attained index converges. It is up to the designer to determine whether the increase in attained index does not outweigh the addition of weight by adding another bulkhead anymore.

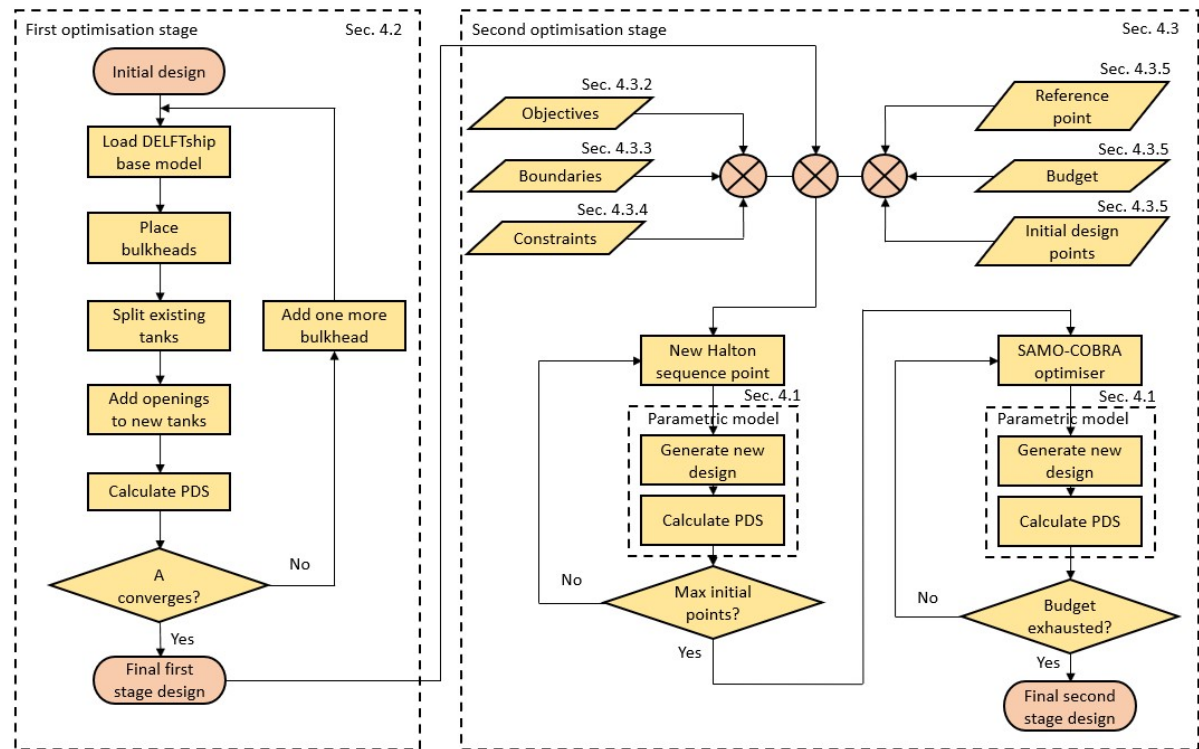


Figure 4.9: Flowchart of the bi-level multi-objective optimisation

The new base ship model is loaded into the DELFTship program, after which a bulkhead is added and the respective tank is split into two new tanks. Openings are added to the new tanks and the new attained index is calculated by the DELFTship program. Next, the same procedure is done but now two bulkheads are added, split evenly over the length of the mid ship section. This procedure is repeated for more and more bulkheads until a convergence threshold is satisfied. To add multiple bulkheads to the model, first a single bulkhead is added and the tank is split, then another bulkhead is added to the newly formed tank which is then split again. This is repeated until enough bulkheads are added. Equation 4.3 is used to add a certain amount of bulkheads split evenly over the length of the midship:

$$x_{BH,j} = \frac{x_{BH\ PR} - x_{BH\ CH\ Aft}}{1 + i} \times (i - j) + x_{CH\ Aft} \quad (4.3)$$

Where i is the total number of bulkheads and j is the current bulkhead that is added to the midship section. Also the location of the pumproom bulkhead and aft cargo hold bulkhead is used. After the total number of bulkheads is determined, the final design of the first stage is used as the base ship of the second optimisation stage, the SA(MO)-COBRA optimiser.

4.3. Setup of the Second Stage

The second stage is the optimisation stage. The amount of bulkheads required are listed and applied to the base ship model, which is then used as input for the optimisation methods. The output of the optimisation method is used as the input for the parametric model and vice versa, as can be seen in figure 4.9. The new infill points generated by the optimiser is used to compute the attained index from the DELFTship program, after which the optimiser uses the attained index to understand the behaviour of the model regarding the damage stability. The algorithm is running either locally or via Amazon Web Services (AWS). Whereby the latter is using a call to provide the algorithm its initial settings and the optimisation problem definition, returning the to be optimised infill points. The optimiser and DELFTship communicate by reading from and writing to a text file their input and output respectively. In this chapter, the setup of the optimisation model is further explained by looking at the optimisation problem definition and initial design parameters of the algorithm.

4.3.1. Objective Function Single-Objective Optimiser (SACOBRA)

The objective function is a single scalar value formulated from a set of design responses and is used to define the objective of the optimisation [87]. These design responses are the variables used in the optimisation, which eventually converge to a combination that both maximises the objective function and satisfies the constraints, resulting in an effective and feasible design.

When the objective function and/or the set of constraints are unknown, unexploitable, or even non-existent, the optimisation becomes what is known as a blackbox optimisation (BBO) [88]. In this case, the objective function is the result of the damage stability calculation. The calculation as described in chapter 2 is applied to all damage cases. The scale of this calculation and damage cases requires a computer simulation to determine the eventual outcome. Therefore, this optimisation is regarded to as a BBO.

The SACOBRA algorithm is only capable of minimizing the defined objective function. Hence, the objective function is transformed without the loss of generality as follows:

$$\max(f(x)) = \min(-f(x)) \quad (4.4)$$

To maximise the attained index, one can simply take the following as a BBO objective function:

$$f(x) = -A \quad (4.5)$$

This approach is used in this research to study the behaviour of the damage stability. However, this research is also applicable to real world problems. Real world problems are also subjected to real world goals. In this case, multiple real world goals are required to ensure an efficient design. The cargo hold volume is one of those goals that is part of the initial design considerations. If the attained index is far above the required index, chances are the designer did not capitalize on a significant margin of cargo carrying capacity. This makes the design less profitable from the perspective of the owner/operator of the ship. To optimise for a model where the attained index is higher than the required index, but lower than a certain value that is based on how much margin the designer wants to have, the objective function takes the following form:

$$f(x) = |R \times (1 + \frac{\mu}{100}) - A| \quad (4.6)$$

Where μ is the safety margin as a percentage of the total required index R:

$$R = 1 - \frac{128}{L_s + 152} \quad (2.3 \text{ revisited})$$

Where the subdivision length L_s is 109.763 according to the DELFTship program. This results in a required index of $R = 0.51101$. In addition an inequality constraint is added that ensures the attained index A is never smaller than the required index R. This is elaborated further in chapter 4.3.4.

4.3.2. Objective Function Multi-Objective Optimiser (SAMO-COBRA)

The multi-objective optimiser uses two objectives, namely the attained index A and the volume of the cargo hold. The latter objective is specifically interesting for this type of ship with regards to the PDS, as well as the cargo carrying capacity. The objective function shown in equation 4.6 combined with constraining the fuel oil tank and pumproom in their maximum volume, indeed resulted in the maximisation of the cargo hold, while maintaining the attained index within a reasonable margin of the required index. The problem with this approach to optimising is that it resulted in exceptionally few feasible solutions, which in turn resulted in less confidence in the solutions being the actual most optimum. In figure 4.10, the number of designs containing a certain number of constraint violations is given. This is the result of 150 iterations including the constrained attained index.

This approach also looks very much like a multi-objective optimisation. Therefore, the decision was made to involve a multi-objective optimiser. The results of the single objective optimiser are still used for explaining certain decisions by the algorithm, as these explain the choices made by the algorithm regarding maximising the attained index and give more insight in the PDS.

The objective functions then become:

$$\begin{aligned} f_1(x) &= -A \\ f_2(x) &= -Vol. \text{ cargo hold} \end{aligned} \quad (4.7)$$

This resulted in an increase in feasible solutions as can be seen in figure 4.10 below, where also 150 iterations were performed. "A" shows the constraint violations for the single objective with a constrained A-index. "B" shows the multi-objective option. The amount of feasible solutions increased from approximately 9% for option "A" to more than 35 % for option B.

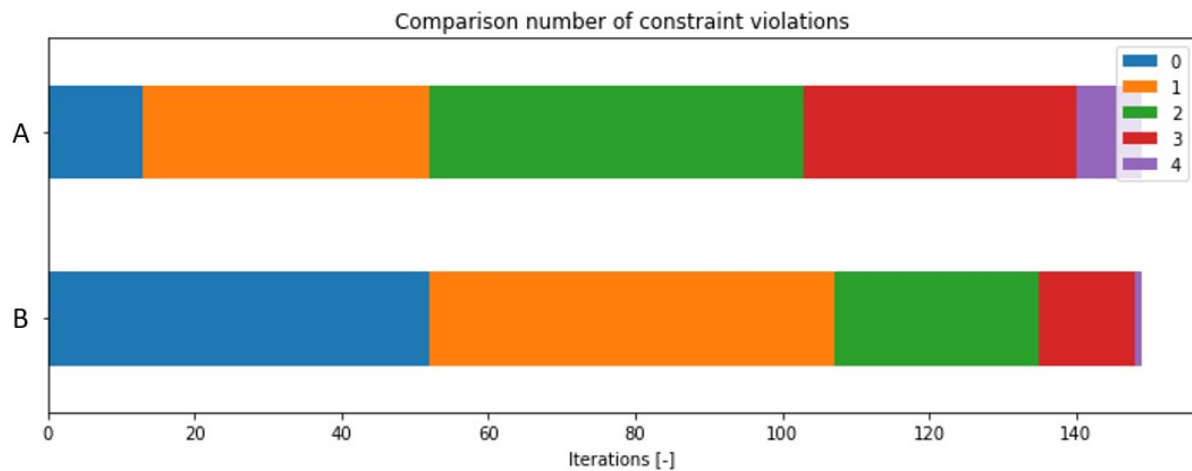


Figure 4.10: Number of constraint violations per option.

4.3.3. Variables

The variables used for this research are all located in the middle section as explained in chapter 4.1.1. The variables and their respective boundaries determine the parameter space the optimisation method can explore. It is therefore important to give special attention to these two properties. In a paper by Bagheri et al. regarding the SACOBRA algorithm, it is stated that:

"Radial basis function (RBF) models are very fast to train, even for high dimensional search spaces. They often provide good approximation accuracy, even when only few training points are given. This makes them ideally suited as surrogate-models for high-dimensional optimisation problems with a large number of constraints" [72].

The notion of "high-dimensional" and a "large number of constraints" is relative of course and depends on the complexity of the model behaviour. In the case of the damage stability optimisation for ships, 10-20 parameters can be considered high dimensional as the behaviour of the model is relatively complex.

As described in chapter 4.1, the variables are subdivided in three categories. The independent and semi-independent variables are applicable to the optimisation. The dependent variables are only applicable to the parametrisation part of this research. These variables do influence the attained index, but they are not used in the setup of the algorithm. For the former two variables, the lower and upper boundaries are inserted in the algorithm. This defines the initial size of the parameter space given a certain amount of variables. Tight boundaries mean a relatively small parameter space, this could potentially result in not finding the optimum design as this is located outside of the boundaries. However, a large parameter space can result in a relatively high percentage of unfeasible solutions. If, during the optimisation a boundary converges to its limit, the decision can be made to increase the limit, provided the increase can be justified within the naval architectural considerations.

The amount of variables can be determined based on the goal of the designer and the time available. The optimisation method can be used to compare a small number of variables, based on certain design choices that are applicable at that moment. This research aims to optimise the entire middle section of the design by varying as many variables as reasonably possible. The combination of a well parameterised model and a cost-efficient optimisation method is used to create an efficient method for understanding and optimising the entire parameter space. Hence, the base ship model would have 16 variables to be subjected to optimisation. 15 parameters comprise the transverse/longitudinal bulkheads and decks and one parameter is used for the height of the openings with respect to the main deck, next to the cargo hold coaming. The openings only vary in vertical direction with every opening between the aft cargo hold bulkhead to the forward cargo hold bulkhead, taking on the same height.

This greatly reduces the amount of variables needed, while still creating some understanding of the influence by the location of these openings. The actual number of parameters that is subjected to optimisation ranges between 12 and 20, depending on the results from the first stage of the optimisation. This only influences the number of bulkheads located in the water ballast tanks. All other parameters remain the same as those of the base ship model.

Table 4.1: Boundaries of all independent variables used for optimisation of the middle section with two bulkheads added, where WF is the web frame distance of 0.55m

	CH Aft	CH Fwd	Tanktop	Double hull	Main deck	Pipe tunnel
LB [m]	$WF \cdot 32$	$WF \cdot 145$	0.84	6.00	11.00	0.50
UB [m]	$WF \cdot 42$	$WF \cdot 160$	2.00	8.00	12.50	2.00

The boundaries of the cargo hold bulkheads are determined by how far aft and forward the cargo hold can extend before it reaches other tanks or compartments. The double hull, main deck and pipe tunnel boundaries are determined empirically by running multiple test optimisations. In figures 4.11 and 4.12, two examples are given of a variable with too stringent boundaries and a variable with the optimum well within the lower and upper boundaries respectively. After the initial design points (48 in this case), the variables either converge straight to its upper boundary or is able to find the most optimum position, the latter being the most desirable.

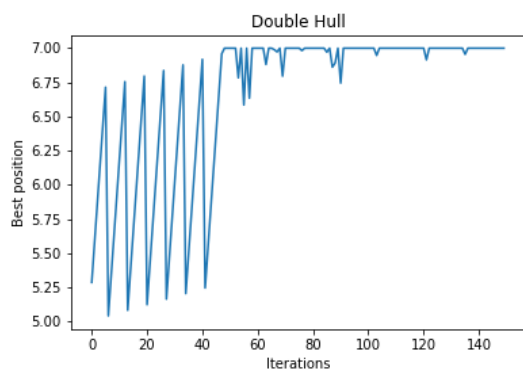


Figure 4.11: Variable reaching its upper boundary

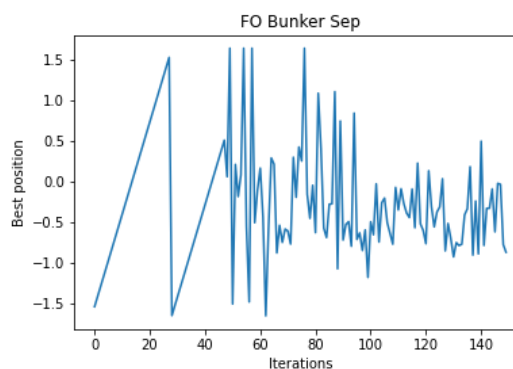


Figure 4.12: Variable well within its boundaries

The minimum height of the tanktop is defined by SOLAS part II-1 Part B-2 Regulation 9 [89] as follows:

$$h = \frac{B}{20} \quad (4.8)$$

Where h is the resulting minimum height of the tanktop and B is the moulded breadth. The regulations also states that the value of h is in no case to be less than 760 mm, and not to be taken as more than 2,000 mm. The resulting minimum height, based on the breadth given in table 3.1, is 840 mm.

Table 4.2: Input data for all semi dependent variables, where WF is the web frame distance of 0.55m

	FO Mid	FO Fwd	Pumproom	FO Height	Pumproom height	Openings
Coupled to	CH Aft	CH Aft	CH Fwd	Tanktop	Tanktop	Main deck
Fixed distance [m]	$WF \cdot 7$	$WF \cdot 14$	$-WF \cdot 14$	4.95	4.95	4.95
LB [m]	$-WF \cdot 3$	$-WF \cdot 3$	$-WF \cdot 7$	-3.00	-3.00	0.00
UB [m]	$WF \cdot 3$	$WF \cdot 3$	$WF \cdot 7$	3.00	3.50	3.00

Using equation 4.2, the following the standard variables to be evaluated can be written as follows and is used in the actual parametric model to update geometry of the design:

$$\mathbf{v}' = \mathbf{x} \cdot \mathbf{v} = \left\{ \begin{array}{l} \left[\begin{array}{c} x_{CH\ Aft} \\ x_{CH\ Fwd} \\ x_{CH\ Aft} + WF \cdot 7 + x_{FO\ Sep} \\ x_{CH\ Aft} + WF \cdot 14 + x_{FO\ Fwd} \\ x_{CH\ Fwd} - WF \cdot 14 - x_{Pump\ room} \end{array} \right] \cdot \begin{bmatrix} 1 \\ 0 \\ 0 \end{bmatrix} \\ \left[\begin{array}{c} x_{Double\ hull} \\ x_{Pipe\ tunnel} \end{array} \right] \cdot \begin{bmatrix} 0 \\ 1 \\ 0 \end{bmatrix} \\ \left[\begin{array}{c} x_{tank\ top} \\ x_{Main\ deck} \\ x_{Tank\ top} + 4.95 + x_{FO\ height} \\ x_{Tank\ top} + 4.95 + x_{Pump\ room\ height} \\ x_{Tank\ top} + 4.95 + x_{Openings} \end{array} \right] \cdot \begin{bmatrix} 0 \\ 0 \\ 1 \end{bmatrix} \end{array} \right. \quad (4.9)$$

This does not include the extra water ballast bulkheads that will be added as a result from the first optimisation stage described in chapter 4.2. These will be added to the top vector as independent variables.

4.3.4. Constraint Handling

The optimisation model uses a number of constraints to prevent certain variables from diverging and to ensure the model remains efficient. The COBRA algorithm has difficulty with handling equality constraints [72]. Therefore, any equality constraints need to be transformed into two inequality constraints. This can be done the as follows without the loss of generality:

$$\begin{array}{ll} \text{Equality constraint} & g(\vec{x}) = 0 \\ \text{Inequality constraints} & \begin{cases} h(\vec{x}) - \mu \leq 0 \\ -h(\vec{x}) - \mu \leq 0 \end{cases} \end{array} \quad (4.10)$$

The COBRA algorithm considers all constraints as being equally important. This ensures a constraint violation by for example the cargo hold is not more important than the fuel tank, just because the constraint violation is larger in an absolute sense. This is reached by scaling every constraint output as follows:

$$c' = \frac{c}{\max(c) - \min(c)} \quad (4.11)$$

Where:

- c' = Normalised constraint violation factor;
- c = Constraint output;
- $\max(c)$ = Maximum constraint violation encountered so far;
- $\min(c)$ = Minimum constraint violation encountered so far.

Different constraint handling techniques are used for the different objective functions used. For instance, in the case of the single objective optimisation, whereby the attained index is maximised, the following constraints are used:

$$\begin{aligned}
\text{Objective : } f(x) &= -A \\
\text{Constraints : } h_1 &= V_{cargo\ min} - V_{cargo\ actual} \\
h_2 &= V_{FO\ aft\ min} - V_{FO\ aft\ actual} \\
h_3 &= V_{FO\ fwd\ min} - V_{FO\ fwd\ actual} \\
h_4 &= V_{pumproom\ min} - V_{pumproom\ actual}
\end{aligned} \tag{4.12}$$

This ensures the minimum volume of the compartments, preventing infeasible solutions as a result of infeasible compartment sizes. The total volume of the ballast tanks in the middle section is not taken into account, as this would severely limit the optimisation freedom of the algorithm. This can however be implemented if the designer deems this necessary.

For constraining the single objective, as is done in the case of equation 4.6, the following constraints are used:

$$\begin{aligned}
\text{Objective : } f(x) &= |R \times (1 + \frac{\mu}{100}) - A| \\
\text{Constraints : } h_1 &= V_{cargo\ min} - V_{cargo\ actual} \\
h_2 &= V_{FO\ aft\ min} - V_{FO\ aft\ actual} \\
h_3 &= V_{FO\ aft\ actual} - V_{FO\ aft\ max} \\
h_4 &= V_{FO\ fwd\ min} - V_{FO\ fwd\ actual} \\
h_5 &= V_{FO\ fwd\ actual} - V_{FO\ fwd\ max} \\
h_6 &= V_{pumproom\ min} - V_{pumproom\ actual} \\
h_7 &= V_{pumproom\ actual} - V_{pumproom\ max} \\
h_8 &= R - A
\end{aligned} \tag{4.13}$$

For this method, the FO tanks and pumproom are constrained also in an upper value. Combined with the objective function that does not result in the highest attained index possible, but rather as close to the required index plus some margin, the cargo hold is expanded as much as possible, in order to lower the attained index towards the right value. The minimum value of A is now constrained as well to ensure the required index is always satisfied. This method is however not deemed viable, as this results in very few feasible solutions due to the three equality constrain like boundaries for the tank volumes and the small margin for the attained index. It is decided that another method should be chosen in order to reach the goals of this research. The decision is made to use multiple objectives instead of constraints to ensure the efficiency of the design. The problem definition then becomes the following:

$$\begin{aligned}
\text{Objectives : } f_1(x) &= -A \\
f_2(x) &= -V_{cargo} \\
\text{Constraints : } h_1 &= V_{FO\ aft\ min} - V_{FO\ aft\ actual} \\
h_2 &= V_{FO\ fwd\ min} - V_{FO\ fwd\ actual} \\
h_3 &= V_{pumproom\ min} - V_{pumproom\ actual} \\
h_4 &= R - A
\end{aligned} \tag{4.14}$$

Here, the basic constraints for the minimum tank volumes can be used again resulting in more feasible solutions. The constraint for satisfying the required index is still used, as otherwise the resulting Pareto front would also show designs that do not satisfy this requirement.

4.3.5. Initial Optimisation Parameters

Both algorithms consist of an initial phase. Where, after defining the optimisation problem, the characteristics of the algorithm can be set. These characteristics, or arguments, influence both the sampling method that is used for exploring the parameter space prior to optimising and the behaviour of the algorithm during optimisation.

The first stage of the algorithm is "learning" the behaviour of the to be optimised model. This creates the initial design for the surrogate model. By using a sampling method, the algorithm aims to explore the entire parameter space as efficient as possible. The COBRA framework allows the user to decide which initialisation approach is most suitable for their respective optimisation problem. In this case, a Halton sequence is used as the initialisation approach. This is the default method offered by the algorithm which is proven by Bossek et al. to be an effective sampling method for sampling with an as small as possible initial sample [90]. The Halton sequence is a generalised low-discrepancy quasi-random sampling method, that is based on the van der Corput sequences for 1D distributions [91].

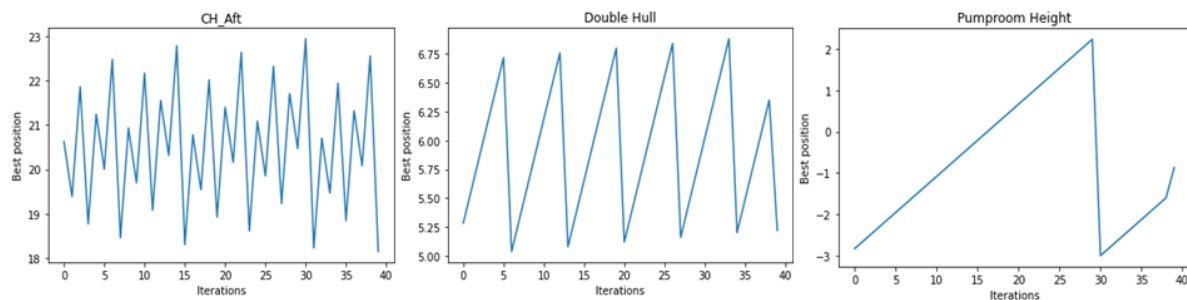


Figure 4.13: Halton sequence applied to the first, middle and last variable respectively

An initial set of sampling points of $3 \cdot d$ where d is the number of dimensions is recommended and used for testing the algorithm on a set of benchmark problems in a paper by Bagheri et al. [72]. Another method is to find a balance between the amount of initial design points and the convergence rate. When using relatively few initial design points, the convergence rate becomes relatively low. A balance can be found that minimises the total time to converge, including the initial stage of the algorithm. It should be noted that this is only done to reduce the calculation time, as it could potentially decrease the confidence in the quality of the results, when the amount of initial design points becomes relatively low.

The COBRA optimiser uses the COBYLA optimiser as a local optimiser for phases I and II of the optimisation stage. Whereby phase I is used to find a feasible solution by searching new infill points and phase II improves the feasible solution with the help of the RBF surrogate model. COBYLA uses a number of starting points and a maximum number of iterations for the surrogate model. To increase the chance of finding the global optimum, the number of starting points should be increased. By increasing the maximum number of iterations, the chance is increased of finding an optimum for every starting point used. By increasing these two parameters, the calculation time of the algorithm increases as well. As the calculation time for finding the attained index is relatively high, the time required for finding new infill points is therefore not considered as very critical. When the algorithm can not find a new set of infill points where at least one of the constraints is satisfied, an error is returned and the least infeasible solution is chosen for that particular iteration.

In order to compute a Pareto front, the algorithm needs a reference point from where the hypervolume can be calculated. This reference point consists of the lowest objective scores possible for both objective functions. For the attained index, this is zero, meaning no damage cases add anything to the attained index. For the cargo hold volume, this is 4126.85 m³ which is the lowest volume taking into account the boundaries of the variables defined in chapter 4.3.3.

4.4. Setup of the Global Sensitivity Analysis

The Morris method is used for performing the sensitivity analysis, as explained in chapter 3.6.3. Python offers an open source library that contains common sensitivity analysis routines such as the Morris method, which was published in the Journal of Open Source Software called SALib (Sensitivity Analysis Library in Python) [92]. Performing a Morris method consists of the following steps:

- Step 1 : Defining the variables with their respective lower and upper bounds;
- Step 2 : Generate parameter sets;
- Step 3 : Run the parameter sets through the model;
- Step 4 : Calculate the Morris indices;
- Step 5 : Interpret the results.

The flowchart in figure 4.14 shows the steps mentioned above to give a more complete overview of the set-up of the sensitivity analysis.

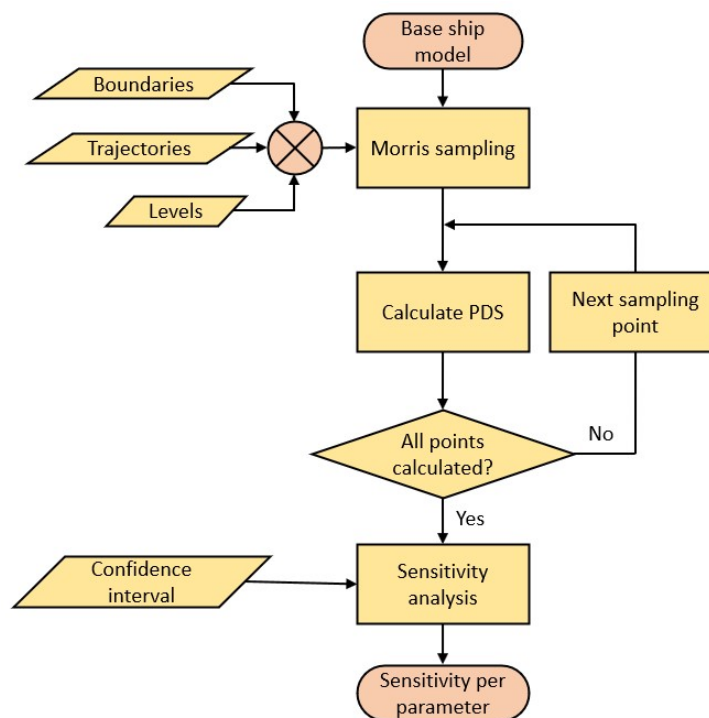


Figure 4.14: Flowchart of the Morris method set-up

Both the variables and their respective lower and upper bounds are the same as used for the input of the optimisation method. This ensures that the results from the sensitivity analysis can be applied to the optimised model. Other options are to use a different set of bounds or more or less parameters if that is deemed desirable. This way, the designer can focus on specific parts of the ship, to create a better understanding of the design freedom within that part.

The number of trajectories (succession of points in which two consecutive elements only differ for one parameter, starting from a random base vector) the Morris method uses is defined by N . The total number of function evaluations is $N(p+1)$, where p is the dimension of the parameter space (16 for this case study). As described in chapter 3.6.3, the Morris method uses few function evaluations compared to other sensitivity analysis methods. Typically, the elementary effects method such as the Morris method uses 10 to 50 trajectories in the input space [93]. Approximately 50 to 60 trajectories are needed according to a paper by Campolongo [94] and a paper by Herman et al. [95], that compares the results of both the Sobol and Morris methods for different sample (trajectory) values, shows that there is little benefit from using a sample size greater than $N=20$. A study was performed that looked at the number of trajectories between 20 and 100 with an interval of 20 for 14 parameters. If less than

10% of the sensitivity index value for the most sensitive parameter is represented for a confidence interval of 95%, convergence was considered acceptable. As this case study uses only two more parameters, a similar strategy is used to determine the right number of trajectories for this research. Three separate model runs are performed with 20, 60 and 100 trajectories respectively with the same confidence interval (95% is also the default value offered by SALib). Which can also be presented as follows:

$$10 > \frac{100 \times \mu_{conf}^*}{\mu} \quad (4.15)$$

Each variable range is broken up into a grid by the Morris sampling method. The default discrete number of values each variable can take on between the lower and upper bound is four and should always be even. These levels correspond to the quantiles of the factor distribution. For four levels, the 12.5th, 37.5th, 62.5th and 87.5th quantiles are taken [96]. It is demonstrated that the choice for the number of grid levels of four has produced valueable results [93, 97, 98] and is therefore also used for this case study.

The resulting parameter sets for the trajectory values of 20, 60 and 100, resulting in 320, 1020 and 1600 sets respectively, are then fit for being run through the parametric model. The same model as was used for the optimisation is used for generating the required output. The only difference being the input and output file handling to fit them into the Morris method. To calculate the Morris indices, the parameter file, the output file and the number of objectives is required. For the optimisation, a multi-objective approach was used, which included the volume of the cargo hold. This objective is not interesting for the sensitivity analysis, as it is trivial what parameters influence it the most, namely the parameters that represent the main dimensions of the cargo hold. The Morris indices are calculated, again in Python, using the SALib package.

Finally, the mean and variance of each parameter's elementary effects, given by μ and σ respectively, can be interpreted. The mean of the absolute values of the elementary effects is given by μ^* and is the best approximation of the "total" sensitivity [92].

Analysis and Discussion

The results from the two optimisation stages and the sensitivity analyses used in this research are combined to create an overview of the behaviour of the PDS calculation with respect to the subdivision of the ship, and to show the results and usability of the design, resulting from the multi-objective optimisation. This chapter aims to answer the following two sub questions, *To what extent is it possible to provide a preliminary design by the use of an optimisation algorithm?* and *What set of parameters has the most influence on the attained index?* The results, analysis and discussion are combined into one chapter. The first optimisation stage is used to establish the amount of bulkheads that is required for the water ballast tanks in both the side shell as well as the double bottom, over the entire length of the cargo hold. Then, the resulting design will be used as a starting point for both the multi- and single-objective optimisation. The multi-objective optimisation will result in the most optimum design to be used for further design and the single-objective optimisation will be used to run certain experiments to show the result of different design choices. After this, the new design will be subjected to three different sensitivity analysis methods, two of which were added later due to insufficient results from the Morris method.

5.1. Results From the First Optimisation Stage

The results from the first optimisation stage are presented in this chapter and later used as the base for the second stage. Figure 5.1 shows the convergence of the attained index when bulkheads are added as described in chapter 4.2.

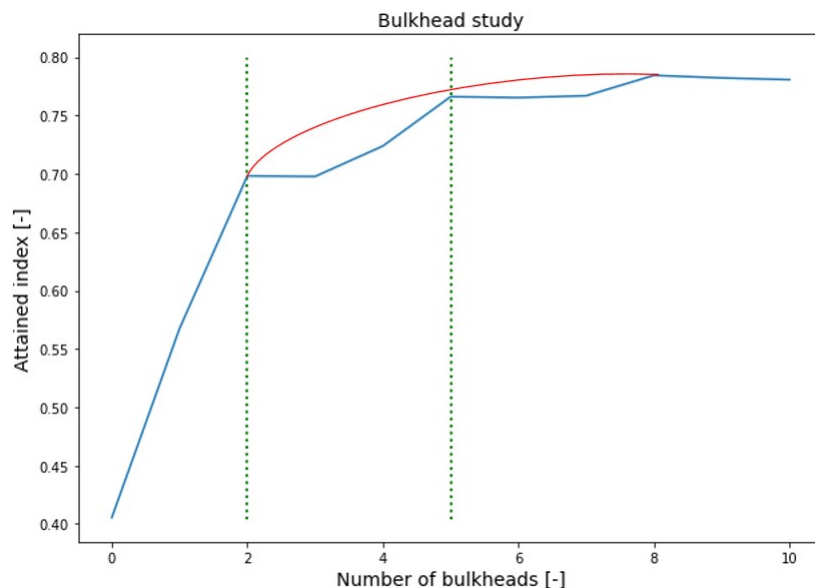


Figure 5.1: Results from the first optimisation stage

Only the attained index is taken into account in the first stage of the optimisation and gives the designer the ability to determine the amount of bulkheads that should be used to further optimise the design. The graph shows that the total attained index does not change significantly after five bulkheads. However, after two bulkheads, the steep increase in attained index halts and continues with a lower slope up till five bulkheads. Here, the increase in attained index between zero and two bulkheads and two and five bulkheads decreases by six times. As explained in chapter 4.2, the distance between the bulkhead is equally divided over the length of the cargo hold. However, it is never established that this is a good division, concerning the damage stability. As every attained index is composed of three service draughts, chances are that the changes in attained indices for the different draughts cancel each other out, therefore resulting in an equal total attained index between two different numbers of bulkheads. In table 5.1, the attained indices for both two and three and five and six bulkheads are compared.

Table 5.1: Comparison between two pairs of designs, comparing the partial attained indices

# BH	2	3	Δ	5	6	Δ
A_l	0.80425	0.83157	0.02732	0.91590	0.91232	-0.00358
A_p	0.79893	0.77245	-0.02645	0.87292	0.85717	-0.01575
A_s	0.54442	0.55601	0.01159	0.58609	0.59990	0.01381
A_{tot}	0.69819	0.69770	-0.00049	0.76678	0.76529	-0.00149

It can be seen that for two bulkheads, the partial subdivision draught is decreased after adding another bulkhead. For five bulkheads, both the light and partial subdivision draught decrease for the same procedure. The origin of this inconsistency can be found in the s_i factor (SFAC) diagrams, which result from the PDS calculation. The diagram is shown in figures 5.2 and 5.3 below for two and three water ballast bulkheads. Due to the increase in subdivision zones, more multi-zone damage area is covered in yellow, meaning it adds to the attained index. The forward side of the ship also shows more orange area instead of the previous red.

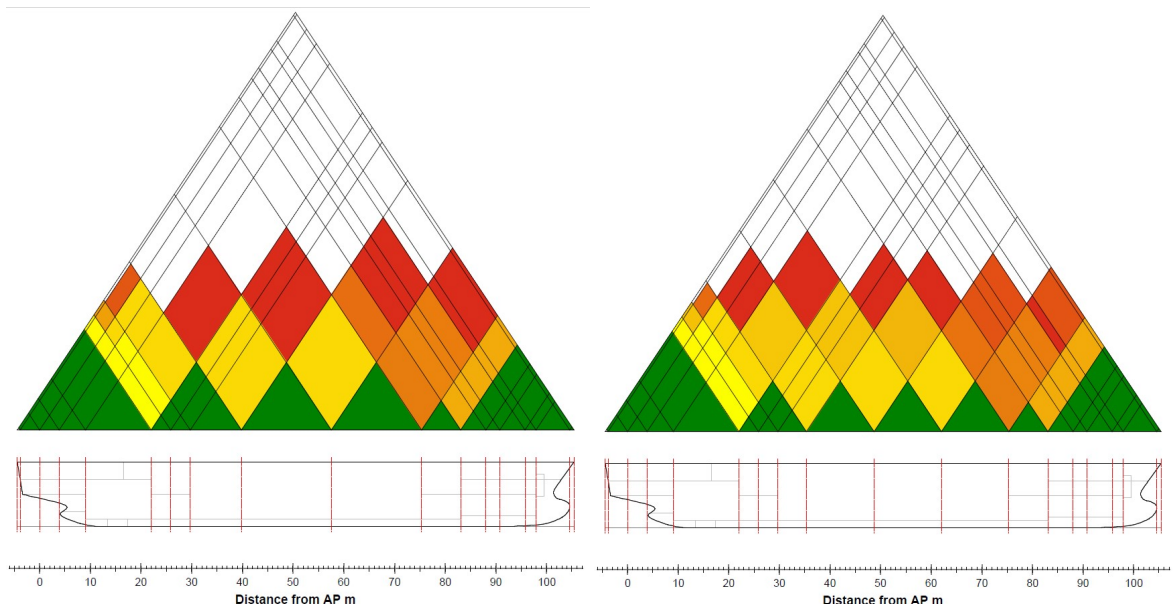


Figure 5.2: SFAC diagram for two bulkheads in partial service draught

Figure 5.3: SFAC diagram for three bulkheads in partial service draught

Diving deeper in the SFAC diagram, allows the designer to compare the attained index per pair of zones damaged. In table 5.2 below, the attained indices and survivability percentages are shown. The total attained index decreases for this particular draught as well as the total survivability percentage. However, the attained index only decreases for 1 damaged zone, while the survivability percentages

only decrease for 2,3,4 and 6 damaged zones. The fact that the single zone damage contribution per zone decreases, is due to their reduction in size. The less volume a zone has, the lower the contribution on the attained index for the same survivability as a larger zonal volume. This decrease in attained index should however, be compensated by the multi-zone damages that follow. This is clearly not the case, as the total attained index for three bulkheads remains below the index for two. This can also be seen in more detail in table 5.2 below.

Table 5.2: Comparison between two pairs of designs, comparing for the partial draught

#BH	2		3	
	Attained	Perc %	Attained	Perc%
1 damaged zone	0.39967	100.0	0.36367	100.0
2 damaged zones	0.23911	65.0	0.24269	63.0
3 damaged zones	0.10234	75.1	0.10486	70.9
4 damaged zones	0.04137	66.0	0.04184	64.5
5 damaged zones	0.01339	60.2	0.01616	61.1
6 damaged zones	0.00282	44.1	0.00285	40.4
7 damaged zones	0.00027	13.5	0.00037	18.8
8 damaged zones	0.00000	0.0	0.00000	9.3
Total	0.79897	80.1	0.77245	77.4

It can be assumed that if every experiment from figure 5.1 was to be optimised for the location of the bulkheads, the line would be closer to an exponential function (red line in figure 5.1), converging to an attained index just below 0.8. An experiment can be run that optimises the design for all every single number of bulkheads to provide the exact graph. The results obtained from this experiment, do not compensate for the time and effort it takes to run it. Therefore, for now, the red line is assumed to be representative for the shape of the optimised graph. Still, one could advocate for both two and five bulkheads at this stage. There are multiple reasons the designer could be interested in either of those numbers. A comparison is made in table 5.3 below:

Table 5.3: Comparison between two and five bulkheads in the ballast water tanks

	Advantages	Disadvantages
Two BH	<ul style="list-style-type: none"> • Low added weight • Lower construction costs • Less extensive ballast system 	<ul style="list-style-type: none"> • Less ballast freedom • Less Attained index • Lower stiffness
Five BH	<ul style="list-style-type: none"> • More Attained index • More ballast freedom • Higher stiffness 	<ul style="list-style-type: none"> • More added weight • Higher construction costs • More extensive ballast system

To determine whether two or five bulkheads is the most optimum amount in this case with respect to for instance, the steel weight and the distance of the GM, the method should be expanded to include the weight and/or centre of gravity of the bulkheads. For now, both the design with two bulkheads as well as five bulkheads are used for further optimisation in the second stage. The results from that stage will show the difference in design between these two numbers of bulkheads. The two designs used for further optimisation are shown in figures 5.4 and 5.5 with tables 5.4 and 5.5 showing their respective

variable boundaries. These extend the base ship variables shown in table 4.1.

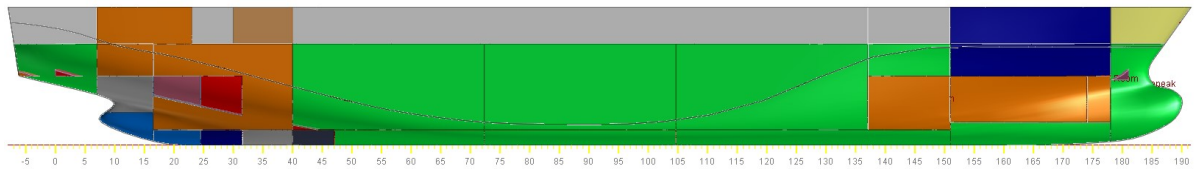


Figure 5.4: Resulting design for two bulkheads

Table 5.4: Boundaries of all variables used for optimisation of the middle section with two bulkheads added, where WF is the web frame distance of 0.55m

	CH Aft	CH Fwd	Tanktop	Double hull	Main deck	Pipe tunnel	WB1	WB2
LB [m]	$WF \cdot 32$	$WF \cdot 145$	0.84	6.00	11.00	0.50	$WF \cdot 50$	$WF \cdot 95$
UB [m]	$WF \cdot 42$	$WF \cdot 160$	2.00	8.00	12.50	2.00	$WF \cdot 85$	$WF \cdot 120$

Figure 4.2 can then be expanded in the x-direction to be defined as follows:

$$\mathbf{v}' = \mathbf{x} \cdot \mathbf{v} = \begin{bmatrix} x_{CH\ Aft} \\ x_{CH\ Fwd} \\ x_{WB1} \\ x_{WB2} \\ x_{CH\ Aft} + WF \cdot 7 + x_{FO\ sep} \\ x_{CH\ Aft} + WF \cdot 14 + x_{FO\ Fwd} \\ x_{CH\ Fwd} - WF \cdot 14 - x_{pumproom} \end{bmatrix} \cdot \begin{bmatrix} 1 \\ 0 \\ 0 \\ 0 \end{bmatrix} \quad (5.1)$$

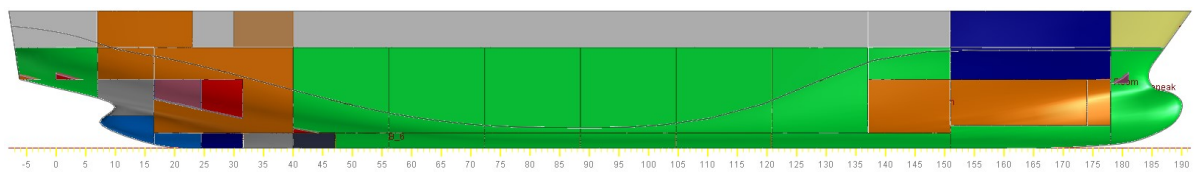


Figure 5.5: Resulting design for five bulkheads

Table 5.5: Boundaries of all variables used for optimisation of the middle section with five bulkheads added, where WF is the web frame distance of 0.55m

	CH Aft	CH Fwd	Tanktop	Double hull	Main deck	Pipe tunnel	WB1	WB2	WB3	WB4	WB5
LB [m]	$WF \cdot 32$	$WF \cdot 145$	0.84	6.00	11.00	0.50	$WF \cdot 44$	$WF \cdot 63$	$WF \cdot 77$	$WF \cdot 91$	$WF \cdot 105$
UB [m]	$WF \cdot 42$	$WF \cdot 160$	2.00	8.00	12.50	2.00	$WF \cdot 61$	$WF \cdot 75$	$WF \cdot 89$	$WF \cdot 103$	$WF \cdot 122$

The boundaries for the water ballast bulkheads are equally divided over the length of the cargo hold. Due to the relatively small boundary compared to the design with two bulkheads, it could potentially result in some boundaries reaching their limit. If that happens the boundaries can be adjusted and a new optimisation can be run. Figure 4.2 can then be expanded in the x-direction to be defined as follows:

$$\mathbf{v}' = \mathbf{x} \cdot \mathbf{v} = \begin{bmatrix} x_{CH\ Aft} \\ x_{CH\ Fwd} \\ x_{WB1} \\ x_{WB2} \\ x_{WB3} \\ x_{WB4} \\ x_{WB5} \\ x_{CH\ Aft} + WF \cdot 7 + x_{FO\ Sep} \\ x_{CH\ Aft} + WF \cdot 14 + x_{FO\ Fwd} \\ x_{CH\ Fwd} - WF \cdot 14 - x_{Pump\ room} \end{bmatrix} \cdot \begin{bmatrix} 1 \\ 0 \\ 0 \end{bmatrix} \quad (5.2)$$

Equations 5.1 and 5.2 can now be used in the parametric model to further optimise the base ship model in the second optimisation stage.

The first optimisation stage is a relatively simple automated procedure. To verify the results, the same procedure as explained in section 4.2, can simply be performed by hand. The bulkheads are added in DELFTship in the GUI as well as their position. The input of the PDS is checked and then run for every design, after which the results are compared with every point in figure 5.1. This showed the exact same results, proving that the automatic addition of bulkheads is correctly programmed and parameterised, and can be applied to other single hold designs as well.

As discussed in this section, due to the inability to really separate the two and five bulkhead design, both designs are used for further optimisation. These designs are defined in tables 5.4 and 5.5 and equations 5.1 and 5.2.

5.2. Results From the Second Optimisation Stage (SAMO-COBRA)

The second optimisation stage consists of the multi-objective optimisation. The results of the multi-objective optimiser that follow from the results of the first optimisation stage from section 5.1 are obtained by first determining the amount of function evaluations required. Then, the results are presented for both the two and five bulkhead designs respectively. The Pareto front for every design is given, as well as the behaviour of the parameters with respect to the attained index. The results are analysed to find a trend in the designs along the front and to verify the outcome of every optimisation.

5.2.1. Convergence

First, the amount of iterations required for this case study is determined. Convergence for a multi-objective optimiser like SAMO-COBRA is measured using the hypervolume progress [73]. The hypervolume is the area or volume between the Pareto front and the reference point as can be seen in figure 5.6. With each new feasible Pareto efficient point, the Pareto front changes and the hypervolume is slightly increased. The highest possible hypervolume value is the area or volume between the reference point and the optimal line.

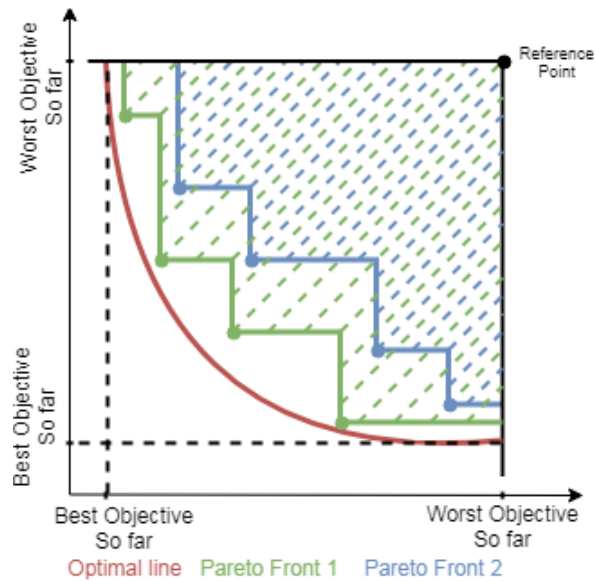


Figure 5.6: Schematic example of the hypervolume [99].

Convergence is reached when the hypervolume progression is decreased to a certain threshold and when the designer has enough confidence that the optimiser is not in a state of premature convergence. Therefore, the method of determining whether the optimiser has converged is a matter of first running an optimisation with many iterations, after which the appropriate amount of iterations for other similar models can be established. In figure 5.7 below, the hypervolume progress of a model with 400 iterations for the two bulkhead design is shown. It can be seen that after approximately 200 iterations the optimiser doesn't show a significant increase in hypervolume anymore, and it can be concluded that this is the appropriate amount of iterations for this model. 200 iterations amounts to approximately 1.5 days of running the model on a single core. If the model is started at the end of the day, this translates to only one full working day of waiting for the optimisation to finish. From an economical standpoint, this is considered reasonable. A side note is that during the optimisation, the DELFTship program cannot be used for other purposes. This can be solved by running multiple instances of the program on external cores, such as via cloud computing.

The hypervolume progress is also calculated for the five bulkhead design as it was found that the number of non-dominated designs reduced significantly for 200 iterations when comparing it to the two bulkhead design with the same amount of iterations. Figure 5.8 shows the hypervolume progress for this design. Even though a higher convergence value was expected, this hypervolume progress also converges after approximately 200 iterations.

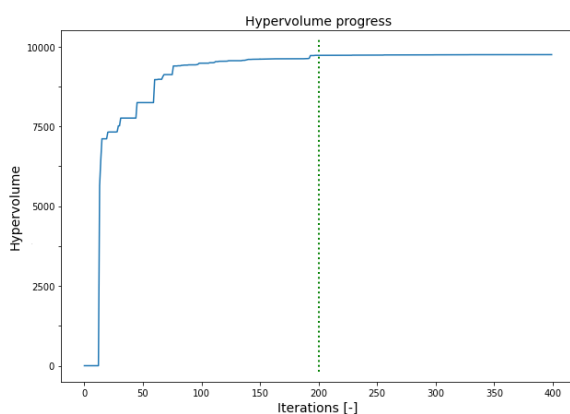


Figure 5.7: Hypervolume progress of the SAMO-COBRA optimiser for 400 iterations and two WB bulkheads

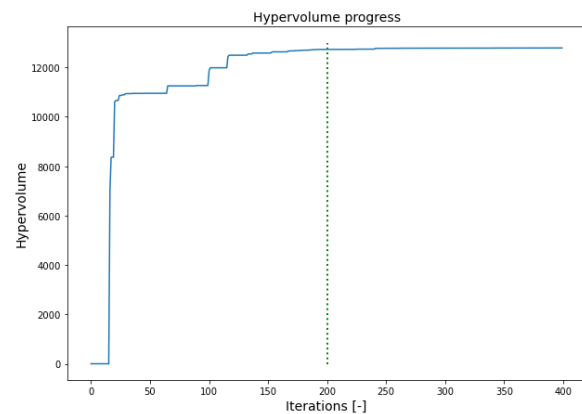


Figure 5.8: Hypervolume progress of the SAMO-COBRA optimiser for 400 iterations and five WB bulkheads

The scatter plot and corresponding Pareto front for the two bulkhead design are presented in figure 5.9 below:

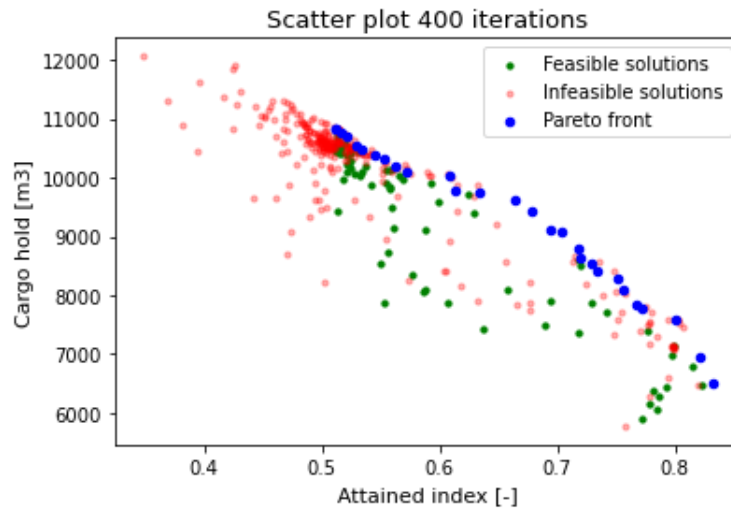


Figure 5.9: Scatter plot and Pareto front for 400 iterations and two WB BH.

Both the scatter plot and the Pareto front show a high concentration of feasible designs between an attained index of 0.5 and 0.6. Most of these points are added in the later stages of the optimisation. This means that the line in figure 5.7 does not actually converge, but keeps increasing all the way till the end. However, this increase in attained index and cargo hold volume is so marginal, that it doesn't way up against the increase in time it takes to obtain these improved designs. The scatter plot and corresponding Pareto front for the five bulkhead design are presented in figure 5.10 below:

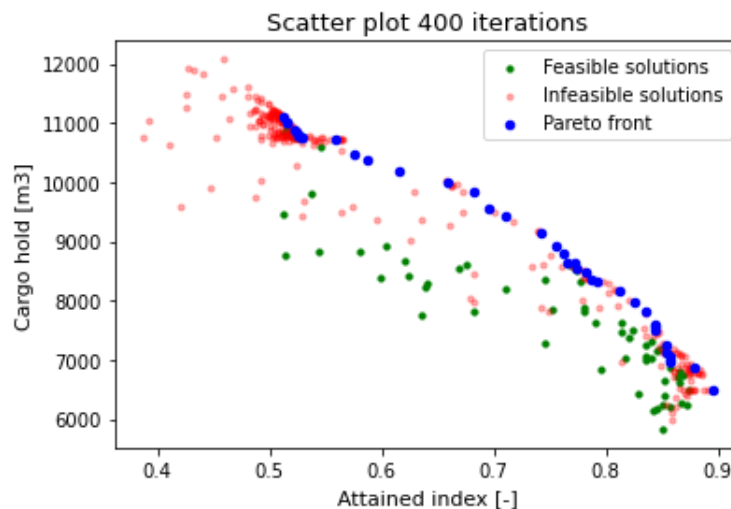


Figure 5.10: Scatter plot and Pareto front for 400 iterations and five WB BH.

The scatter plots for 400 iterations show the large amount of infeasible solutions (one or more constraint violations) compared to the feasible solutions (no constraint violations). This ratio is as was expected, as can be seen in figure 4.10 and is considered as . The hypervolume progress shows that both designs reach a state of convergence after approximately 200 iterations. Hence, for both designs 200 iterations will be used to determine the most optimum design.

5.2.2. Results For the First Design

Below, the resulting designs for two bulkheads are shown. 200 iterations were used as discussed in the beginning of this section. The design with the lowest attained index and the highest cargo hold volume is presented in figure 5.11 and the highest attained index and lowest cargo hold volume in figure 5.12. The particularities of the layout of both extremes are discussed below the figures. They are then discussed to understand the decisions by the algorithm and to prove that it is likely to be the optimum.

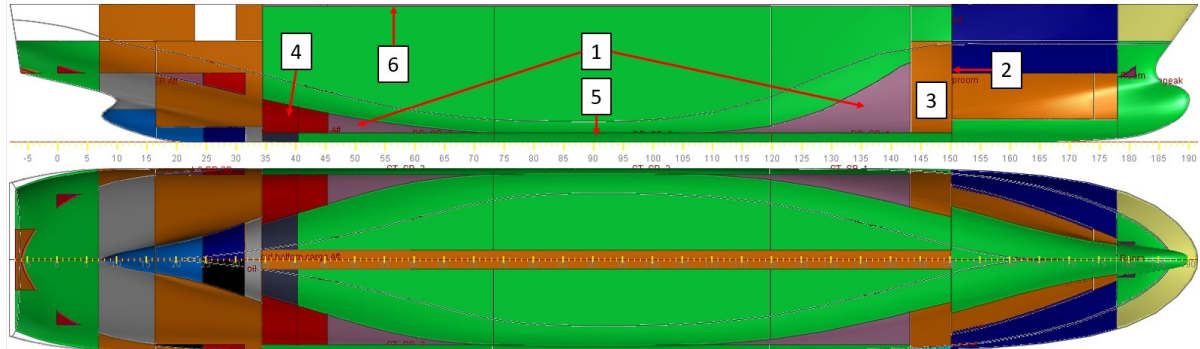


Figure 5.11: Design corresponding with the lowest attained index on the Pareto front and the highest cargo hold volume for two water ballast bulkheads

Looking at the design, some properties stand out:

1. Cargo hold is not located within the double hull;
2. Forward cargo hold bulkhead is shifted towards the bow;
3. Pump room to its maximum height and minimum length;
4. Fuel oil tanks became higher and more located to the aft;
5. Double bottom to its minimum height;
6. Main deck maximum height.

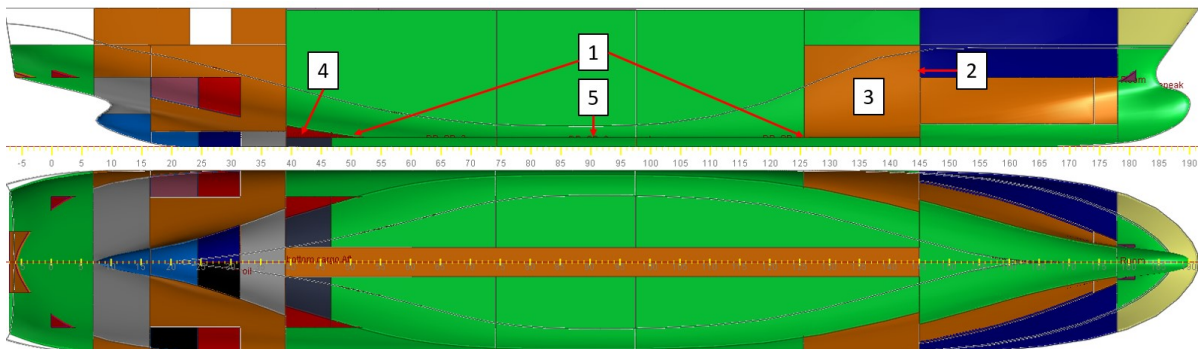


Figure 5.12: Design corresponding with the highest attained index on the Pareto front with a maximum cargo hold volume for two water ballast bulkheads

For this design, the following properties stand out:

1. Cargo hold is located inside double hull by a considerable margin;
2. Forward cargo hold bulkheads shifted towards aft, creating the largest possible volume;
3. Pump room bulkhead shifted towards aft;
4. FO tanks still not located inside double hull.
5. Double bottom stayed its minimum height;

Figure 5.13 shows the non-dominated points that form the Pareto front. The Pareto front consists of 22 points, which is considered enough for generating sufficient initial designs. The original Pareto

front, with 400 iterations from figure 5.9 had 28 non dominated points. This means that in the last 200 iterations, 6 new non-dominated points were added. There is a significant less concentration between the 0.5 and 0.6 region. As already discussed, these designs are ignored as they only added marginal improvements to both objectives and are located in the same region. In figures 5.14, 5.15 and 5.16 below, the behaviour of the bulkhead/deck location of all Pareto front points are shown with respect to the increase in attained index. This is used to try and explain the decisions made by the algorithm with regards to the Pareto front designs. For further clarification of the behaviour of the model, appendix A.1 shows the values obtained from the constraint functions per iteration.

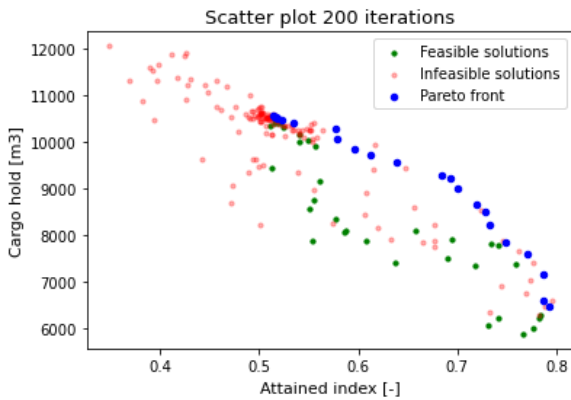


Figure 5.13: Pareto front for two bulkheads and 200 iterations

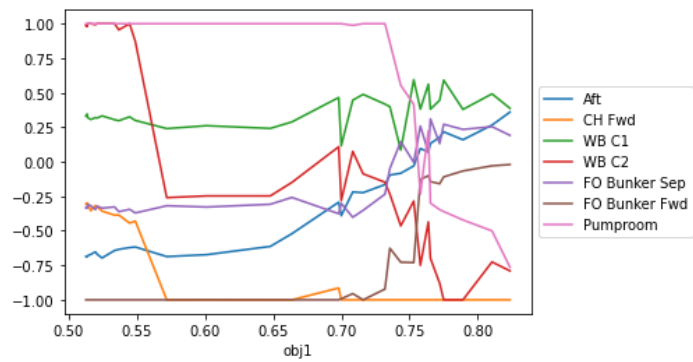


Figure 5.14: Location trans. BHs for A-index.

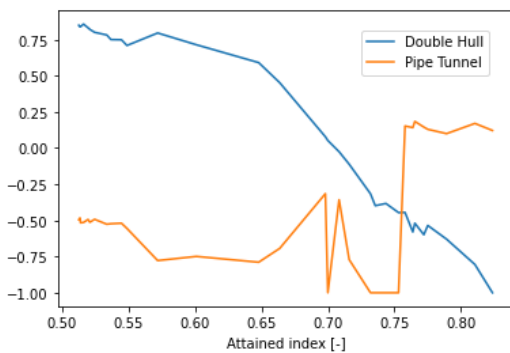


Figure 5.15: Location long. BHs for A-index.

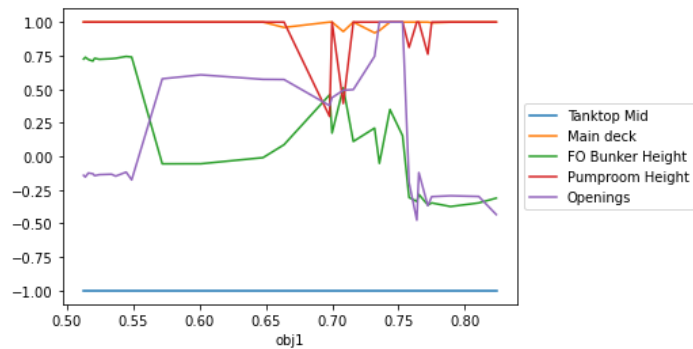


Figure 5.16: Location vert. BHs for A-index.

The cargo hold volume is influenced most by the location of the longitudinal cargo hold bulkheads, or side shell. Figure 5.15 shows that the higher the attained index becomes (the lower the cargo hold volume), the more the cargo hold sides move to the inside of the ship. Hence, creating more space between the side shell and the cargo hold. The aft and forward bulkhead of the cargo hold do not show the same behaviour as can be seen in figure 5.14. They both influence the size of the cargo hold equally and determine the size of the aft and forward sections of the ship. There is however, one significant difference regarding the influence on the subdivision of these two parameters. As the forward section of the ship is slimmer than the aft section, the position of the forward bulkhead greatly influences the distance of the cargo hold to the side shell of the ship.

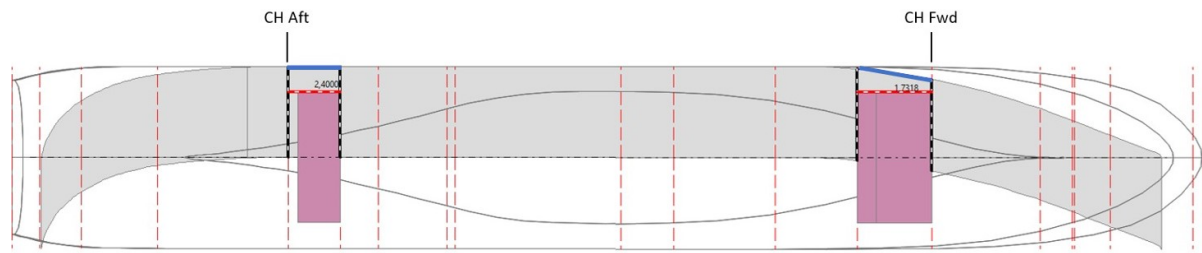


Figure 5.17: Penetration depth overview showing the distance of the cargo hold to the side shell at the aft and forward bulkheads

The blue lines show the position of the side shell while the red/white dotted line show the boundaries of the cargo hold. As can be seen, the "CH Fwd" bulkhead greatly influences the distance of the cargo hold to the side shell due to the geometry of the hull at this section of the design. The more the bulkhead is located to the aft, the bigger this distance and the higher the attained index becomes.

The height of the pump room can be explained by the permeability of the pump room compared to the tanks and spaces above. The pump room is considered a machinery space, which has a permeability of 0.85, while the other tanks and spaces (water ballast tank, fresh water tank and cargo hold) all have values of 0.95. By flooding the pump room instead of the other tanks and spaces, less weight is added to the ship i.e. less buoyancy is lost. A single objective experiment is run in section 5.3 to confirm this statement.

The reason the fuel oil tanks are still not located within the double hull is because they are relatively small compared to the cargo hold. In fact, they form a barrier between the cargo hold and the side shell, making it less problematic that the cargo hold is not located within the double hull anymore. The shape of the FO tanks can not be explained at this point. The permeability of the tanks is the same as of those surrounding it, which means that it does not have the same reason to increase its height as the pump room. In fact, it only decreases in height, the higher the attained index becomes. The transverse FO bulkheads only move to the bow at higher attained index designs.

Regarding the allowability of FO tanks located against the outer hull, regulation 12A is only applicable to ships with an aggregate fuel oil capacity of $600m^3$ and above. Fuel tanks should then be located inside the moulded line of the bottom and side shell plating. The minimum distances of these two are defined as follows [100]:

$$h = \frac{B}{20} \text{ or,} \quad (5.3)$$

$$= 2.0 \text{ m, whichever is less}$$

$$w = 0.4 + 2.4 \frac{C}{20,000} \text{ m} \quad (5.4)$$

Where:

- h = Minimum height of the tanktop;
- w = Minimum width of the side shell plating;
- B = Moulded breadth of the ship;
- C = Ship's total volume of FO, including that of the small FO tanks, in m^3 , at 98% tank filling.

Oil fuel capacity is defined as the volume of a tank in m^3 , at 98% filling. In this case, the tanks each have a volume of approximately $100m^3$. In some designs, this volume increases to approximately $200m^3$, but it never reaches the $600m^3$. This means that its possible to store the FO as is shown in the designs of this chapter. However, if its not desired, the distances calculated by equations 5.3 and 5.4 can be used to create a verified distance between the hull and the tank.

The tanktop is at a minimum height for every single point on the Pareto front, as can be seen in figure 5.16. The tanktop is in its entire range located below the light subdivision draught. This means that the PDS calculation always assumes everything below the tanktop to not add any buoyancy. Every compartment above the tanktop has volume that is located above one of the waterlines. Therefore, if

the tanktop height increases, the tanks located above have less volume and are therefore adding less buoyancy, resulting in a lower attained index. The tanktop is therefore always located at its minimum height which is described by SOLAS chapter II-1 part B-2 regulation 9 [89].

As explained in chapter 2.2.4, the maximum heeling angle for cargo ships is 30°, with an additional 16° for TRange. Openings that are designed to extend beyond this maximum heeling angle do not contribute to the attained index. Figure 5.18 shows the damaged waterline for this PDS calculation and the openings at their lowest allowed value. The starboard openings are located below the waterline at this point. When the openings are located approximately 60 cm higher, they do not add anything to the attained index anymore. Note that this distance only counts for the base ship as the openings are changed relative to the main deck. This means that for the full influence of the openings the total variables space should be investigated by means of a global sensitivity analysis or a similar method.

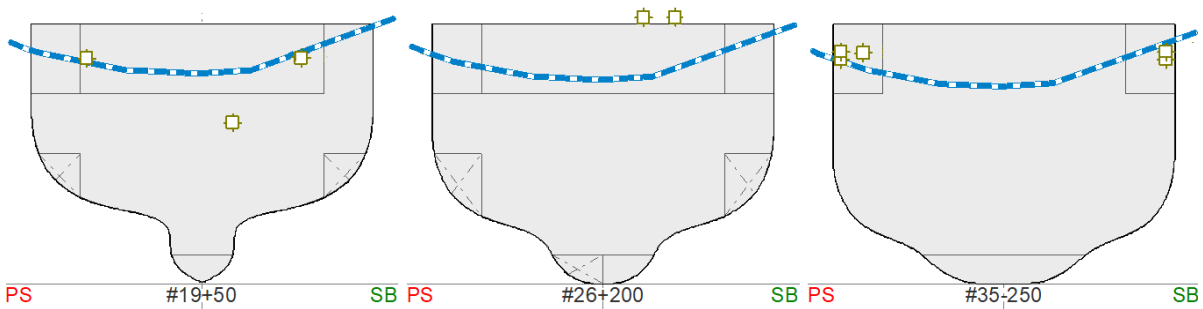


Figure 5.18: Damaged waterline (blue/white line) and location of openings at position zero for different cross section locations.

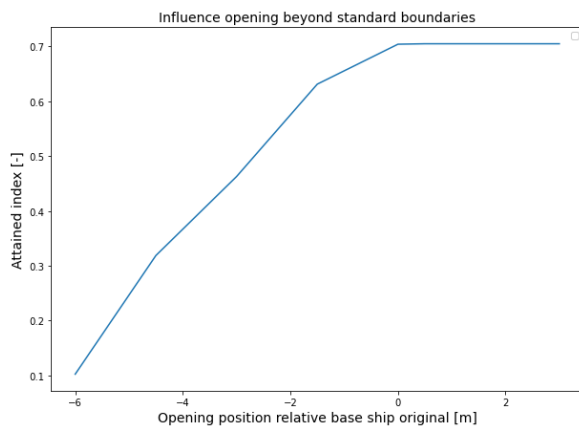


Figure 5.19: Influence of openings beyond their respective boundaries

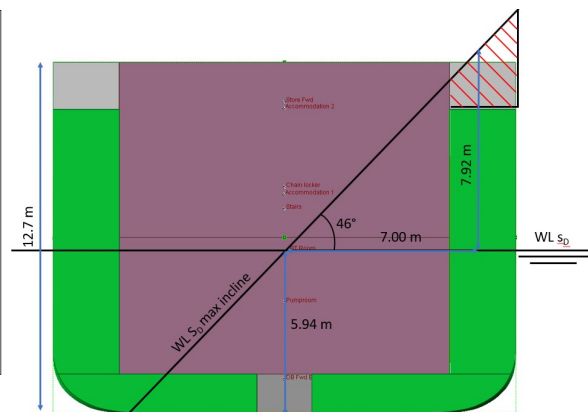


Figure 5.20: Zone of influence according to chapter 2.2.4

Figures 5.19 and 5.20 show the influence of the height of the openings beyond their initial boundaries and a schematic showing the height at which the openings have no influence on the attained index anymore respectively. As can be seen in figures 5.18 and 5.20, the openings can be made lower the more they are located inward of the ship. The height of the schematic, based on the equations, is not the same as the height of the damaged waterline from the DELFTship program. For passenger ships, the K factor becomes zero after the equilibrium heeling angle becomes higher than 30° according to equation 2.35. Figure 5.20 shows the 30° together with the TRange of 16° at the deepest subdivision draught. This is the absolute maximum case for which the openings do not influence the attained index anymore. In reality, the DELFTship program creates a damaged waterline graph, taking all damages for all three subdivision draughts and combining the highest damaged waterlines into a new 3D waterline that could be lower than what is depicted in the figure above.

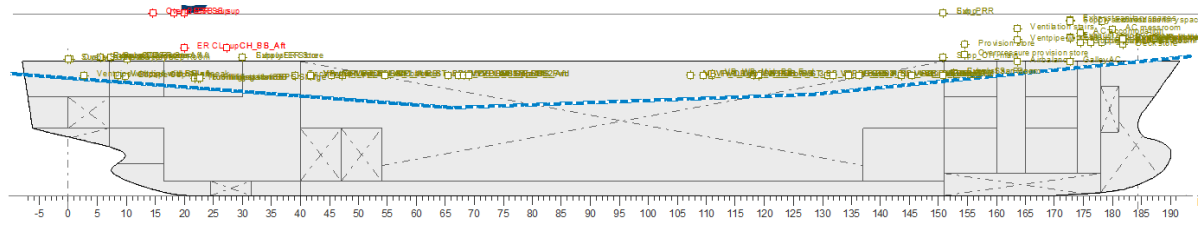


Figure 5.21: Damaged waterline (blue/white line) over the length of the ship.

As can be seen in figure 5.21, the damaged waterline is not at the same height over the entire length of the ship. Around the engine room, the damaged waterline is significantly lower than at the other sections. This is a result from the trim induced by flooding of the forward and aft compartments. If the engine room is flooded, the survivability or s_i goes to zero. This results in far less damage cases adding to the attained index, reducing the damage waterline height even more.

Appendix A.2 show the parallel coordinate plots for this design. They can be used to confirm the finding in this chapter. They show the trends for not only the Pareto efficient designs, but for all iterations after the initial design points.

5.2.3. Results For the Second Design

Next, the results for the design of five water ballast bulkheads is presented and analysed. The results are compared with those of the two bulkhead design. The more non-dominated points, the more options the designer has to choose the best fit for their respective further requirements. For 400 iterations, 39 non-dominated designs are identified by the algorithm. The Pareto efficient points are spread more evenly over the Pareto range than for two bulkheads. For 200 iterations 13 non-dominated designs are identified, as can be seen in figure 5.22 below.

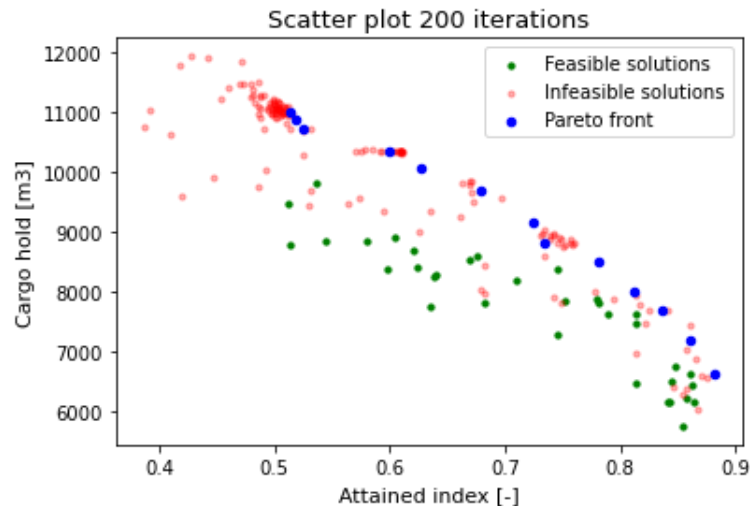


Figure 5.22: Pareto front for 200 iterations and five WB BH

In figures 5.23 and 5.25 below, the designs for both the lowest and highest attained index of the Pareto front are presented.

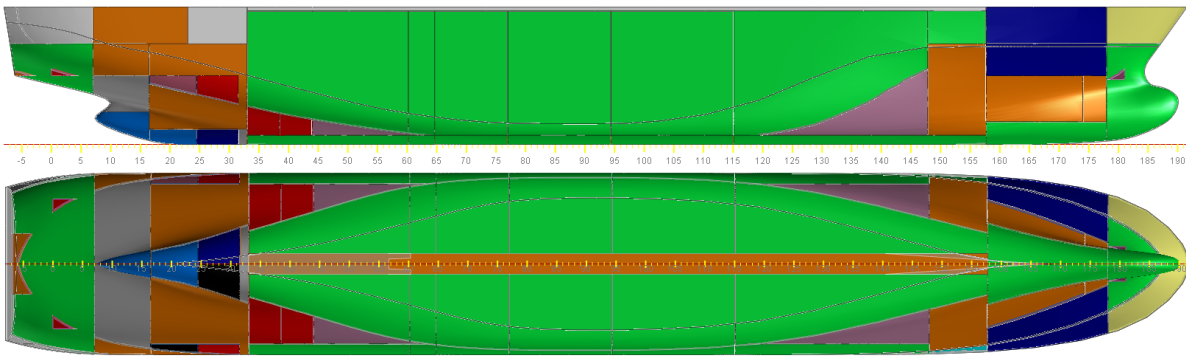


Figure 5.23: Design corresponding with the lowest attained index on the Pareto front and the highest cargo hold volume for five water ballast bulkheads

Here, one other particularity is found, leaving out the particularities from the first design. Namely, the uneven distribution of the water ballast bulkheads. When diving deeper in the results it can be seen that both the forward and aft section of the cargo hold have an s_i factor of zero. When these zones are damaged, they show a zero percent survivability as the cargo hold is immediately penetrated as well. An explanation would be that the algorithm accepts this and tries to move the bulkheads in such a way that they add as much attained index as possible in the other sections that do contribute to the attained index. However, after manually shifting the bulkheads towards an even distribution, a higher attained index is obtained. Further investigation is necessary to explain why the algorithm does not find an optimum for these bulkheads, compared to the others, which could be proven to be in their optimal position. A separate optimisation is performed that focused on the attained indices between 0.5 and 0.65. This gave the results shown in figure 5.24 below:

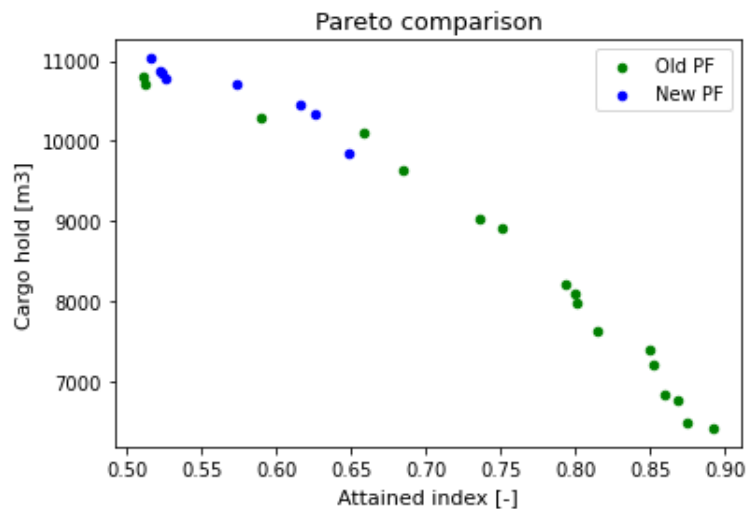


Figure 5.24: Comparison between the new Pareto front with the old front.

It can be seen that over almost the entire range, the new Pareto front dominates the old front. By focusing on this region, a higher attained index was reached for the same, or even a higher cargo hold volume. The following possible solutions have been explored, which all resulted in equal or less favourable results:

- Change the infill criteria from the exploiting (PHV) criteria to the exploration (SMS) criteria;
- Use more initial design points, 100 instead of $3*d$;
- Use less initial design points, $d+1$ instead of $3*d$, as is used in [5];

This concludes that the algorithm is not able to find the optimum solution for these bulkheads in the lower attained index and higher cargo hold volume region. However, the proposed designs are only

flawed by the water ballast bulkheads in that particular region of the Pareto front. It can therefore be assumed that the design is still located around the global optimum, making it a suitable method for optimisation.

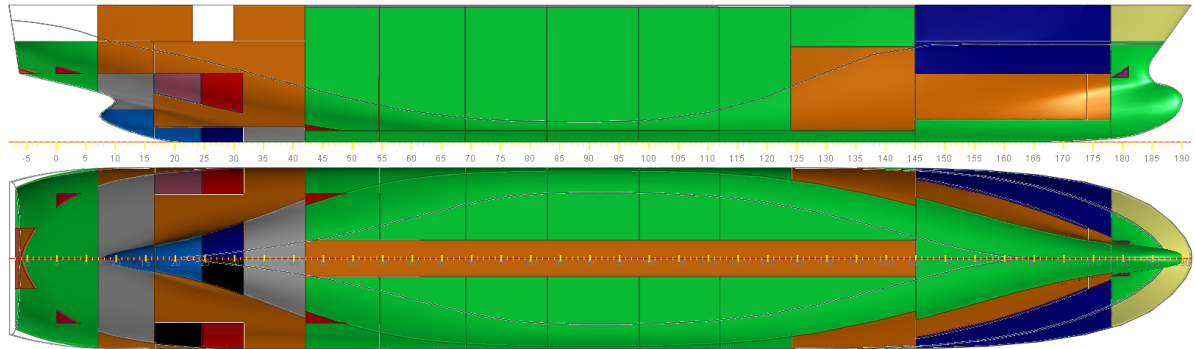


Figure 5.25: Design corresponding with the highest attained index on the Pareto front with a maximum cargo hold volume for five water ballast bulkheads

The water ballast bulkheads are now distributed evenly as the side of the cargo hold is shifted towards the midship and the other parameters behave approximately the same as the design in figure 5.12. For further clarification of the behaviour of the model, appendix A.1 shows the values obtained from the constraint functions per iteration.

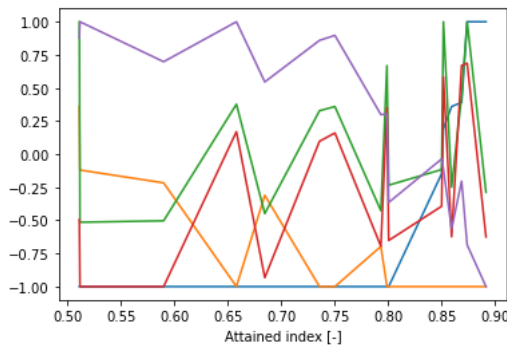


Figure 5.26: Location transverse BHs for A-index.

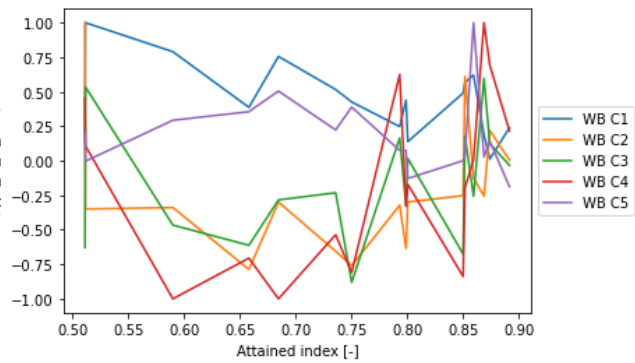


Figure 5.27: Location water ballast BHs for A-index.

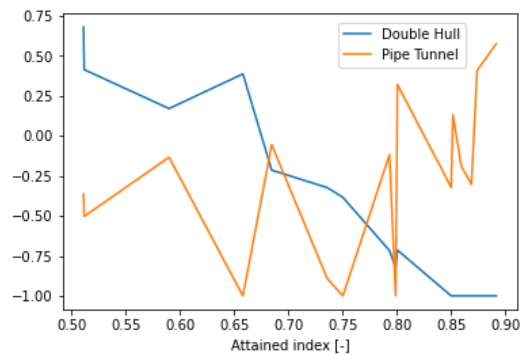


Figure 5.28: Location longitudinal BHs for A-index.

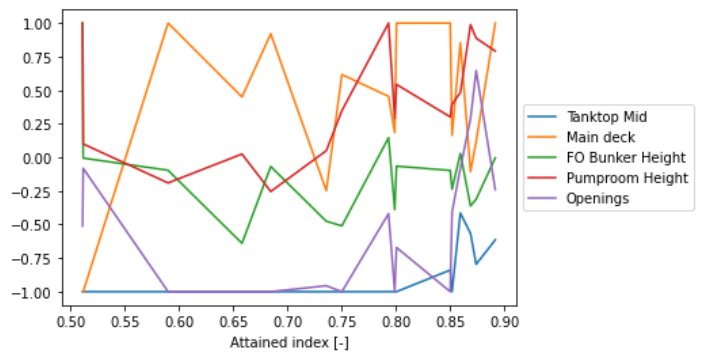


Figure 5.29: Location vertical BHs for A-index.

Figures 5.26 till 5.29 show the behaviour of the parameters of the Pareto efficient designs in relation to the attained index. Similar behaviour is observed compared to the two bulkhead design, except for the water ballast bulkheads as explained in this section. Appendix A.2 show the parallel coordinate plots for this design and are used to further strengthen the findings in this section.

The verification of the multi-objective optimiser started in the beginning of this chapter with the

hypervolume study. This showed that 200 iterations were sufficient for both the two and five bulkhead configuration. Next, the results were given and discussed. For now, the verification of the results is based on the consistency of the designs and naval architectural choices made by the algorithm. Listed below are the identified demands that aim to increase confidence in the model and its results prior to the sensitivity analyses.

- Double checking all coding and calculations with the methodology;
- Comparing the value of the infill points with the actual skeleton plane locations;
- Comparing the constraint function results with the actual tank/space volumes;
- Consistency between designs that lay in the same vicinity on the Pareto front;
- Identifying a trend in ship design along the Pareto front;
- Compare results from sensitivity analyses (Chapter 5.4).

Except for the last item, the model was verified for all items on the list. The results are compared to the sensitivity analysis results in chapter 5.4.

5.2.4. Conclusion

This section provided the results of the multi-objective optimisation for both the two and five bulkhead designs obtained from the first optimisation stage. The behaviour of the algorithm was analysed and discussed, and verified using the PDS calculation as described in chapter 2 and tested using the items listed above.

What becomes apparent is that most of the decisions by the algorithm with respect to increasing the attained index can be linked to the increase in distance from the cargo hold to the hull. The following decisions are related to that cause:

- The position of the forward cargo hold is much more critical as it has more impact on the distance between the cargo hold and the hull than the aft bulkhead;
- The pump room is used as a sort of crumple zone between the cargo hold and the hull;
- The FO tanks show this behaviour as well, where it does not matter that the tanks are located against the hull, but they are creating this same distance;
- The longitudinal bulkheads of the cargo hold move inwards, the more focus is placed on the attained index.

Only the openings, main deck and the height of the tanktop are not related to the protection of the cargo hold. The openings stop contributing to the attained index after a certain height and the tanktop is kept at a minimum due to the increase in buoyancy of compartments that are (partially) located above the waterline.

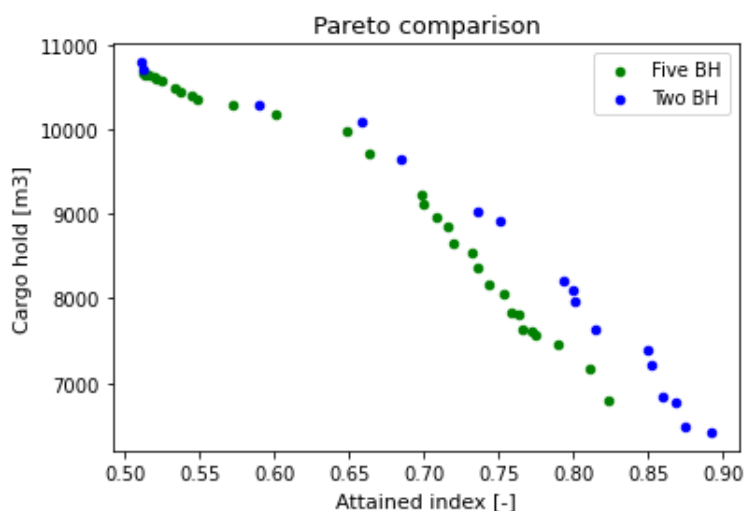


Figure 5.30: Comparison of the Pareto front for the two respective designs.

Figure 5.30 shows the Pareto frontiers for both designs. What can be concluded is that for the lower attained index regions (approximately up till 0.65), No increase can be seen in both attained index and cargo hold volume. As shown in figure 5.24, this is not the most optimum line. However, the small improvement shown in that figure is significantly less than in the higher attained index region. Following the double hull line from figures 5.15 and 5.28, it can be concluded that the size of the water ballast tank in the side shell continuously increase in size the higher the attained index becomes. That explains the low increase in attained index in its lower regions between the two designs. Once the side shell ballast tanks actually start to contribute to the buoyancy, difference start to build between the two designs.

This conclusion does not answer the question which design (two or five water ballast bulkheads) is the absolute best. More aspects need to be taken into account to determine this. This chapter shows the possibilities of the algorithm with respect to providing an optimum subdivision for a given amount of bulkheads. Also, the difference between the two designs shows the changes to expect when adding more or less bulkheads to the design. Regarding figure 5.24, the design needs to be manually optimised with respect to the water ballast bulkheads. Fortunately, this is a small percentage of the total hypervolume, and the overall design appears to be located in the global optimum when looking at all other parameters. Therefore, the optimisation is still considered as an effective method.

5.3. Single-Objective Optimisation (SACOBRA)

The single objective optimisation is, as said in previous chapters, used to verify the multi-objective optimiser and to run experiments to create more insight in the PDS calculation. If these last experiments show good results, it can also be concluded that this method can be used for researching many different design choices without having to use the PDS calculations from chapter 2.

5.3.1. Convergence

Multiple convergence criterion have been tested to determine the convergence threshold of the single objective optimisation. A method commonly used is to compute the change in the objective function in the last x iterations. An example is the definition given in equation 5.5, where x is 10, OF is the objective function and i the current iteration number [101].

$$\epsilon_i = \frac{|\sum_{i-9}^{i-5} OF_i - \sum_{i-4}^i OF_i|}{\sum_{i-4}^i OF_i} \quad (5.5)$$

This is however not possible to implement for this case study as the algorithm tries different routes and starting points to increase the attained index once it seized to increase in the current route. That means that large dips in the convergence plot can be observed which shows the algorithm taking a different approach. This can be clearly be seen in figure 5.31, where the maximum attained index hardly increases after approximately iteration 67, but has some significant dips. Another risk that comes with this method is premature convergence, or getting stuck on a local optimum. It is possible for the algorithm to find another route to a higher attained index much further in the process. By only looking back 10 or 20 iterations, chances are that this can happen. Therefore the convergence of the first model run is checked by performing many more iterations than are initially believed to be needed to reach a state of convergence. This can be seen in figure 5.31 below. 400 iterations where used to check the behaviour of the model far beyond the first convergence state.

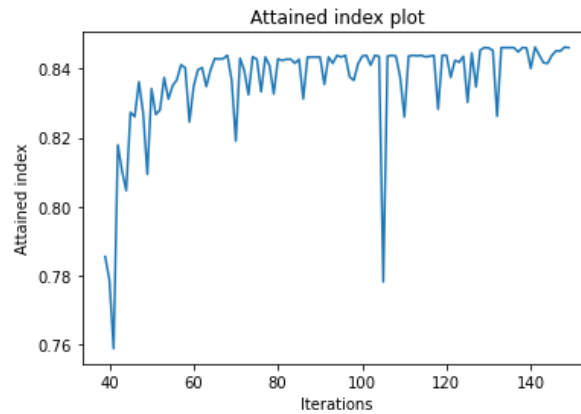


Figure 5.31: Attained index plot for 150 iterations

The convergence attained in figure 5.31 shows that the increase in attained index converges after only 80 iterations, at around 120 iterations a slight increase in attained index can be seen. For 400 iterations, it is found that after 150 iterations, no significant increase in attained index is observed. This shows that at 150 iterations the optimiser has reached a level of convergence that is considered acceptable. To verify the results from the single objective optimiser the following list of verification requirements is identified:

- Double check all coding and calculations with the methodology;
- Comparing the value of the infill points with the actual skeleton plane locations;
- Comparing the constraint function results with the actual tank/space volumes;
- Consistency in design between the best designs;
- Compare results from sensitivity analyses (Chapter 5.4).

The optimisation is applicable to real world optimisation problems, this has the added benefit of comparing the results with what is to be expected based on other ship designs. The first design is to verify that the optimiser shows the same result as the design from figure 5.12.

5.3.2. Experiment 1 - Maximum Attained Index

The first experiment is to verify that the converged single objective optimiser shows the same design as the highest non-dominated point with respect to the attained index of the multi-objective optimiser. The two bulkhead design is used for these experiments.

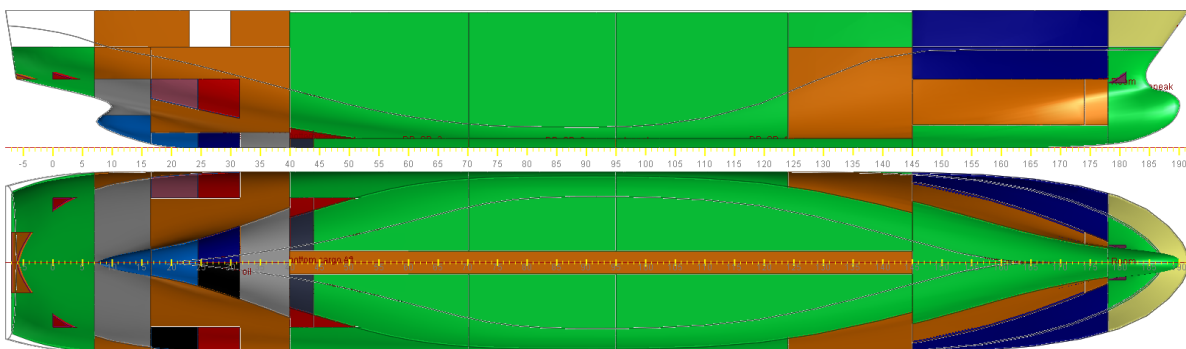


Figure 5.32: Best design for two bulkheads, after 150 iterations.

There are two significant design differences between the single- and multi-objective optimisation results. The first is the shape of the FO tanks. For the single-objective optimiser, the tanks were high and located more to the aft cargo hold bulkhead, while the multi-objective resulted in lower and longer tanks. Both tank designs cover the patch of cargo hold where there is no water ballast tank located.

One explanation is that the shape of the fuel oil tanks does not influence the attained index much, making it irrelevant if its high and short or low and long. If the most important function of the FO tanks is to protect the cargo hold, then this could very well be the case. This feeling is strengthened by the fact that the size of the tanks do not influence the cargo hold volume, as they are located fully inside the cargo hold. Figures 5.33 and 5.34 show these two different FO tank designs. The second difference between the two optimisers is the height of the openings. This can be contributed to the same principle as described in chapter 5.2 and in particular figures 5.18, 5.19 and 5.20. The height of the openings is very likely a random value between the minimum height of when it does not contribute anymore to the attained index, to the upper boundary of the variable. Table 5.6 shows the numerical differences between the single and multi objective optimiser.

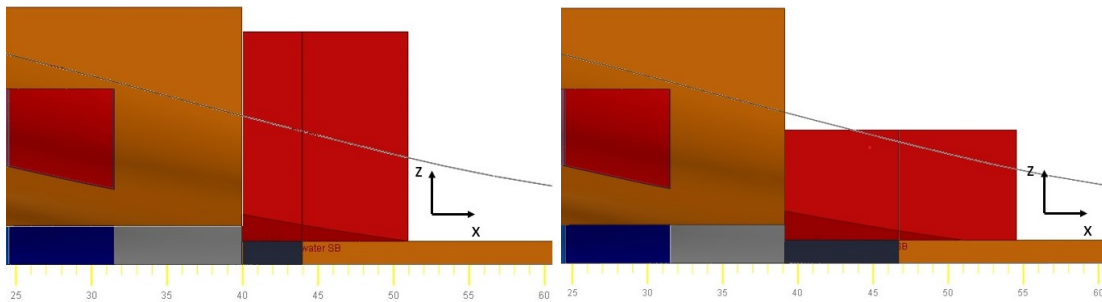


Figure 5.33: Single objective FO tanks result

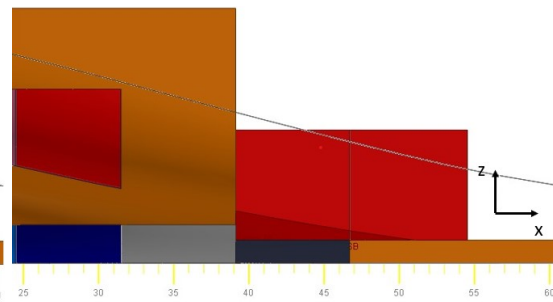
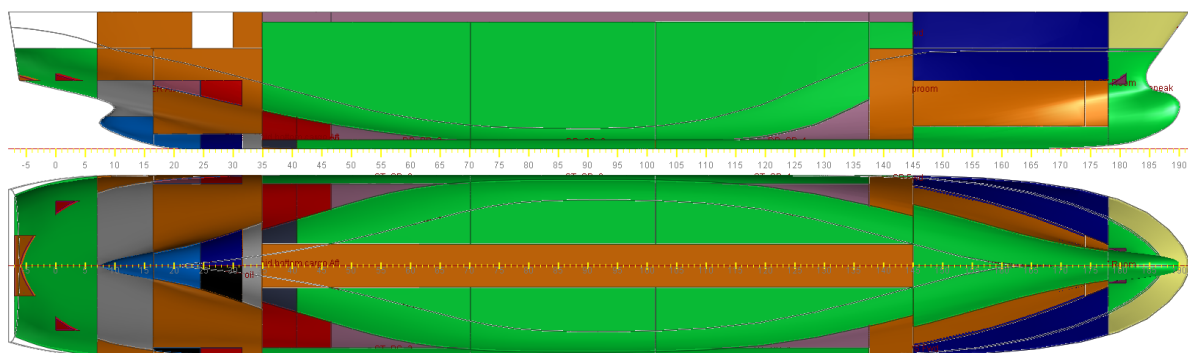


Figure 5.34: Multi objective FO tanks result

The rest of the design shows a similar result as the multi-objective optimiser from section 5.2. Together with the explanations regarding the differences between these two designs, more confidence is created in the multi-objective optimiser. This experiment encompassed one extremity of the Pareto front, while the aim of the second experiment is to verify the other extremity.

5.3.3. Experiment 2 - Minimum Cargo Hold Volume

A minimum cargo hold volume is introduced to see what the behaviour of the single-optimiser is when subjected to a relatively large constraint and to verify the same layout is reached for the multi-objective optimiser. This constraint is a minimum cargo hold volume of $10,000m^3$. In figure 5.35, the layout of the resulting design is shown.

Figure 5.35: Layout of the design for which a minimum cargo hold volume of $10,000m^3$ was introduced as a constraint.

Comparing this to figure 5.11, again, few differences can be spotted. Table 5.6, shows the differences between the single and multi objective design for both experiment one and two. The multi-objective design that is used for this comparison is a Pareto efficient design with the cargo hold volume closest to $10,000m^3$.

Table 5.6: Comparison between the infill points for the single and multi-objective optimisers for both their maximum attained index design and with a minimum cargo hold volume of 10,000m³

Parameter	SO_{maxA}	MO_{maxA}	SO_{minCH}	MO_{minCH}
CH Aft	21.97	21.52	19.20	19.11
CH Fwd	79.95	79.97	79.75	79.75
Tanktop	0.84	0.84	0.84	0.84
Double hull	6.00	6.00	7.61	7.59
Main deck	12.50	12.50	11.75	12.5
Pipe tunnel	1.05	1.34	2.0	0.66
WB C1	38.58	40.84	38.57	39.44
WB C2	52.25	53.69	55.80	57.42
FO sep	-1.64	0.32	-0.65	-0.51
FO fwd	-1.65	0.77	-1.30	-1.65
Trans. pump room	-3.85	-2.94	3.58	3.85
Vert. FO	2.62	-0.93	-0.85	-0.02
Vert. pump room	3.50	3.50	3.50	3.50
Openings	2.66	0.85	2.21	2.36

Although the designs are relatively similar, the single-objective design only had five feasible solutions as a result from 150 iterations, where 108 iterations were allocated to the optimiser and 42 for the Halton sequence initial sampling. This means that from the optimiser, only 4.6% of the concepts were considered a feasible design. This may seem like a low feasibility ratio, but to put this in perspective, for the multi-objective optimiser, the Pareto front consisted of 22 points, where most were not in the vicinity of such a high cargo hold volume. This also left only a hand full of designs with cargo hold volumes, higher than 10,000m³.

The table shows similar designs. This experiment is used to verify the other extremity, namely the highest cargo hold volume. However, because the cargo hold volume chosen was not the absolute extreme from the multi-objective (approximately 600m³ below), the designs are slightly different from figure 5.12. The forward cargo hold bulkhead is shifted aft. This is, as was expected, one of the first steps taken by the algorithm to increase the attained index when less cargo hold volume is required.

5.3.4. Experiment 3 - Cargo Hold Container Cutout

It can be seen from and explained in the multi objective results from chapter 5.2, that for designs with higher attained indices, the optimiser tries to shield the cargo hold with the pump room and to some extent with the FO tank. This creates more volume in the tanks and pump room and might unnecessarily reduce the cargo hold volume. An experiment is run to see what the difference in design is when on certain points in the cargo hold, shown in figures 5.36 and 5.37, cutouts are created with the width and height of a standard 20/40 foot container. The length is dependent on the position of the pump room bulkhead. For clarification, 1 is the pump room against the forward cargo hold bulkhead and 2 the water ballast tanks in the side shell. 3 is the hull that is now makes up the boundary of the cargo hold, where 4 is the cargo hold cutout that provides distance between the cargo hold and the hull.

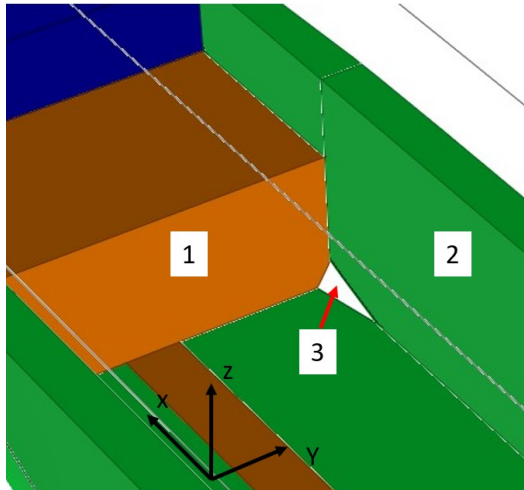


Figure 5.36: Cargo hold without cutout sections.

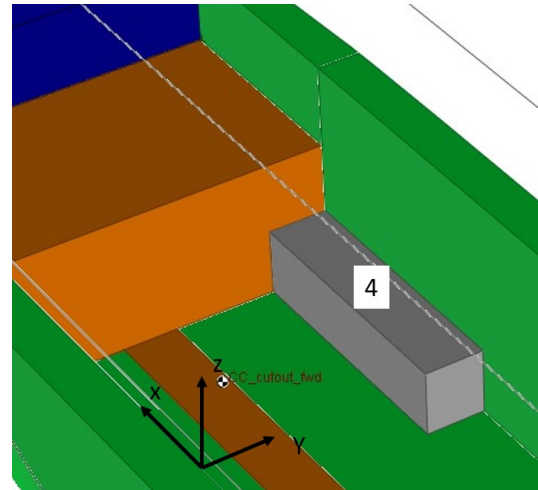


Figure 5.37: Added cargo hold cutout section

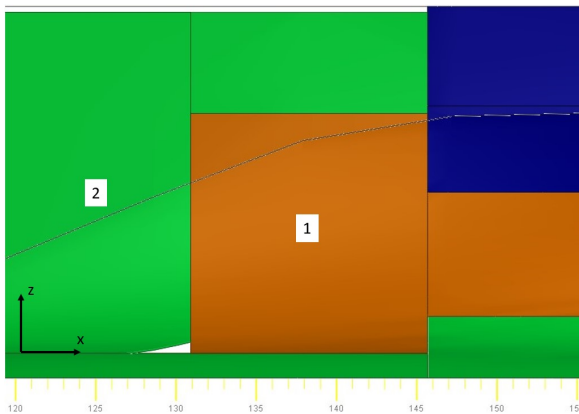


Figure 5.38: Pump room size with no cutout.

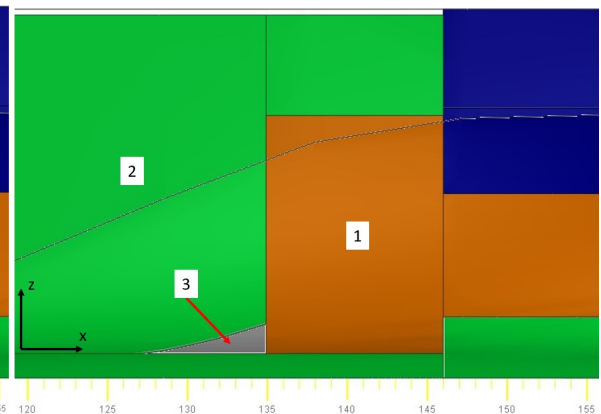


Figure 5.39: Pump room size with cutout.

A first experiment did not show any significant changes, the cargo hold volume remained approximately $6400m^3$ and the pump room height and longitudinal position remained at their upper and lower boundary respectively. However, when introducing a minimum cargo hold volume of $8500m^3$, a significant change in behaviour between the two models was observed. This is due to a single zone puncture of the cargo hold results in an s_i of zero. This means that for higher cargo hold volumes, the cutouts become more and more important for creating that distance to the hull. Figures 5.38 and 5.39 show the result in the design when a cutout in the cargo hold is used to create distance between the cargo hold and the hull.

The volume of the pump room prior to the cutouts was $967m^3$, after the cutouts this is reduced to $710m^3$. The total volume occupied by the cutouts is $101m^3$. This increases the cargo volume by $156m^3$. Although more volume is available for cargo, this does not mean that it is a benefit per se. For project cargo for instance, this cutout in the cargo hold can obstruct the sheer size of the cargo itself. For bulk carriers, this is no problem as the cargo can take on any shape or form. Hence, to determine if a lower volume of pump room is desired over a more uninterrupted cargo hold area, the designer must ask itself the question what type of cargo the ship will handle. The FO tanks did not seem to show significant changes compared to the design without cutouts. This can be contributed to the same property described in chapter 5.2.

5.3.5. Experiment 4 - Change of Permeability

To see the impact of a change in permeability of tanks and spaces, a fourth experiment is run where the pump room and FO tanks have a lower permeability. As the pump room has a higher permeability than the tanks above, and the FO tank have the same permeability as the cargo hold. The pump room gets a higher permeability and the FO tanks a lower permeability. These changes are summarised in table 5.7 below:

Table 5.7: Changes in permeability for experiment 4

Tank/space	Permeability		
	Initial	Tank above	New
FO tanks	0.95	0.95	0.85
Pump room	0.85	0.95	0.95

This results in the following results after running the optimisation again:

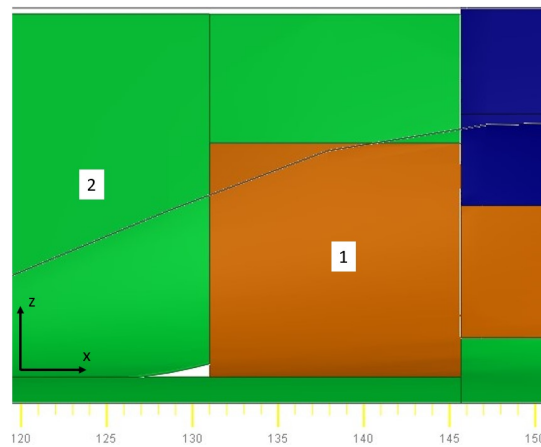


Figure 5.40: Resulting layout of the pump room after the change of permeability as shown in 5.7.

What can be seen is that the height of the pump room decreases compared to figure 5.32. The shape of the FO tank did not change compared to the other design. This can be caused by the same principle as was explained in chapter 5.2. The pump room volume decreased by $96m^3$

Table 5.8, shows the possibilities in permeability of the compartments in the design. This is provided to give a feeling of the potential that the change in location of some spaces with respect to the permeability can offer.

Table 5.8: Permeability of each general compartment according to SOLAS part B-1 regulation 7-3 [102]

Spaces	Permeability
Appropriated to stores	0.60
Occupied by accommodation	0.95
Occupied by machinery	0.85
Void spaces	0.95
Intended for liquids	0 or 0.95 ¹

1. Whichever results in the more severe requirement.

The cargo hold also has different permeability's for all three subdivision draughts. However, these permeability's are fixed for the type of cargo that can be transported. All of the values are the same, except for Ro-Ro applications, but they are not part of this scope and therefore this is not investigated any further.

5.3.6. Conclusion

The conclusion for the single-objective optimisation experiments can now be presented. The first two experiments aimed to verify the results from the multi-objective optimiser, while the other two showed how the algorithm would respond to creating more distance between the cargo hold and the hull and how it would respond to a change in permeability. The conclusion for every experiment is listed below:

- Optimising for a maximum attained index showed similar results as the multi-objective optimiser, whereby any dissimilarities could be explained;
- Optimising for a maximum attained index with a minimum cargo hold volume of $10,000m^3$ showed similar results as the multi-objective optimiser, whereby any dissimilarities could be explained after a certain cargo hold volume;
- The cargo hold cutout showed a significant difference of $156m^3$ in the design after a certain cargo hold volume;
- The permeability change in selected tanks showed a significant difference of $96m^3$ in the design after a certain cargo hold volume.

It was found that the effect of the cargo hold cutout and the permeability changes significantly increased when a single zone damage that penetrated the cargo hold resulted in an s_i of zero. These findings create more confidence in the optimiser and show the designer the possibilities of the PDS calculation. It can also be concluded that the single-objective optimiser can successfully be used as a framework to test many other design choices.

5.4. Results From the Sensitivity Analysis

In this chapter the results from the sensitivity analysis is shown. An answer is given to the sub question of this research, *What set of parameters has the most influence on the attained index?* The Morris method is used to indicate the influence of the parameters across the entire parameter space. However, it doesn't show the correlation between the variables. During the research, the decision was made to include a correlation matrix to further provide insight into the behaviour of the variables. For validation purposes, a local sensitivity analysis is performed by hand. In chapters 5.1 and 5.2, two different designs are optimised and presented. However, only one of these designs is used for the sensitivity analysis, as the use of two designs would result in an unnecessary amount of results that does not lead to a significant increase in insight. Therefore, the design with five water ballast bulkheads is used simply for the fact that it has more variables, which mean that the methods will also work for less variables.

5.4.1. Morris Sensitivity Analysis Method

As explained in chapter 4.4, three different sensitivity analysis experiments are performed. The first experiment uses 20 trajectories, while the other two use 60 and 100 trajectories respectively. For these experiments, the base ship from chapter 3.1 and figures 4.2 and 4.4 is used, as this was performed prior to any optimisation, and its only used to determine the minimum number of trajectories. The results can be seen in figure 5.41 below. A 95% bootstrap confidence interval is used, which should not exceed more than 10% of the highest influential parameter. In appendix C.1, the results for all three trajectories are listed and the size of the confidence interval is calculated.

In table 5.9, the resulting confidence intervals for both the N=20 and N=100 run are shown:

Table 5.9: Total size of the confidence interval when compared to the total size of the largest parameter w.r.t. the elementary effect

Number of trajectories N [-]	20	100
Confidence interval vs Elementary effect [%]	8.56	4.80

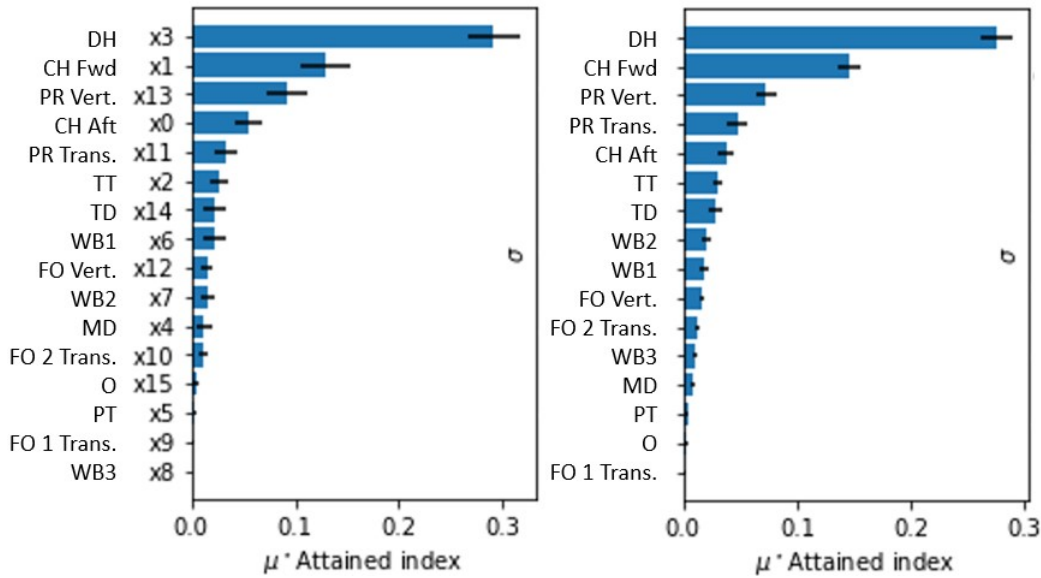


Figure 5.41: Results of the Morris method for N=20 and 100 respectively

The N=20 experiment already satisfies the threshold set in equation 4.15. This means that this is the number of trajectories that is going to be used for the further calculation of the Morris method on the new optimised design. However, looking at CH fwd and PR and CH aft and FO 1 trans. in the N=20 experiment, it can be seen that the confidence intervals overlap one another. For clarification this is illustrated in figure 5.42 below:

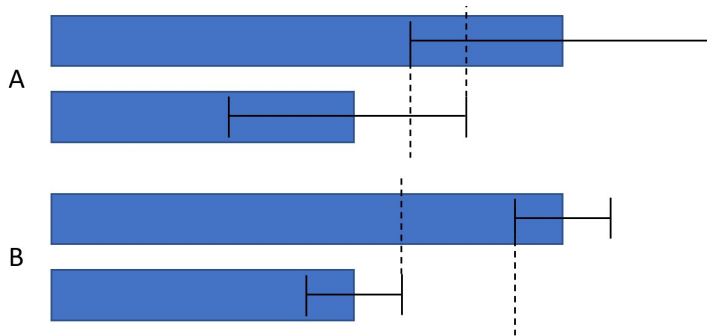


Figure 5.42: Bootstrap confidence interval where situation A is not desired and situation B is desired.

This means that it there is a chance for the two parameters to be in the wrong order. In both the N=100 experiment, the CH Aft and FO1 Trans. parameters are displayed in a different order. It is also much more clear from this experiment that the forward cargo hold bulkhead is much more distinguished from the height of the pumproom. However, the time required to perform the sensitivity analysis is reduced drastically if only 20 iterations are being used. 20 trajectories require 360 function evaluations for 17 parameters, therefore taking approximately 48 hours to complete instead of approximately six or ten days for 60 and 100 trajectories respectively. It is still clear which individual parameters have the most influence on the attained index for the N=20 experiment. Therefore it is used as the default number of trajectories for this case study.

Figure 5.43 shows both the elementary effect as well as the standard deviation that makes up the bootstrap confidence interval in two ways. The first is the same as is shown in figure 5.41 and provides a quick overview of the most influential parameters. The second figure aims to indicate if the parameter behaves linear, non-linear, monotonic or non-monotonic as was first discussed in figure 3.14 in chapter 3.6.3.

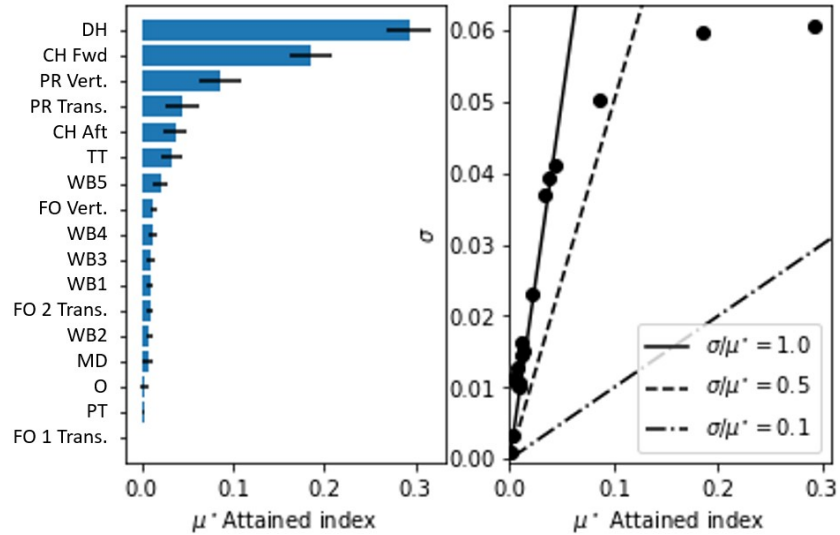


Figure 5.43: Results of the Morris sensitivity analysis method of the second optimisation stage for five bulkheads.

Almost all parameters, except the top three, are located on the line of non-linearity and non-monotonic. In appendix C.1 table C.4, it can be seen that the confidence bootstrap interval is approximately 8.1% of the total elementary effect of parameter DH. This is, again, within the limit and confirms that 20 trajectories is good enough for this case study. However, a parameter like the openings shows that the confidence interval is more than 100% of the absolute value for the elementary effects regarding that specific parameter. For the next couple of parameters in the vicinity of the openings, this lays around 50%, which is still considered as unreliable. This number decreases the higher the elementary effect per parameter goes, but only the last three parameters show reliable results concerning figure 5.42.

The non-linear/non-monotonic behaviour of most of the parameters make it a complex task to determine what level of influence they actually have on the PDS and the parametric model. For instance, it was expected that the openings had a significant influence on the attained index. However, its elementary effect value is only marginal compared to the other parameters. To better understand the level of influence, more research is performed to expand on the current results. The Morris method itself does not show a graph with the behaviour of the attained index over all trajectories. In the next section and section 5.4.3, a correlation matrix and one-at-a-time method by hand are performed respectively, that do include graphs of the behaviour of the attained index. This makes the verification of the sensitivity analysis more easy. It also generates more insight in the correlation between the variables.

5.4.2. Pearson Correlation Matrix

Post processing methods are used to visualise certain aspects and properties of large numbers of data that would otherwise not be easy to understand or visualise. In this case, the input and output of the multi-objective optimisation is used as input to calculate the Pearson correlation coefficients. Especially for models with costly function evaluations like the PDS calculation in this case, post-processing methods can be implemented relatively quick. The correlation matrix is comprised of Pearson correlation coefficients $r_{X,Y}$. These coefficients can be calculated as follows.

$$r_{X,Y} = \frac{\sum_{i=1}^{m} (X_i - \bar{X})(Y_i - \bar{Y})}{\sqrt{\sum_{i=1}^{m} (X_i - \bar{X})^2} \sqrt{\sum_{i=1}^{m} (Y_i - \bar{Y})^2}} \quad (5.6)$$

Where X and Y are the two instances that contain m attributes and \bar{X} and \bar{Y} are defined as:

$$\bar{X} = \frac{1}{m} \sum_{i=1}^m X_i \tag{5.7}$$

$$\bar{Y} = \frac{1}{m} \sum_{i=1}^m Y_i \tag{5.8}$$

The Pearson correlation coefficient shows the linear correlation between two variables. $r_{X,Y}$ ranges from -1 to 1, or from a strong negative to a strong positive correlation. Zero means that two variables are uncorrelated [103]. All these values are combined into a symmetric $n \times n$ matrix, where n is the number of instances.

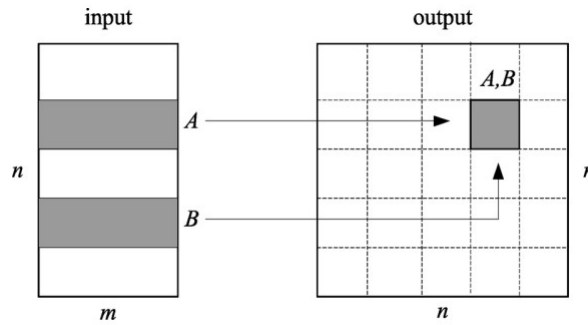


Figure 5.44: Partitioning correlation coefficient matrix [103]

In figure 5.45 below, the correlation matrix is shown consisting the Pearson correlation coefficients for the objectives, constraints and the five most influential parameters according to the Morris method from chapter 5.4.1 and this correlation matrix.

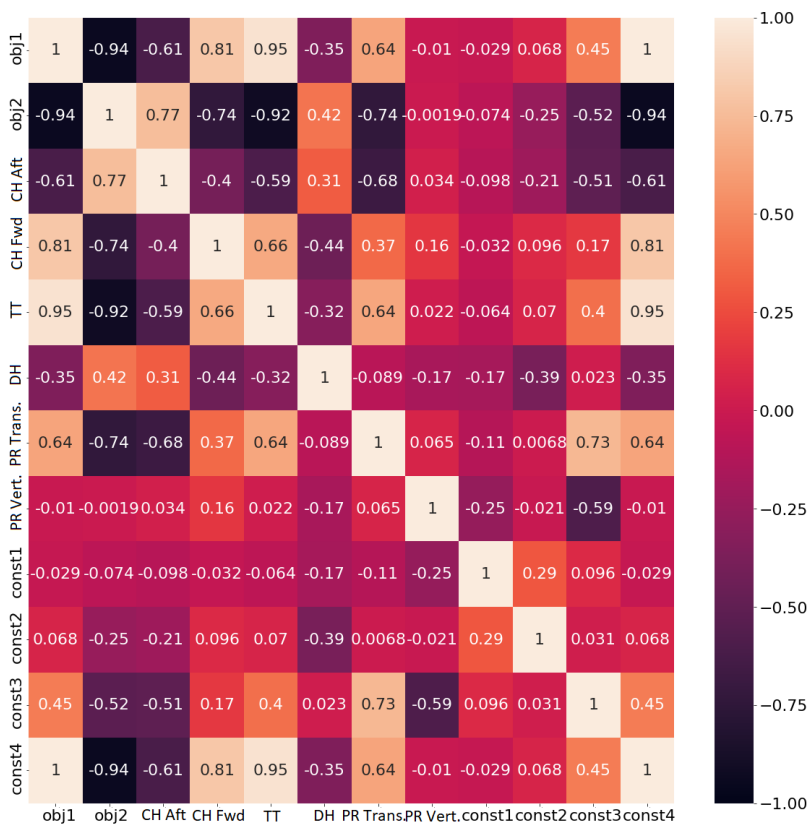


Figure 5.45: Matrix containing all Pearson correlation coefficients for the objectives, constraints and the five most influential parameters according to the Morris method.

To verify the results of the correlation matrix, some (sanity) checks are performed. Listed below are some of the identified checks for this case study, that determine whether the results from the matrix are reliable or not.

- Correlation between the same two parameters should be "1";
- Attained index and 4th constraint strong correlation;
- Parameters show the same correlation between attained index and 4th constraint;
- Objectives should have a strong negative correlation;
- Correlation between parameters and size of the cargo hold are as expected;
- Correlation between parameters and the attained index are as expected.

The first sanity check is to check whether the parameters have a strong positive correlation of value "1" with themselves, which is true in this case. The first objective and the last constraint have the same strong positive correlation as the constraint is defined by the attained index and a constant R. The constraints and objectives are defined in equation 4.14. This also means that the parameters that influence the attained index should have the same correlation coefficient for both the first objective and the last constraint. This is the case as it can be seen that the whole left column consists of the same values as the bottom row. Both objectives should have a strong negative correlation, as they are chosen such that they can form an efficient Pareto front. The parameters that influence the cargo hold geometry also show the to be expected correlations, therefore the correlation matrix satisfies the first set of sanity checks.

The highest correlation between the first objective (A-index) from figure C.3 and the parameters shows the level of influence of these parameters on the attained index, just like the results from the Morris method. The difference is of course that the Morris method uses a global sampling method to explore the entire parameter space, while this matrix only uses a number of initial design points as a sampling and then obtains the rest of the results from a converging optimiser. In table 5.10 below, the difference in outcome between the Morris method and correlation matrix is shown:

Table 5.10: Difference between Morris and Pearson sensitivity analyses

		CH_{Aft}	CH_{Fwd}	TT	DH	MD	PT	WB1	WB2	WB3
Morris	EE μ^*	0.036	0.185	0.033	0.293	0.007	0.002	0.0089	0.008	0.010
	Ranking	5	2	6	1	14	16	11	13	10
Pearson	Coefficient	0.61	0.81	0.18	0.95	0.26	0.13	0.14	0.022	0.072
	Ranking	4	2	8/9	1	6	11	10	16	15
Difference		-1	0	+2/3	0	-8	-5	-1	+3	+5
		WB4	WB5	FO_{Sepx}	FO_{Fwdx}	PR_x	FO_z	PR_z	O	
Morris	EE μ^*	0.012	0.021	0.000	0.0088	0.044	0.013	0.087	0.003	
	Ranking	9	7	17	12	4	8	3	15	
Pearson	Coefficient	0.18	0.078	0.22	0.35	0.64	0.11	0.01	0.098	
	Ranking	8/9	14	7	5	3	12	17	13	
Difference		-1/0	+7	-10	-7	-1	+4	+14	-2	

When examining only the row indicating the differences between the two methods, significant deviations can be identified. When looking at the results from figure 5.43, from approximately ranking 8 till 17, the differences between the influence of the parameters is so marginal that it is not possible to give a reliable ranking. However, the correlation matrix hardly shows any correlation between the height of the pumphouse and the attained index, whereas the Morris method shows a relatively high elementary effect. The low correlation between the pump room height and the attained index does not necessarily mean that the influence of the parameter is low, in fact it could just mean that there is actually a very strong correlation between the parameter and the attained index. This is because the correlation matrix is a post-processing method that uses the results from the optimisation. If the algorithm finds that the higher the pump room height, the higher the attained index becomes, it will automatically use the highest possible value for this parameter at all times, resulting in a low correlation. The correlation matrix does not include the findings of the algorithm prior to the beginning of the optimisation. It is therefore not possible to use the current correlation matrix to verify the results of the Morris method. Hence, to obtain reliable values, a pseudo random sampling method is used to generate the correct correlation between the objectives and the parameters. As the correlations of the objectives and constraints are considered to not be related to the correlation between the parameters, a new, combined correlation matrix can be made that shows the correct coefficients. This improved matrix is shown in figure 5.46 below:

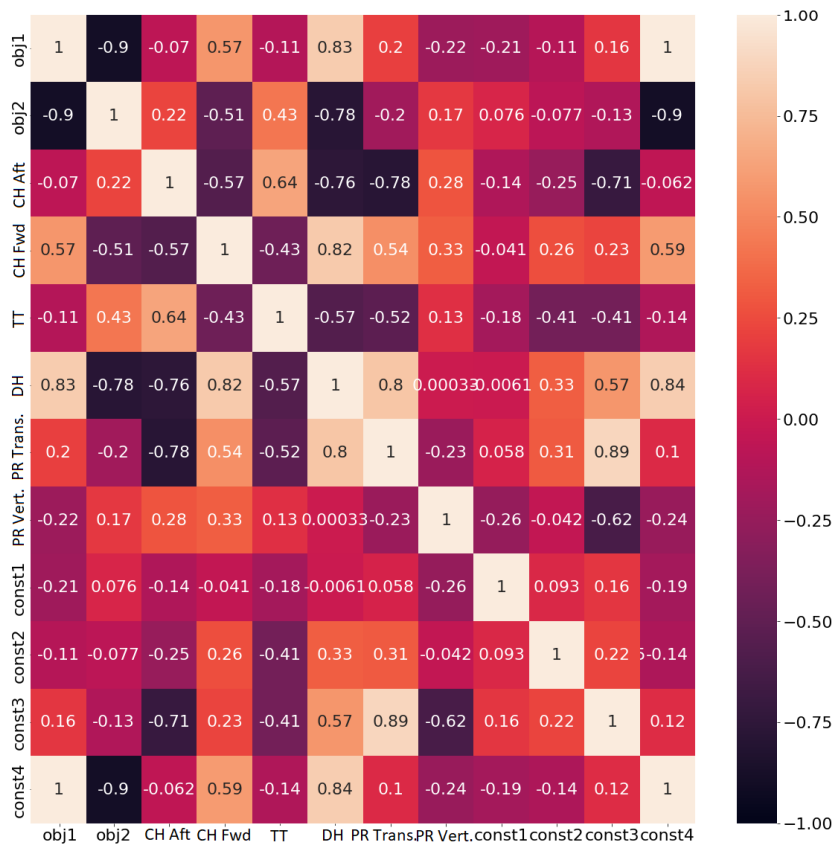


Figure 5.46: Improved correlation matrix that combines a random sampling with the optimiser to show the correct correlation coefficients for both the parameters as well as the objectives and constraints.

Table 5.11: Difference between Morris and Pearson sensitivity analyses for the improved correlation matrix

		CH_{Aft}	CH_{Fwd}	TT	DH	MD	PT	WB1	WB2	WB3
Morris	EE μ^*	0.036	0.185	0.033	0.293	0.007	0.002	0.0089	0.008	0.010
	Ranking	5	2	6	1	14	16	11	13	10
Pearson	Coefficient	-0.07	0.57	-0.11	0.84	-0.027	0.012	-0.093	0.075	-0.056
	Ranking	8	2	5	1	15	17	6	7	9
Difference		+3	0	-1	0	+1	+1	-5	-6	-1
		WB4	WB5	FO_{Sepx}	FO_{Fwdx}	PR_x	FO_z	PR_z	O	
Morris	EE μ^*	0.012	0.021	0.000	0.0088	0.044	0.013	0.087	0.003	
	Ranking	9	7	17	12	4	8	3	15	
Pearson	Coefficient	-0.052	-0.053	0.052	-0.036	0.2	0.034	0.22	-0.022	
	Ranking	11	10	12	13	4	14	3	16	
Difference		+2	+3	-5	+1	0	+6	0	+1	

This method shows better results when comparing it to the Morris method. The highest four variables show the same ranking as those of the Morris method results. After that, the elementary effects and correlation coefficients become low and their values lay close together. The correlation coefficients also suffer from high confidence intervals at this point as was shown in table C.4 for the Morris method. Therefore, after these four values, the ranking can not be trusted to be in the correct order. It can be seen that below a correlation coefficient of approximately 0.1, the values can not be used anymore to say something about the correlation. Hence, for the correlation between the variables, only variables with higher correlations are discussed. All listed requirements to verify the correlation matrix, listed below figure 5.45, are now satisfied. Another test to add to the verification requirements is that the correlation coefficients between the variables when only random sampling is used should be low. This is true, as can be seen in figure C.2 in appendix C.2. The results are now analysed.

Pump room - The size of the pump room has a positive correlation with the attained index, this means that for a high attained index, the pump room volume should become high as well. This can be seen in figures 5.12 and 5.25, where the size of the pump room increased between the lowest and highest attained index designs. Also the transverse bulkhead and deck of the pump room show a similar correlation. The transverse bulkhead also shows high correlation with many of the other parameter. This is because it significantly influences both objectives, resulting in other parameters adjusting to its position. This phenomenon can be seen for all variables that have a high influence on one or both objectives. A particularly interesting results, is the high correlation of the fourth water ballast bulkhead with both the pump room deck and the openings. The strong positive correlation means that the more the bulkhead is located forward, the higher the deck and openings tend to be located. This also goes the other way around, which is more likely as the influence of the water ballast bulkheads on the attained index is very low.

FO tanks - The FO tanks both have a negative correlation with the attained index. It can be seen that between the different designs, the fuel tanks remain relatively small compared to the increase in size of the pump room. The two transverse bulkheads and deck of the FO tanks show a marginal correlation between them and the attained index. This explains the difference between the two designs from the single and multi objective runs shown in figure 5.33 and 5.34. If the size of the tanks do not matter, the two slightly different optimisers may show different FO tank designs that both have the same level of influence on the attained index. Both transverse bulkheads also show a strong correlation with the double hull and forward cargo hold bulkhead. This can be contributed to the fact that they all determine the size of the cargo hold, therefore depending on each other to determine this size, while maintaining a high attained index.

Water ballast bulkheads - As discussed above, the 4th and 5th water ballast bulkheads seem to have a high correlation with both the pump room and FO bulkheads respectively. As the water ballast bulkheads do not show a significant correlation with the attained index, it can be assumed that they are being influenced by the pump room and FO tanks instead of the other way around.

Cargo hold main bulkheads/decks - The main bulkheads are the cargo hold aft, forward and double hull bulkheads and the tanktop. These define the shape of the cargo hold, where the FO tanks and pump room are located in. The difference in correlation for the cargo hold aft and forward bulkheads is shown in figure 2.10, this verifies the difference between the two bulkheads. The longitudinal cargo hold bulkheads both influences the attained index and the cargo hold volume the most. Part of this reason is that the distance defined by DH, defines the distance of both the PS and SB longitudinal cargo hold bulkhead. The tanktop correlation with the attained index and the cargo hold volume shows that it is much more important for the algorithm to maintain a low tanktop height as this greatly increases the cargo hold volume. That explains the reason the tanktop height remains minimum for all designs during this research. All main cargo hold bulkheads and decks have a high correlation with each other.

Main deck and openings - The main deck and openings are linked as the height of the openings is semi-dependent on the main deck height. What stands out is that these two variables are not highly correlated. Their correlation is in the same vicinity as these variables have with many of the others. This could be attributed to the fact that after a certain height, the height of the openings does not matter and the height of the openings becomes almost from a certain point, lowering the correlation coefficient. Furthermore, these show a very low correlation with the attained index as their range is not sufficient enough to affect the attained index as is shown in figure 5.19 for the openings.

5.4.3. Verification by Hand

As both sensitivity analyses presented in this chapter lack unambiguous answers or contain some form of flaws, a final verification is performed to really connect the two analyses with, the research, each other and the optimisation. This final verification is derived from a paper by Simopoulos et al. [32]. The behaviour of the parameters is examined by changing one variable at a time, for which its value is determined by a certain interval:

$$p_{i,j} = \frac{UB_i - LB_i}{x} \quad (5.9)$$

Where:

- $p_{i,j}$ = i^{th} parameter with the j^{th} position in the interval;
- UB_i = Upper boundary of the i^{th} parameter;
- LB_i = Lower boundary of the i^{th} parameter;
- x = Number of intervals as an integer.

The base ship is used as a starting point, where all variable values return to if they are not subjected to change. The number of function evaluations for this sensitivity analysis is $x+1$ times the number of variables. This means that for this case study 176 function evaluations are necessary to obtain the results. The results are normalised and combined into three groups of graphs representing behaviour of the transverse, longitudinal and vertical location of the parameters respectively. The range is normalised to show the relative influence of the parameters with respect to their total allowable range. This allowable range is the same as is used in the optimisation. This way, a better comparison can be made between the sensitivities of the variables. Comparing the absolute influence is not considered realistic as this doesn't show the true potential of the parameters in the feasible space. Figures 5.47, 5.48 and 5.49 show these normalised graphs. A discussion is provided below each graph regarding the results. The verification of the sensitivity by hand is relatively easy, as the method is quite simple and straightforward.

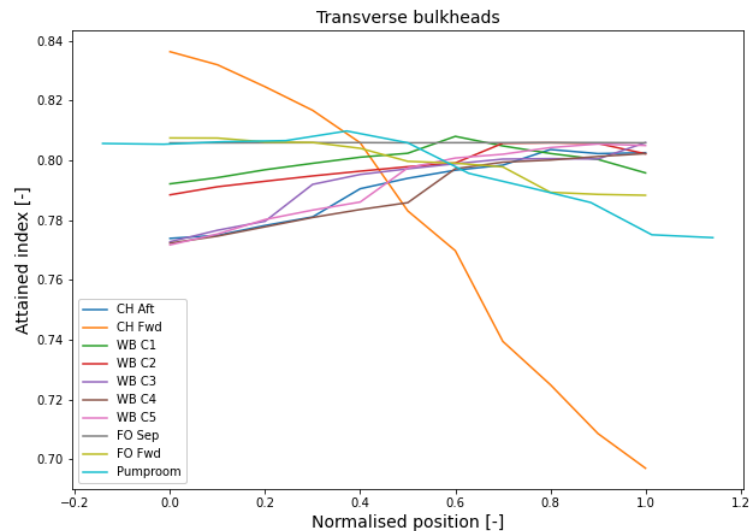


Figure 5.47: Sensitivity in the normalised range of the transverse bulkheads with respect to the attained index A.

As can be seen in figure 5.47 above, most of the variables have the same level of influence on the attained index. They do not change the attained index by approximately more than 5% over their entire range. However, the transverse bulkhead that represents the front of the cargo hold shows a significantly higher influence. With the attained index dropping from 0.84 to 0.70, a difference of 0.14 in attained index is recorded between the lower and upper boundary of this variable. The more the bulkhead is positioned to the aft of the ship, the higher the attained index becomes. However, this also reduces the size of the cargo hold significantly. This strengthens the results described in section 5.2 and the correlation matrix results of section 5.4.2, where the forward cargo hold bulkhead also showed the same behaviour. This also applies to the pump room bulkhead, that shifts more to the aft of the ship to increase the attained index, and the water ballast bulkheads that converge to equal spacing for the same reason.

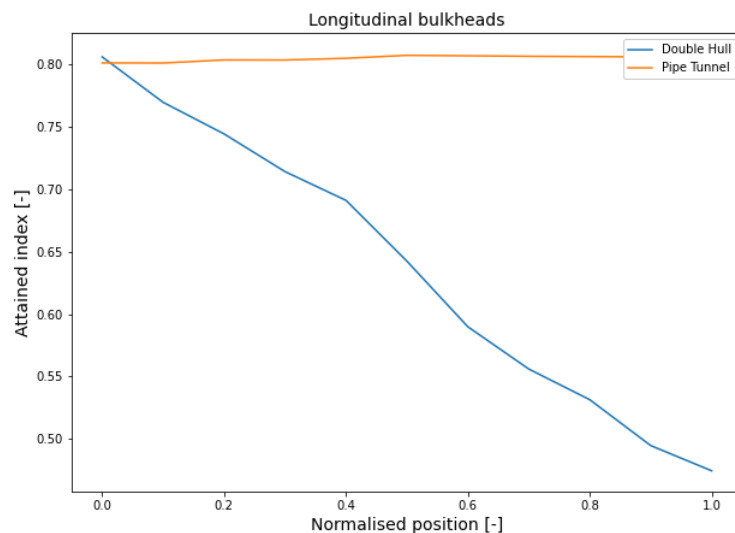


Figure 5.48: Sensitivity in the normalised range of the longitudinal bulkheads with respect to the attained index A.

Only two longitudinal bulkheads are located in the middle section. The difference in influence by these two variables is clearly visible in figure 5.48. The pipe tunnel is located in the middle of the double bottom. Together with the small range it can extend from the middle, an increase in breadth of the pipe tunnel does not influence many new damage cases due to the penetration depth of these cases simply not reaching the pipe tunnel. The inside of the double hull changes the size of the cargo hold and distance from the side shell significantly, which results in a relatively large influence on the attained index.

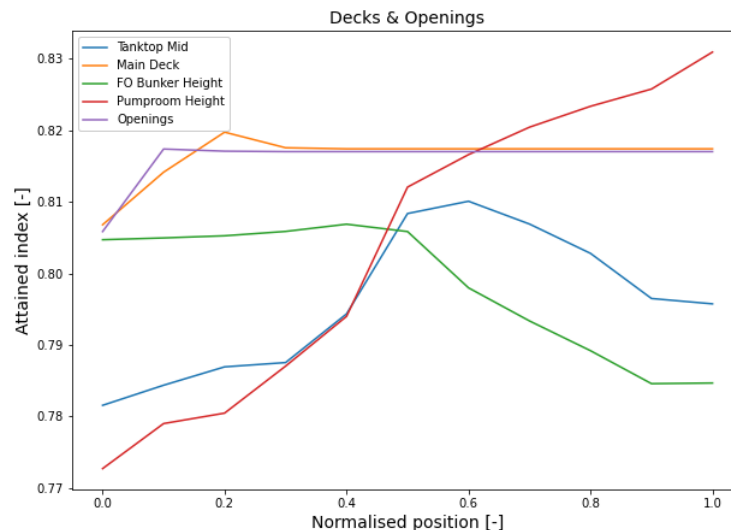


Figure 5.49: Sensitivity in the normalised range of the decks and openings with respect to the attained index A.

The level of influence on the attained index is relatively the same for the decks and openings. However, some particularities can be observed from figure 5.49. The height of the openings show a relatively large influence in the first quarter of its range, but then suddenly stops influencing the attained index at all. The height of the FO bunker tank only negatively influences the attained index the higher it becomes. This is in contrast to the height of the pumproom, where an increase in height seems to increase the attained index almost exponentially.

The sensitivity analysis by hand discussed in this chapter only shows the influence of the parameters with respect to the base ship model. This is therefore not a global analysis that results in the sensitivity of the parameters over the entire parameter space. However, as the base ship model is a realistic model, it does show the behaviour of the parameters in the vicinity of a reasonably optimised model. Combined with the post processing Pearson correlation matrix and the Morris sensitivity analysis, the optimisation can be verified and insight in the PDS calculation is generated.

5.4.4. Conclusion

The conclusions following the results of the three sensitivity analysis methods are combined and summarised in this section to verify these methods, as well as to further strengthen the confidence in the results of the optimisation methods.

By combining the results of all three sensitivity analysis methods the following insight is generated:

- Most parameters behave non-linear/non-monotonic;
- Influence of parameters on the attained index can be distorted by their respective boundaries;
- Morris method is therefore only reliable for most influential variables;
- Correlation matrix can be useful, but should be viewed with suspicion at all times;
- The combination of different sensitivity analysis methods together with an optimisation method, provides significant insight in the behaviour of the PDS calculation.

The non-linear and non-monotonic behaviour of the parameters greatly influences the ability of the Morris method to distinguish the influence of the parameters as the relative confidence interval increases significantly due to this behaviour. Although the bias of the correlation matrix is partially solved, the correlation coefficients of the parameters are still influenced by this. Therefore, when looking at the sensitivity analysis methods on their own, they can show a distorted image of the real behaviour of the parameters. By combining the three methods, a clear image can be computed.

The following behaviour of the optimiser is verified and further insight is given by the sensitivity analyses:

- Differences between aft and forward cargo hold bulkhead due to their respective distance from the hull;
- Openings and main deck do not significantly influence the attained index in their current boundaries, but do so beyond these boundaries;
- Even though the number of water ballast bulkheads has a lot of influence on the attained index, their location, within their respective boundaries, do not;
- A higher pump room volume results in a higher attained index;
- The shape of the FO tanks is not of importance to the attained index;

These conclusions are applicable to ships with a similar design, where the focus is on the parameters surrounding a single cargo hold. Generality is important as it can help designers create different rules for designing similar ships, resulting in less time spent on the subdivision of these designs due to a more favourable starting point.

5.5. Design Process Implementation

The results from sections 5.1 till 5.4 make up the framework described in the main research question. The research focuses on the preliminary design stage of ship design and the aim is to show that the results can be used to create a starting point for the designer, and to verify the starting point and understand the behaviour of the PDS calculation.

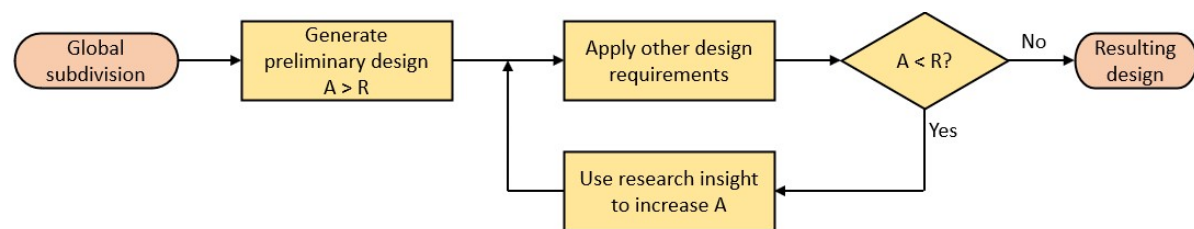


Figure 5.50: Flowchart showing the use of the research results as a base of design

It is shown in section 5.1 that the addition of bulkheads significantly influences the survivability of the ship. However, to obtain the exact increase, every design should be optimised. This is not feasible due to the available time and corresponding time that is spent in these first stages of the design. Therefore, the first stage can be used to quickly determine one or more designs that is further investigated. This does not significantly change the current method of adding bulkheads. The optimisation however, shows good results in understanding the behaviour of the PDS calculation and can be used to establish a Pareto front, where a selection of different ship designs can be selected that each provide the highest cargo hold volume for their respective attained index (vice versa the same applies). Together with the insight generated for generalised single hold ships, a new approach to ship design is presented where the PDS calculation is used as a base of design. The choice in preliminary design can be chosen such that the margin the attained index has from the required index, corresponds with the expected level of change the design is going to be subjected to. This level of change is based on all other design requirements that are applicable to the respective design project. Figure 5.50 shows a flowchart of how the research can be used as a base of design.

By using the PDS calculation as a base of design, the full freedom potential can be capitalised on and more design freedom can be created for the other design requirements. This can lead to a significant improvement compared to other design approaches, where the PDS requirements are implemented after many other requirements are implemented and the subdivision of the ship, with respect to the damage stability, already lost much of its freedom.

Not only the lead time estimation saving is an important factor in the design process, also the increase in design exploration must be taken into account. During a normal design process, the designer uses a reference ship as a starting point to identify the to be expected capabilities of the design. Then,

a small number of designs are created which are made up off the knowledge and experience of the designer. Depending on the designer, a part of the parameter space is used to determine these designs. The advantage of an optimisation method is that it fully explores the parameter space, creating far more designs than the designer is able to generate in the same amount of time. This way, the chances of finding more fitting and innovative designs increases significantly. In this case, 200 ship designs are generated over approximately 36 hours with a minimum of approximately 13 Pareto efficient designs.

The lead time of computing the Pareto front is a summation of the processes listed in table 5.12:

Table 5.12: Summation of the lead time of all processes required to use the framework proposed in this thesis

Process	Time required (hrs)
Parametric model	2
Optimisation set-up	1
Optimisation run	36
Sensitivity set-up	1
Sensitivity analysis run	48
Interpreting results	2
Total	89

A total of 89 hours is approximately required to set-up, run and interpret both the methods proposed in this framework. The total hours spent by the designer is however only six hours, as the execution of the methods can be performed in the background. Even better would be to start the methods simultaneously on different available computers just before the weekend. This way, the effective time of the whole optimisation and sensitivity analysis during worktime is reduced to six hours. Regarding the set-up, the parametric model requires the most time as all bulkhead and openings should be defined and connected to the lists. The model should be checked to determine everything is done accordingly. Setting up the optimisation and sensitivity analysis is a relative quick method as the same code is used for every single project. Only the boundaries and constraint functions should be determined for the optimisation. The sensitivity analysis only requires the boundaries to be determined. The same goes for the other two sensitivity analysis methods proposed in this thesis. Running the methods requires the longest lead time, approximately 36 and 48 hours respectively.

The biggest gain in the process is the quality and variety of the proposed designs in a relatively short amount of time. In an interview with one of the lead naval architects of C-Job (appendix D, it is said that approximately the same amount of time is needed to produce the initial design. However, the method of finding the resulting design is similar to a local optimisation, where a certain starting point is chosen that is changed slightly, whereby the winner is used for further optimisation by hand. This is where the proposed global SAMO-COBRA optimiser distinguishes itself from the current method used. The global optimiser is able to fully explore the parameter space, preventing the convergence to a local optimum due to bias of the designer. The knowledge added by the sensitivity methods strengthens the confidence in the designs and enables the designer to resolve any issues that come up in later stages of the design, increasing the efficiency even more.

According to the interview, a similar view on the implementation is given regarding the prevention of unused margin on the attained index. Not a huge difference is expected by the naval architect, but these last percents advantage do have the potential to distinguish the companies designs from the competition.

6

Validation

This chapter aims to show the validity of the results and methods used in this research. Results do not only need to be verified, but also validated. This means that the even though the results may be correct, they should also satisfy the research requirements set by the research goal and research questions. In this chapter, a validation method is used to validate the methods and their applicability to the problems of this research. For validating the results obtained by the different methods in this research, the validation square by Peterson et al. [34] is used. The main goal of the validation method is to: "Validate design research in general, and design methods in particular.". The validation square consists of four quarters as can be seen in figure 6.1 below.

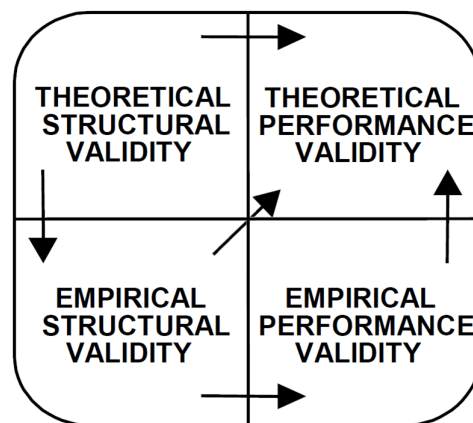


Figure 6.1: Validation square by Peterson et al. [34]

6.1. Theoretical Structural Validity

The theoretical structural validity consists of, accepting the construct's validity and accepting the method consistency. This is the first step in the validation square process and will be handled in this chapter.

The construct is in this case the methods that constitute the optimisation method and sensitivity analysis, so the SACOBRA [72], SAMO-COBRA [73], Morris [79] and Pearson [104] method. The Morris method and Pearson correlation coefficient are two widely accepted and used methods. They are used for all kinds of problems throughout the literature. Also the fact that both methods are relatively old (1991 and 1896 respectively) and are still widely used today, shows the validity of both of these methods. The SACOBRA and SAMO-COBRA methods are relatively new compared to the sensitivity analysis methods (2017 and 2021 respectively). Therefore, more literature research needed to be performed to increase the confidence in these methods. The SACOBRA optimisation method is published in applied soft computing volume by Elsevier and is cited 37 times. The SAMO-COBRA optimisation method is based on the SACOBRA optimisation method and is developed by R. de Winter, a C-Job employee. The algorithm was previously used by P.D.H. Bronkhorst for his master thesis regarding

concept design by involving seakeeping for offshore service ships [105]. This research showed good results with using this algorithm for its optimisation problem. The method has been published in the book "Evolutionary Multi-Criterion Optimization" and published by Researchgate. It has only been cited four times, but that can be contributed to its relatively short time since its been published. The DELFTship program, that is used to create the parametric model and perform the PDS calculation, is a well accepted and tested visual hull modelling and stability analysis program. It is used by many top naval architect bureaus, shipbuilders and shipping companies like, Huisman, IHC, Ulstein, DEME and Van Oord [10]. The program is subjected to strict requirements set by ship classification societies that inspect and maintain technical standards for the construction and operation of ships. The DELFTship program is therefore regarded to as a trusted and suitable program to use.

To validate the method consistency, flow chart representations are used as shown in figures 4.1 4.9 and 4.14. They show a clear overview of the method and its inputs and creates more confidence in the consistency of the methodology. For both the optimisation and sensitivity analysis, the flow charts are based on the needs and properties of the methods themselves, leaving little room for a wrong approach. There is more freedom to the parametrisation of the base ship model. Different approaches have been devised and tested as is explained in chapter 4.3. However, it is relatively easy to validate the working of the parametric model, as its only function is to translate the output of the optimisation and sensitivity methods into a new design. The new design can simply be compared to the output of the methods to show the design is correct. The output of the PDS calculation is then assumed correct, as this is performed by the DELFTship program itself.

6.2. Empirical Structural Validity

The second quarter is building confidence in the example problem, in this case the base ship design combined with a PDS calculation. This is done the following way:

- Document that the example problem is similar to other problems that have been used on these methods;
- Document that the example problem represents the actual problem for which the method is intended;
- Document that the data associated with the example problems can support a conclusion.

Chapters 3.3 and 3.5.1 describe the search for a fitting optimisation method for this particular optimisation problem, while chapters 3.4 and 3.5.2 describe the same thing for the sensitivity analysis. Therefore, it is already relatively clear that the problem fits the used methods in this research. For further increase in the fitting of the problem to the methods used, it can be stated that the SAMO-COBRA algorithm used by Bronkhorst was also applied to a parametric model built in the NAPA software and an expensive optimisation model. The correlation matrix was also used by Bronkhorst as a method of analysing the sensitivity of the parameters. The Morris method can be applied to many different models as can be seen in the literature. For determining the amount of trajectories in chapter 5.4, a paper was used a base, that also used an expensive model with a similar amount of parameters as is used for this problem.

The problem presented in this research can be regarded to as a "real world problem". The ship modelled in the DELFTship program is based on an actual ship design and represents one of the stages of designing a ship. By optimising the parametric model and performing a sensitivity analysis, an actual new proposed design method is executed. Therefore, it is safe to say that the problem presented in this research represents the actual problem for which the method is intended.

The data associated with the example problem is partly based on the actual base ship design and is partly determined by both the researcher (Boundaries, constraints and objectives) and the optimisation and sensitivity method. The parametric model makes sure that all desired data (Attained index) can be computed from the input of the model (infill points). Both the optimisation and sensitivity analysis use the same type of infill points to "steer" the parametric model and to obtain the attained index as output. The method as it is set-up now, is very suitable for generating the desired results, as can be seen in chapters 5.2 and 5.4.

6.3. Empirical Performance Validity

The third quarter consists accepting the usefulness of the method for some example problems and accepting that usefulness is linked to applying the method.

The first part is all about proving that the results and conclusions from these respective results, are useful for industrial purposes, scholar purposes, or both. In other words proving that cost can be reduced, safety improved and knowledge is produced that can help produce more scientific knowledge. This relates back to the research question stated in chapter 1.5 and the societal relevance of chapter 1.3. The framework set up in chapter 4 and its results, discussed in chapter 5, contribute to less time needed to generate an initial design, create more insight in the behaviour of the PDS and to lay a base from which a more extensive and holistic framework can be created (Recommendations for future research are presented in chapter 7.2).

The second part of the empirical performance validity is comparing the solutions with and without the construct. This way, a quantitative comparison can be made between using the methods from this study and trying to obtain the results without the use of these methods. The problem is that it is simply not possible to compare the use of the optimisation and sensitivity analysis methods with other methods for this specific case study. There is simply not enough time to perform a complete optimisation and global sensitivity analysis by hand or the use of other methods for this case study. However, a paper by Boulougeris et al. showed that the use of a genetic algorithm used between 192 and 1536 iterations, where the latter number of designs showed much better results than the former. The SACOBRA and SAMO-COBRA optimisers only require 150 iterations before significantly better designs are proposed by the methods. Therefore it is a much better method to be used, regardless of the computation time per iteration. In the papers by de Winter [73] and Bagheri [72] regarding the optimisers, it is proved that they show significant increase in reaching a state of convergence compared to other state-of-the-art methods. The Morris method is proven to be the most time efficient method by a significant margin in chapter 3.4. The minimum number of trajectories can be used for the 5.4.1 and further in appendix C.1. This means that the Morris method is not only the fastest method in general, but it can be assumed it is as well for this application.

6.4. Theoretical Performance Validity

Theoretical performance validity is the last step in the validation square. It is the expansion of the empirical performance validity, which was meant to show the usefulness for some limited instances (case study problem). This last step is to accept the usefulness of the methods beyond the example problem. In other words, to claim generality of both the research methods as well as the constructs used. This research aimed to show the possibility of applying a state-of-the-art optimisation methods on parametric models and the PDS calculation as well as to generate more insight in the behaviour of the variables for single hold ships. Although a case study was used as a "vessel" to generate all the results, generality was always the goal of this research. The use of a base ship to be used as a case study should not have the effect of limiting the research to that case. By focusing on the middle section and running different single objective optimisation experiments next to the multi-objective optimisation, a more general conclusion and recommendations were reached. As explained by Pederson et al. [34]:

"The purpose of going through the Validation Square is to present 'circumstantial' evidence to facilitate a leap of faith, i.e., to produce belief in a general usefulness of the method with respect to an articulated purpose."

This refers to the "External validity" of the research [106], or the validity of using the applied methods outside of this case study. The conclusion at the end of sections 5.2 and 5.3 present the verification that the used constructs, or methods, can be applied to the base ship model. However, they also show the certain design choices that were made by the algorithm. These design choices are described in such a way that they can be applied to any single hold ship design. An example is the behaviour of the openings, or the result of the difference in permeability. The base ship showed that these two variables influenced the design of the design, but this goes for all ship designs. Conclusions that were specifically applicable to single hold ships are the findings regarding the shielding of the cargo hold and how the algorithm tried to accomplish that.

7

Discussion, Recommendations and Conclusion

This final chapter aims to combine all the results from the methods used in this research and to draw a conclusion based on the knowledge gained. First, the research questions are listed again and the answers to these questions provided. Next, the contributions of this research to the scientific community are presented that can be used to expand the research regarding this subject. Recommendations are then given as to what these expansions might be, based on the limitations of this research. A conclusion is drawn to complete the research, based on all items listed above. Finally, a personal reflection is added that gives me, the author, the opportunity to review the personal developments over the course of this research and to present personal advice to anyone starting their thesis.

7.1. Discussion of the Main/Sub-question(s)

What parameters influence the attained index based on the PDS calculation?

This sub-question was used to provide a basis to not only identify the parameters that influenced the attained index, but also to summarise and understand the PDS calculation in order to link the results back to the requirements and explain the choices by the algorithm. This proved to be helpful as can be seen in chapter 5.2, where many references are made to chapter 2 in order to provide evidence for the resulting behaviour of the model. It was established that the parameters found, could be categorised into two different sets, namely the discrete and continuous parameters and parameters that influence the actual design or only the settings of the calculation. The identification of these two categories and the choices of which to use defined the course of this research.

Based on the properties and requirements, what optimisation and sensitivity analysis method is most suitable for the PDS calculation?

The choice of what parameters to use and the base ship model were the foundation of the search for suitable methods. The SACOBRA algorithm was first identified and selected as the importance of multiple objectives instead of stringent constraints was first overlooked. During later stages of the research, the choice of adding a second objective, namely the cargo hold volume was made. A new algorithm was chosen (SAMO-COBRA), which was an extension of the single-objective optimiser. This proved to be very efficient and showed the desired results. As the single-objective optimiser was already fully operational at this stage, the decision was made to include it in the research as a way of verifying the multi-objective optimiser and to use it as a tool to experiment with different design choices. The use of a global sensitivity analysis proved to be rather difficult, as most of the methods required an excessive amount of function evaluations in order to acquire a reasonable confidence interval. The Morris one-at-a-time method was identified as it required the lowest amount of function evaluations. As this method does not provide any information regarding the correlation between the parameters, the choice was made to include a Pearsons correlation matrix. To verify the results of both of these methods, a small sensitivity analysis by hand was performed. This combination proved to be an effective method of providing insight in the PDS calculation.

How can the base ship model be parameterised in order to be subjected to different optimisation and sensitivity analysis methods?

The parameterisation of the base ship model proved to be the most important aspect of this research. A well parameterised model can be used for many different applications and is able to generate a significant amount of results and therefore knowledge. As the ship is composed of many different independent and semi-independent variables, the decision was made to only focus on the middle section of the ship. The parameters in this area were more linked to the actual research question of the application to a single hold ship. This also presented the opportunity of using all parameters in this section due to the removal of the parameters in the aft and forward sections of the design on the optimisation.

To what extent is it possible to provide a preliminary design by the use of an optimisation algorithm?

The preliminary design resulted from the two optimisation stages, where the amount of bulkheads was determined in the first optimisation stage, and the multi-objective optimiser was used for the second. As the first optimisation stage proved to be needing more information to determine the actual best design, two designs were used as input for the second optimisation stage. The SAMO-COBRA optimiser showed good results for providing a preliminary design based on the input (objectives, constraints and variable boundaries). Notable is the result of comparing the two designs. The two bulkhead design proved able to reach the same attained index and have an equal relation between the attained index and the cargo hold volume as the five bulkhead design. This indicates that the graph provided in figure 5.1, does not accurately depict the difference between the number of bulkheads and can therefore not be used as a first indication of how many bulkheads are needed without optimising their location first.

What set of parameters has the most influence on the attained index?

This sub-question is answered by a combination of all methods used during this research. The Morris method provided an indication of the influence of the individual parameters. Due to the non-linear, non-monotonic behaviour of the parameters, the confidence interval of the other parameters increased, removing the ability to confidently determine the order of influence of the parameters. The decision was made to combine the individual correlation matrices for the sampling and optimisation and create an improved matrix. This proved better than the initial matrix. The results of the sensitivity analysis by hand were used to clarify the other results and to increase confidence in the other methods.

An important note regarding the influence of the parameters is that the boundaries given to the parameters were within the realistic naval architectural considerations. Therefore the resulting influence of the parameters is not their absolute influence, but their influence within realistic boundaries. The following insight is generated by the optimisation stages and sensitivity analyses regarding the influence of the parameters and their analysis methods:

- Most parameters behave non-linear/non-monotonic;
- Influence of parameters on the attained index can be distorted by their respective boundaries;
- Morris method is therefore only reliable for most influential variables;
- Correlation matrix can be useful, but should be viewed with suspicion at all times;
- The combination of different sensitivity analysis methods together with an optimisation method, provides significant insight in the behaviour of the PDS calculation.

The following behaviour of the multi-objective optimiser is verified and further insight is given by the sensitivity analyses:

- Differences between aft and forward cargo hold bulkhead due to their respective distance from the hull;
- Openings and main deck do not significantly influence the attained index in their current boundaries, but do so beyond these boundaries;
- Even though the number of water ballast bulkheads has a lot of influence on the attained index, their location, within their respective boundaries, does not;
- A higher pump room volume results in a higher attained index;
- The shape of the FO tanks is not of importance to the attained index;

7.2. Recommendations

In order to efficiently perform a research, the subject is demarcated such that a certain level of depth can be reached. This is also done for this research, resulting in many elements of the ship design spiral to be purposefully ignored. However, during the research, some of the elements that are ignored or new elements that have been found, prove to be of high value for the results. Due to the limited time available and desired depth of the research, these elements are not further researched, but listed below and serve as inspiration for future research.

Performing the actual weight calculation in the first stage

The method of determining if the first stage optimisation is converged yes or no, now relies solely on the difference of attained index. This means that it is still the designer who decides whether or not the addition of another bulkhead and therefore increasing the attained index is worth the increase in weight. By expanding the first stage so that it is able to include the addition of weight, a more educated decision can be made to determine the state of convergence of the first optimisation stage.

Multi-Threading

This research was a quest for not only the best possible solution, but also the most efficient algorithm to use for finding this solution. The SACOBRA and SAMO-COBRA algorithms were indeed very efficient, time saving algorithms that simultaneously performed very well. However, the DELFTship program and SAMO-COBRA algorithm allow for multi-threading. As explained in chapter 3.3.4, multi-threading is an effective tool to speed up the process of optimisation, provided that there are enough cores available to support this method. Due to the available time, no multi-threading was used to further decrease the run time of the optimisation. However, this is relatively easy and quick addition to this framework and would be the first addition to add in my view.

Expand on GM (wave scatter plots)

Determining the amount of bulkheads also influences the roll period of the ship, as the GM changes quite significantly during this exercise. The distance of the GM could therefore be coupled to wave scatter diagrams provided for the operational area the ship will be designed for. This way, more pleasant roll periods for both the ship and crew could be realised. It is been long known that the operating economics of the ship are influenced by the roll period as it can reduce crew efficiency, cause damage to cargo and therefore ship and increase the resistance [107]. By determining the amount of bulkheads based on the resulting roll period, new insight can be generated that could potentially change the designers view on handling the weight of the ship compared to the resulting attained index.

Expanding the research to a more holistic approach

In an ideal world, an optimisation and sensitivity analysis method is able to create feasible designs and compare all parameters corresponding with every single item on the design spiral by Evans [4] or similar. This is not a realistic goal, at least not for anywhere in the "near" future as there are many fundamental issues often encountered in optimisation problems. A paper by Weise et al. shows a part of these fundamental issues, which include premature convergence, ruggedness, causality, deceptiveness, neutrality, epistasis, robustness, overfitting, oversimplification, multi-objectivity, dynamic fitness, the No Free Lunch Theorem, etc. [108]. Combining these issues to an all encompassing optimisation method is therefore unrealistic. However, there are many different ways to expand this research to include more parameters (aft/fwd sections), regulatory items (such as deterministic double bottom regulations), different objectives, etc. that are within a feasible scope of work and reliability of the model and result in great new insight.

Another global sensitivity analysis

This research concluded that the Morris method was, even though it is regarded to as the least time consuming global sensitivity analysis, not able to accurately determine the influence of all parameters with a low confidence interval. There are however, many more different sensitivity analysis methods that can be investigated that show good results for a sufficient parameter space exploration. Now, only post processing methods for the output of the optimisation methods were applied due to insufficient time left to investigate a new approach. This resulted in great insight, but the use of another advanced sensitivity analysis could provide even more insight.

7.3. Conclusion - Main Research Question

To conclude this research, the main research question is restated and the findings are summarised and their significance to the scientific community and maritime industry is presented. The main research question the following: *To what extent can a design framework study and optimise the parameter space influencing the attained index during initial stages of the design for ships with a single hold, while maintaining the effectiveness of the design?*

The framework consists of two primary methods to answer the main research question. Namely, the use of an optimisation method and global sensitivity analysis method that aimed to provide a preliminary design and show the level of influence of the parameters respectively. Generality was aimed for in order to extend the applicability of the research from the current case study to single hold ships in general. Although it is still found that any optimisation method should be viewed with suspicion at all times, the multi-level optimisation showed good results in proposing a set of preliminary designs. The only limitation of the algorithm was shown in the lower attained index region for the water ballast bulkheads. However, this is only a small percentage of the hypervolume and is relatively easy to improve by hand. It is still assumed that the design is located in the global optimum for all other parameters. Therefore the algorithm is still considered as a suitable method. The proposals showed interesting trends with respect to the decisions made by the algorithm. It could be seen that the highest priority for single hold ships is the protection of the cargo hold. This is not a shocking realisation in itself. However, the methods used by the algorithm to reach this goal provide great insight in how to approach such a kind of ship during this stage in the design. The single objective optimiser showed that it could be used to investigate certain decisions and properties of the design. This comes especially handy as there are numerous methods to, for instance, create more distance between the cargo hold and the hull. These methods can be implemented in the optimiser and their influence on the design is then provided. The sensitivity analysis results provided by the Morris method showed that the parameters behaved mostly non-linear and non-monotonic and were therefore difficult to distinguish when looking at their influence on the attained index. The use of the correlation matrix and the verification by hand provided the rest of the insight that was needed to answer the main and sub research questions of this thesis. In the end, the sensitivity analysis explained and verified the decisions made by the algorithm and provided some interesting insight in the characteristics of the parameters and the compartments that were assigned to them. The influence of the parameters was measured over their respective boundaries. These boundaries were chosen such that they represented realistic locations in an actual ship design. This greatly influenced the level of influence these parameters had on the design. However, as this research is performed from the perspective of the designer, this is exactly the type of influence that is aimed for. Therefore, all results for the sensitivity analyses are normalised.

As was stated in chapter 1, the freedom potential offered by the PDS regulations to use them as a base of design is difficult to capitalise on when it is unclear what the behaviour of- and coherence between the parameters is. By providing an optimised preliminary design and insight in this behaviour and coherence, the design freedom that comes with the PDS regulations can now be fully explored. Ship designers can use the framework as a base of design and can continue using it in later stages as well, when, due to other design requirements, the design does not satisfy the required index anymore. The aim of this research is therefore fulfilled.

7.4. Personal Reflection

In 2013, I started as a first year student Maritime Officer at the Maritime Institute Willem Barentsz. Interested in technical challenges and wanting to be part of a group of professionals that excelled in their respective field of expertise. Although I had no previous connection to the maritime sector, I figured the two previous named requirements for my future career choice where to be found in this sector. The more I learned about what was necessary to operate and maintain the machinery on board, the more I became interested in the fundamentals of ship design itself. During my time at sea (which I thoroughly enjoyed) I realised that for me, there was more to be discovered about the choices and compromises that are part of the design process, rather than to just accept that things were designed the way they were. This knowledge I hoped to find at the TU Delft, where I started studying in 2019. In the beginning of my pre-master I questioned myself whether it wasn't a little too much fundamentals for me, and that I should go back to the more practical side of shipping/ship building. But the more I began to understand the basic math and science, the more I became aware of the potential that a good understanding of

the fundamentals had to offer. To me, the possibilities became endless and I decided that this was the right path for me to continue. When people ask me why ship design is so much more interesting for me than other technical disciplines, I find it hard to give a single answer. Maybe the fact that ships are highly advanced, complex "beings" that are designed to operate autonomously in one of the most hostile environments on the planet. Or the versatility of the maritime sector with a very open minded perspective towards the future. Notice that I refer to ships as "beings", as I have the same problem of finding a single answer when I think of what a ship is to be referred to. Some would say it is a structure, as it is just like a building, a composition of structural elements that is build around whatever it needs to house. Some would say it is a piece of machinery, as the main purpose of a ship is to convert energy into the moving of the ship or other types of movement it is designed for. The simplest one you frequently hear is that a ship is referred to as a vessel, implying it is just a floating object. For me, its all of those combined and much more than that. A ship has a function, characteristics and is, together with the crew and its highly automated systems, self thinking and regulating. It only needs fuel and supplies in order to perform complex task without the need of others, but is also able to communicate and operate together with other ships. To me this feels like a living "being", and I feel that it is much more interesting to look at ships that way.

For my thesis I tried to aim for two personal development goals, namely, increasing my knowledge in one of the disciplines that is part of the base of design of a ship and to increase my programming skills. This thesis definitely satisfied these goals and gave a lot more insight in the process of designing a ship, taking the damage stability as a starting point. It also gave me a sense of the potential and limitations of using optimisation and sensitivity analysis methods during the design. Using an optimisation algorithm on real world problems defined by many variables, constraints and objectives requires many hours of research and literature review in order to come up with a feasible plan of approach. I can safely say that I misjudged the scale for different parts of the process, such as creating a well defined parametric model, or the amount of decisions that where necessary to create a robust, "watertight" research. I approached the thesis based on a statement made by Peter de Vos, MT Master coordinator. He said that the thesis was to be seen as a project, where you are your own project manager. This helped me to create a network of people that where interested in my research and could provide me with their professional opinion about my choices during this research. The ability to bring all of these opinions together and channel it into the best possible research approach was for me the most interesting part of this period. The personal development goals that I set out to achieve during this research where definitely met, with the help of all people involved. I discovered the potential and limitations of the PDS, the potential and limitations of programming, but also my personal potential and limitations and how to further improve myself in the future. In the end, I tried to enjoy my thesis as much as possible. It could very well be the last time during your career that you can focus on one subject for such a long period of time, without people expecting you to use your time for other work as well. This made the journey more pleasant and made me realise that it wasn't so bad as how people sometimes portray it. But, there are always things that I would do differently if I had to start again or would like to give as a piece of advice for anyone starting their thesis. It is important to share these findings, as other people did the same for me, when I first started nine months ago. The tips shared with me before the start of my thesis that helped me throughout are:

- The thesis is a project, where you are the project manager;
- Surround yourself with people that motivate you and show interest in your thesis;
- Try to gather as much opinions as reasonable and channel them into an approach that fits you best;
- The literature review is the most important part of the thesis.

Next, the tips I would like to give to students based on my own experience:

- Start by teaching yourself how to manage a project, learn to use tools that help you maintain an overview at all times;
- There are many more people interested in helping you than you would think;
- Don't stare yourself blind on a subject when you loose inspiration, reach out or temporarily focus on other parts of the thesis;
- You can't have your best day every single day. Sometimes its okay to call it a day when you don't have the focus.

Bibliography

- [1] Apostolos Papanikolaou. *Ship design: Methodologies of preliminary design*. Springer Netherlands, Jan. 2014, pp. 1–628. ISBN: 9789401787512. DOI: 10.1007/978-94-017-8751-2.
- [2] Kurt Wendel. *Subdivision of ships*. USA: Universitat Hannover, 1968.
- [3] Philip A Wilson and Ship Stability. *Basic Naval Architecture*. Tech. rep.
- [4] J Harvey Evans. “Basic Design Concepts”. In: *Journal of the American Society for Naval Engineers* 71.4 (1959), pp. 671–678. URL: <https://onlinelibrary.wiley.com/doi/abs/10.1111/j.1559-3584.1959.tb01836.x>.
- [5] Roy de Winter et al. “Optimizing Ships Using the Holistic Accelerated Concept Design Methodology”. In: *Practical Design of Ships and Other Floating Structures*. Springer, 2019, pp. 38–50.
- [6] Herbert J Koelman and Jakob Pinkster. *Rationalizing the practice of probabilistic damage stability calculations*. Tech. rep. 3. 2003, pp. 239–253.
- [7] Dracos Vassalos et al. *Design implications of the new harmonised probabilistic damage stability regulations*. Tech. rep. 2007, pp. 339–361.
- [8] Cantekin Tuzcu. “Development of the factor-s: The damage survival probability”. In: *8th International Conference on the Stability of Ships and Ocean Vehicles (2003)*.
- [9] C-Job. *About us*. 2022. URL: <https://c-job.com/about-us/>.
- [10] DELFTship Maritime Software. *DELFTship: Visual hull modelling and stability analysis*. URL: <https://www.delftship.net/>.
- [11] Walter Mattli and Ngaire Woods. *The Politics of Global Regulation*. Princeton University Press, 2009.
- [12] *Safety and Shipping Review 2021 -An annual review of trends and developments in shipping losses and safety*. Tech. rep. Allianz global corporate & specialty, Aug. 2021. URL: www.agcs.allianz.com.
- [13] *Marine Insurance Act 1906*. 2020.
- [14] Jan Babicz. *Encyclopedia of ship technology*. 2nd ed. Helsinki: Wartsila Corporation, 2015.
- [15] *The 2020 World Merchant Fleet Statistics*. Tech. rep. Equasis - Electronic Quality Shipping Information System, Dec. 2020.
- [16] *Maritime Safety Committee (MSC), 92nd session, 12 to 21 June 2013*. 2013.
- [17] Marine Casualties Investigative Body. *Cruise Ship Costa Concordia Marine Casualty on January 13, 2012 Report on the safety technical investigation*. Tech. rep. Ministry of Infrastructures and transports.
- [18] Alan Taylor. *The Wreck of the Costa Concordia*. Jan. 2012. URL: <https://www.theatlantic.com/photo/2012/01/the-wreck-of-the-costa-concordia/100224/>.
- [19] Kathrine Ilje Nerland. *A proactive approach for safety - Updated*. July 2019.
- [20] Tony R. Walker et al. “Environmental Effects of Marine Transportation”. In: *World Seas: An Environmental Evaluation*. Halifax: Elsevier, 2019. Chap. 27.
- [21] Hassan Partow et al. *X-Press Pearl Maritime Disaster Sri Lanka*. Tech. rep. UN Environmental Advisory Mission, June 2021.
- [22] Willem de Niet. *‘Problemen X-Press Pearl al langer bekend’*. June 2021. URL: <https://www.schuttevaer.nl/nieuws/zeevaart/2021/06/18/problemen-x-press-pearl-al-langer-bekend/?gdpr=accept>.

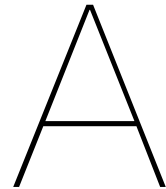
- [23] X-Press Pearl Containership partially sinks during tow attempt. June 2021. URL: <https://www.maritime-executive.com/article/x-press-pearl-containership-begins-sinking-during-tow-attempt>.
- [24] Nishan Degnarain. *Global Shipping's moral authority plunges in Mauritius as pope intervenes in Wakashio saga*. Sept. 2020. URL: <https://www.forbes.com/sites/nishandegnarain/2020/09/03/global-shippings-moral-authority-plunges-in-mauritius-as-pope-intervenes-in-wakashio-saga/?sh=11b3fbc953a1>.
- [25] Haakon Lindstad, Inge Sandaas, and Sverre Steen. "Assessment of profit, cost, and emissions for slender bulk vessel designs". In: *Transportation Research Part D: Transport and Environment* 29 (2014), pp. 32–39. ISSN: 13619209. DOI: 10.1016/j.trd.2014.04.001.
- [26] Oyvind Buhaug et al. *Second IMO GHG*. Tech. rep. London: International Maritime Organization, 2009.
- [27] Theo Notteboom, Thanos Pallis, and Jean Paul Rodrigue. "Disruptions and resilience in global container shipping and ports: the COVID-19 pandemic versus the 2008–2009 financial crisis". In: *Maritime Economics and Logistics* 23.2 (June 2021), pp. 179–210. ISSN: 1479294X. DOI: 10.1057/s41278-020-00180-5.
- [28] Ole Martin Djupvik. "Probabilistic Damage Stability Maximizing the Attained Index by Analyzing the Effects of Changes in the Arrangement for Offshore Vessels". PhD thesis. Norwegian University of Science and Technology, June 2015.
- [29] Stian Røyset Salen. *Probabilistic Damage Stability Evaluating the Attained Subdivision Index by Analysing the Effect of Changes in the Arrangement and Intact Stability for an Offshore Vessel*. Tech. rep.
- [30] Erik Sonne Ravn. *Probabilistic Damage Stability of Ro-Ro Ships*. Tech. rep. 2003.
- [31] Evangelos K Boulougouris, Apostolos D Papanikolaou, and George Zaraphonitis Ntua-Sdl. *Optimization of Arrangements of Ro-Ro Passenger Ships with Genetic Algorithms*. Tech. rep.
- [32] George Simopoulos, Dimitris Konovessis, and Dracos Vassalos. "Sensitivity analysis of the probabilistic damage stability regulations for RoPax vessels". In: *Journal of Marine Science and Technology* 13.2 (May 2008), pp. 164–177. ISSN: 09484280. DOI: 10.1007/s00773-007-0261-x.
- [33] Dracos Vassalos and Luis Guarín. *Designing for Damage Stability and Survivability-Contemporary Developments and Implementation*. Tech. rep. 5. 2009, pp. 57–69.
- [34] Kjartan Pedersen et al. "Validating Design Methods and Research: The Validation Square". In: *2000 ASME Design Engineering Technical Conferences*. Baltimore, Maryland, Aug. 2000.
- [35] Odd Olufsen and Gunnar Hjort. *Probabilistic damage stability*. Tech. rep. DNV GL AS, Mar. 2014.
- [36] A.B. Biran. *Ship Hydrostatics and Stability*. Butterworth-Heinemann, 2003.
- [37] D.G.M. Watson. *Practical Ship Design*. 1st ed. Vol. 1. Elsevier, 1998.
- [38] IMO. "01 ICLL 1966 International Convention on Load Lines 1966 (MSC.172(79))". In: (July 1968).
- [39] Odd Olufsen and Gunnar Hjort. *An introduction to revised chapter II-1 of SOLAS- 74*. Tech. rep. 2013.
- [40] Marie Lützen. *Ship collision damage*. Tech. rep. 2014. URL: <https://www.researchgate.net/publication/264374677>.
- [41] IMO. *Resolution MSC.194(80) (adopted on 20 May 2005) Amendments to the International Convention for the Safety of Life at Sea, 1974, As amended*. Tech. rep. 2005.
- [42] IMO. "IMO Resolution MSC.216(82), amendments to the international Convention for the Safety of Life at Sea, 1974". In: (Dec. 2006).
- [43] Myung-II Roh. *Ship Stability*. 2018.
- [44] HARDER. *Harmonization of rules and design rationale. FP5 Project funded by the European Community, Contract No. G3RD-CT-1999- 00028, 1999–2003*. May 2003.

- [45] IMO. *Chapter II-1 - Construction - Structure, subdivision and stability, machinery and electrical installations, Part B - Subdivision and stability*. 2020.
- [46] Hakan Akyildiz. *Probabilistic Damage Stability: Knowledge and Understanding*. Tech. rep. Istanbul Technical University, 2018.
- [47] Maciej Pawłowski. *Comparison of s-factors according to SOLAS and SEM for Ro-Pax vessels*. Tech. rep. Gdansk: School of Ocean Engineering and Ship Technology, 2010.
- [48] *Introduction to Hill Climbing | Artificial Intelligence*. Oct. 2021. URL: <https://www.geeksforgeeks.org/introduction-hill-climbing-artificial-intelligence/#:~:text=Hill%20Climbing%20is%20a%20heuristic,good%20solution%20to%20the%20problem..>
- [49] Jeffrey Perkel. *The quest to design better experiments*. Mar. 2018.
- [50] Abdullah Konak, David W. Coit, and Alice E. Smith. "Multi-objective optimization using genetic algorithms: A tutorial". In: *Reliability Engineering and System Safety* 91.9 (Sept. 2006), pp. 992–1007. ISSN: 09518320. DOI: 10.1016/j.res.2005.11.018.
- [51] Qin A kai, Vicky Ling Huang, and Ponnuthurai N Suganthan. "Differential evolution algorithm with strategy adaptation for global numerical optimization". In: *IEEE transactions on Evolutionary Computation*. Vol. 13. IEEE, 2008, pp. 398–417.
- [52] Rammohan Mallipeddi and Ponnuthurai N. Suganthan. "Ensemble of constraint handling techniques". In: *IEEE Transactions on Evolutionary Computation* 14.4 (Aug. 2010), pp. 561–579. ISSN: 1089778X. DOI: 10.1109/TEVC.2009.2033582.
- [53] Singiresu S. Rao. *Engineering Optimization - Theory and Practice*. 4th ed. John Wiley & Sons, 2009.
- [54] Joel Emer et al. "Single threaded vs. Multithreaded: Where should we focus?" In: *IEEE Computer Society* (2007).
- [55] Taya Hoskin. "Data types". Rochester.
- [56] Steve Barg, Forest Flager, and Martin Fischer. "Decomposition strategies for building envelope design optimization problems". In: Alexandria, Virginia, USA: Symposium on Simulation for Architecture & Urban Design, Apr. 2015. URL: <https://www.researchgate.net/publication/282923621>.
- [57] S N Sivanandam and S N Deepa. *Introduction to Genetic Algorithms*. Berlin: Springer, 2008.
- [58] David B Fogel. "An Introduction to Simulated Evolutionary Optimization". In: *IEEE Transactions on Neural Networks* 5.1 (Jan. 1994).
- [59] Anand Deshpande and Manish Kumar. *Artificial intelligence for big data: complete guide to automating big data solutions using artificial intelligence techniques*. Packt, May 2018.
- [60] H Christopher Frey and Sumeet R Patil. *Identification and Review of Sensitivity Analysis Methods*. Tech. rep. 2002.
- [61] A Saltelli and K Chan. "Sensitivity Analysis. (Wiley Series in Probability and Statistics)". In: *Wiley* (Mar. 2009).
- [62] Lisa Rivalin et al. "A comparison of methods for uncertainty and sensitivity analysis applied to the energy performance of new commercial buildings". In: *Energy and Buildings* 166 (May 2018), pp. 489–504. ISSN: 03787788. DOI: 10.1016/j.enbuild.2018.02.021.
- [63] Tian Wei. *A review of sensitivity analysis methods in building energy analysis*. 2013. DOI: 10.1016/j.rser.2012.12.014.
- [64] An Van Schepdael, Aurélie Carlier, and Liesbet Geris. *Sensitivity analysis by design of experiments*. Tech. rep.
- [65] Bertrand Iooss and Andrea Saltelli. "Introduction to Sensitivity Analysis". In: *Handbook of Uncertainty Quantification*. Springer International Publishing, 2015, pp. 1–20. DOI: 10.1007/978-3-319-11259-6_{_}31-1.

- [66] M. D. McKay, R. J. Beckman, and W. J. Conover. "A Comparison of Three Methods for Selecting Values of Input Variables in the Analysis of Output from a Computer Code". In: *Technometrics* 21.2 (May 1979), p. 239. ISSN: 00401706. DOI: 10.2307/1268522.
- [67] Henrik Wann Jensen, Co-Chair Matthias Zwicker, and Co-Chair R Samuel Buss Per H Christensen David J Kriegman Falko Kuester. *Efficient Monte Carlo Methods For Light Transport In Scattering Media*. Tech. rep. 2008.
- [68] R Simuta-Champo and G S Herrera-Zamarrón. *Convergence analysis for Latin-hypercube lattice-sample selection strategies for 3D correlated random hydraulic-conductivity fields*. Tech. rep. 3. 2010, p. 2010.
- [69] R.A. Fisher. *The Design of Experiments*. Edingburgh, London: Oliver & Boyd, 1935.
- [70] Benjamin Durakovic. "Design of experiments application, concepts, examples: State of the art". In: *Periodicals of Engineering and Natural Sciences* 5.3 (Dec. 2017), pp. 421–439. ISSN: 23034521. DOI: 10.21533/pen.v5i3.145.
- [71] Laura Pennington and Cena Christianly. *Properties of algorithms*. Mar. 2018. URL: <https://study.com/academy/lesson/properties-of-algorithms.html>.
- [72] Samineh Bagheri et al. "Self-adjusting parameter control for surrogate-assisted constrained optimization under limited budgets". In: *Applied Soft Computing Journal* 61 (Dec. 2017), pp. 377–393. ISSN: 15684946. DOI: 10.1016/j.asoc.2017.07.060.
- [73] Roy de Winter, Bas van Stein, and Thomas Bäck. "SAMO-COBRA: A Fast Surrogate Assisted Constrained Multi-objective Optimization Algorithm". In: *Lecture Notes in Computer Science (including subseries Lecture Notes in Artificial Intelligence and Lecture Notes in Bioinformatics)*. Vol. 12654 LNCS. Springer Science and Business Media Deutschland GmbH, 2021, pp. 270–282. ISBN: 9783030720612. DOI: 10.1007/978-3-030-72062-9_{_}22.
- [74] Rommel G Regis. "Constrained optimization by radial basis function interpolation for high-dimensional expensive black-box problems with infeasible initial points". In: *Engineering Optimization*. 2nd ed. Vol. 46. Taylor & Francis, 2014, pp. 218–243.
- [75] Martin D Buhmann. *Radial Basis Function: Theory and Implementations*. Vol. 12. Cambridge university press, 2003.
- [76] I.M. Sobol. *Sensitivity estimates for Nonlinear Mathematical models*. Tech. rep. Moscow: M.V. Keldysh Institute of applied mathematics, Russian Academy of Sciences, 1990.
- [77] Kai Cheng et al. *Surrogate-assisted global sensitivity analysis: an overview*. Mar. 2020. DOI: 10.1007/s00158-019-02413-5.
- [78] Anh Tuan Nguyen and Sigrid Reiter. "A performance comparison of sensitivity analysis methods for building energy models". In: *Building Simulation* 8.6 (Dec. 2015), pp. 651–664. ISSN: 19968744. DOI: 10.1007/s12273-015-0245-4.
- [79] Max D Morris. "Factorial Sampling Plans for Preliminary Computational Experiments". In: *Technometrics* 33.2 (May 1991), pp. 161–174.
- [80] Anna Franczyk. "Using the Morris sensitivity analysis method to assess the importance of input variables on time-reversal imaging of seismic sources". In: *Acta Geophysica* 67.6 (Dec. 2019), pp. 1525–1533. ISSN: 18957455. DOI: 10.1007/s11600-019-00356-5.
- [81] Song Yang et al. "Comparison of Sensitivity Analysis Methods in Building Energy Assessment". In: *Procedia Engineering*. Vol. 146. Elsevier Ltd, 2016, pp. 174–181. DOI: 10.1016/j.proeng.2016.06.369.
- [82] M Balesdent and J Morio. *Morris Method Methods for high-dimensional and computationally intensive models*. Tech. rep.
- [83] Fanny Peyre. "Comfort Index in BES: Sensitivity study". PhD thesis. Paris Saclay: Ecole Normale Supérieure, 2017. URL: <https://lhypercube.arep.fr/en/methodes-numeriques/analyse-de-sensibilite/>.
- [84] Aphrodite Kanellopoulou et al. "Parametric ship design and optimisation of cargo vessels for efficiency and safe operation in adverse weather conditions". In: *Journal of Marine Science and Technology (Japan)* 24.4 (Dec. 2019), pp. 1223–1240. ISSN: 09484280. DOI: 10.1007/s00773-018-00620-1.

- [85] Herbert J Koelman. "A New Method for Probabilistic Damage Stability". In: *Schifftechnik*. Vol. 53. 2006, pp. 183–193.
- [86] Mike Cardinale et al. *Permeability of tanks intended for liquids in cruise vessels*. Tech. rep. Helsinki: 17th International Ship Stability Workshop, June 2019.
- [87] *Objective and constraints*. 2017. URL: <https://abaqus-docs.mit.edu/2017/English/SIMACAEANLRefMap/simaanl-c-optobjectives.htm>.
- [88] Stéphane Alarie et al. "Two decades of blackbox optimization applications". In: *EURO Journal on Computational Optimization* 9 (Jan. 2021). ISSN: 21924414. DOI: 10.1016/j.ejco.2021.100011.
- [89] "Chapter_II_1_Construction_Structure_subdivision_and_stability_machinery_and_electrical_installations". In: ().
- [90] Jakob Bossek, Carola Doerr, and Pascal Kerschke. "Initial design strategies and their effects on sequential model-based optimization: An exploratory case study based on BBOB". In: *GECCO 2020 - Proceedings of the 2020 Genetic and Evolutionary Computation Conference*. Association for Computing Machinery, June 2020, pp. 778–786. ISBN: 9781450371285. DOI: 10.1145/3377930.3390155.
- [91] J H Halton. *On the efficiency of certain quasi-random sequences of points in evaluating multi-dimensional integrals*. Tech. rep. Numerische Mathematik 2, 1960.
- [92] Jon Herman and Will Usher. "SALib: An open-source Python library for Sensitivity Analysis". In: *The Journal of Open Source Software* 97 (2017).
- [93] Francesca Campolongo, Jessica Cariboni, and Andrea Saltelli. "An effective screening design for sensitivity analysis of large models". In: *Environmental Modelling and Software* 22.10 (Oct. 2007), pp. 1509–1518. ISSN: 13648152. DOI: 10.1016/j.envsoft.2006.10.004.
- [94] F Campolongo et al. *Enhancing the Morris method*. Tech. rep. Ispra: European Commission, Joint Research Centre, 2005. URL: <http://library.lanl.gov/>.
- [95] J.D. Herman et al. "Method of Morris effectively reduces the computational demands of global sensitivity analysis for distributed watershed models". In: *Hydrology and Earth System Sciences* 17 (2013), pp. 2893–2903.
- [96] Andrea Saltelli et al. *Sensitivity Analysis in Practice : A Guide to Assessing Scientific Models*. John Wiley & Sons, 2004.
- [97] Francesca Campolongo and Andrea Saltelli. *Sensitivity analysis of an environmental model: an application of different analysis methods*. Tech. rep. 1997, pp. 49–69.
- [98] F Campolongo, S Tarantola, and A Saltelli. *Tackling quantitatively large dimensionality problems*. Tech. rep. 1999, pp. 75–85.
- [99] Ibrahim Demir, Fatma Corut Ergin, and Berna Kiraz. "A New Model for the Multi-Objective Multiple Allocation Hub Network Design and Routing Problem". In: *IEEE Access* 7 (2019), pp. 90678–90689. ISSN: 21693536. DOI: 10.1109/ACCESS.2019.2927418.
- [100] MARPOL - International Convention for the Prevention of Pollution from Ships. "Annex I - Regulation 12A - Oil fuel tank protection". In: IMO, Aug. 2007.
- [101] Osvaldo M. Querin et al. "Discrete Method of Structural Optimization * *Additional author for this chapter is Prof. Dr.-Ing. Dr.-Habil. George I. N. Rozvany." In: *Topology Design Methods for Structural Optimization*. Elsevier, 2017, pp. 27–46. DOI: 10.1016/b978-0-08-100916-1.00003-9.
- [102] SOLAS - International Convention for the Safety of Life at Sea. "Chapter II-1-Construction-Structure, subdivision and stability, machinery and electrical installations - Part B-1 - Stability - Regulation 7-3 - Permeability". In: IMO, 1974.
- [103] Ekasit Kijispongse et al. "Efficient large Pearson correlation matrix computing using hybrid MPI/CUDA". In: *Proceedings of the 2011 8th International Joint Conference on Computer Science and Software Engineering, JCSSE 2011*. 2011, pp. 237–241. ISBN: 9781457706875. DOI: 10.1109/JCSSE.2011.5930127.

- [104] K Pearson. "Mathematical contributions to the theory of evolution.—III. Regression, heredity and panmixia". In: *Philos. Trans. R. Soc. London* 187 (1896), pp. 253–318.
- [105] P D H Bronkhorst. *Enhancing offshore service vessel concept design by involving seakeeping*. *Developing a framework to efficiently design high-performance offshore service vessel concepts*. Tech. rep. Delft: TU Delft, July 2021. URL: [http://repository.tudelft.nl/..](http://repository.tudelft.nl/)
- [106] Mark L. Mitchell and Janina M. Jolley. *Research design explained*. Wadsworth, 2010, p. 645. ISBN: 9780495602217.
- [107] F.H. Sellars and J.P. Martin. "Selection and evaluation of ship roll stabilization systems". In: *Marine Technology and SNAME News* 29 (Apr. 1992), pp. 84–101.
- [108] Thomas Weise et al. *Why is optimization difficult?* 2009. DOI: 10.1007/978-3-642-00267-0{_}1.



Multi-Objective Optimisation Results

A.1. Constraint Function Results

To further support the findings in chapter 5.2, the plots for all four constraint functions are presented and analysed in this appendix. First the constraints for the two bulkhead design are presented in figure A.1 to A.4. As explained in chapter 4.2, the constraint function satisfies the constraint if the result is negative. The more a constraint function is converging towards the zero line, the more critical this constraint is. This can be helpful in establishing insight in the behaviour of the algorithm.

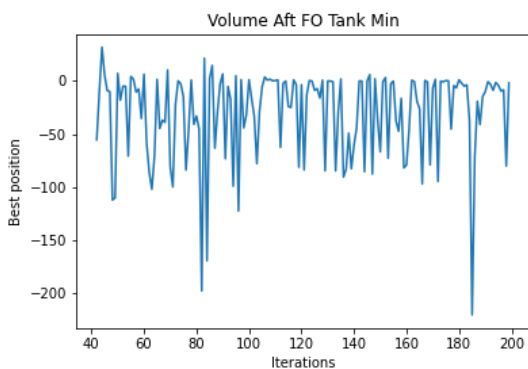


Figure A.1: Constraint plot volume Aft FO tank

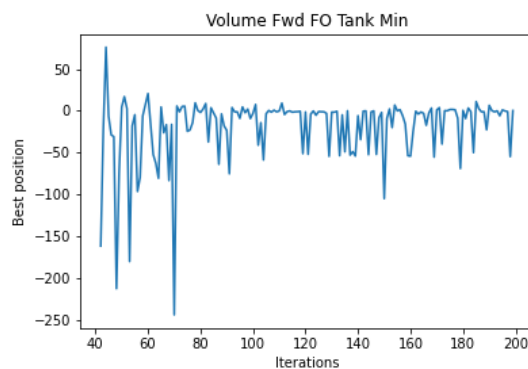


Figure A.2: Constraint plot volume Fwd FO tank

The volume of both fuel oil tanks can be seen above. The FO tanks show a similar behaviour regarding their constraint results as they form a single compartment to shield of the cargo hold. The parameters influencing the FO tanks are not used to describe other compartments, therefore their volume is not influenced by any other compartment that needs to satisfy a certain requirement. Although the aft FO tank shows a little more fluctuation and the forward FO tank some higher peaks, the plots can be considered equal in behaviour.

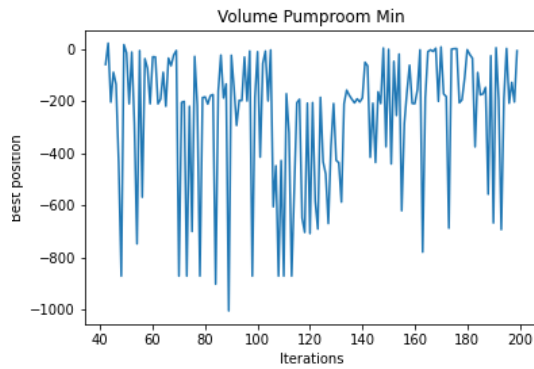


Figure A.3: Constraint plot volume pump room

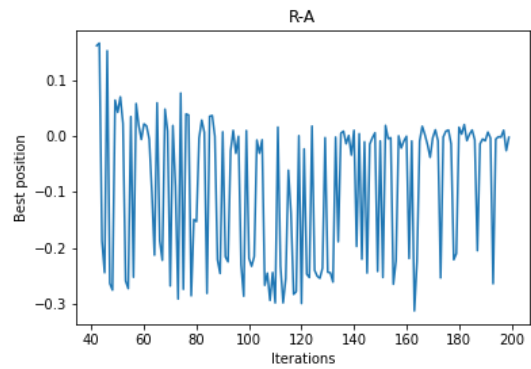


Figure A.4: Constraint plot R-A

The volume of the pump room is not a critical constraint as the graph does not converge around zero. For the higher attained indices, the pump room is used to shield of the cargo hold. Because the pump room volume has more influence on the attained index than the FO tanks, the pump room is used more to do this shielding practice. Between iteration 100 and 140, the constraint function seems to focus on a certain pump room volume. This can be explained by looking at figure 5.9. The $600m^3$ pump room designs were located at the higher attained index designs, while the minimum pump room volume of $300m^3$ were used for the lower ones. The focus on the higher pump room volume is likely the algorithm focusing more on achieving higher attained indices. Figure A.4 supports this claim.

Figures A.5 to A.8 show the constraint function plots for the five bulkhead design.

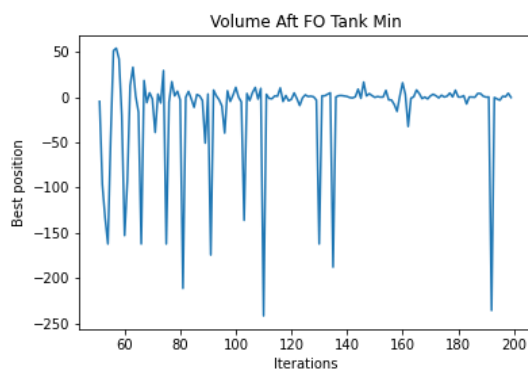


Figure A.5: Constraint plot volume Aft FO tank

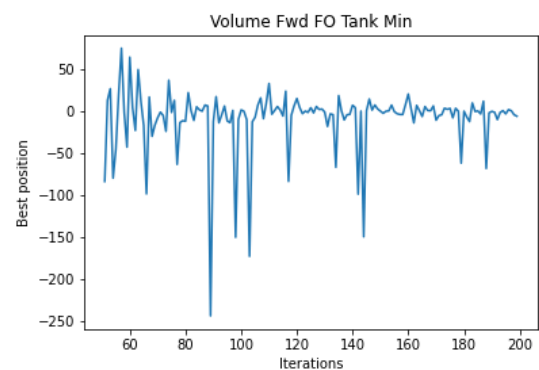


Figure A.6: Constraint plot volume Fwd FO tank

The volume of the FO tanks is now more critical than for the two bulkhead design. This has no clear reason, but it can be seen that even though the constraint shows less fluctuation, it still shows the same properties as the two bulkhead design as it converges around the zero line.

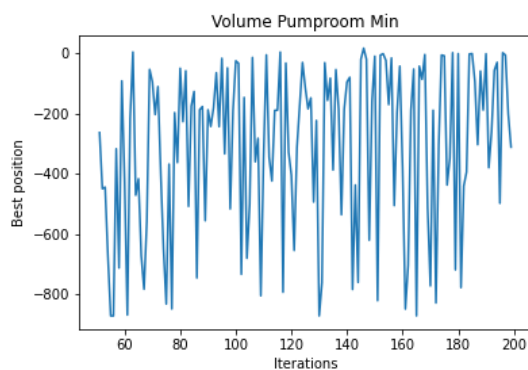


Figure A.7: Constraint plot volume pump room

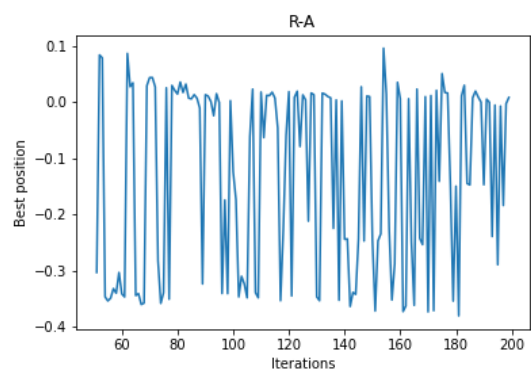


Figure A.8: Constraint plot R-A

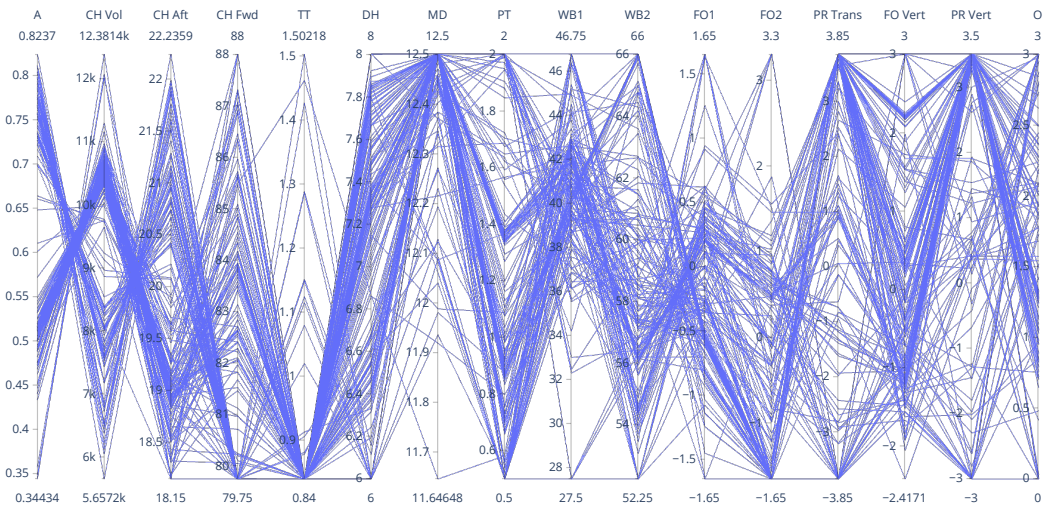
The volume of the pump room shows a similar behaviour as the two bulkhead design. This is expected as the boundaries of the pump room are used to create a as large as possible volume to protect the cargo hold for the higher attained indices. The minimum attained index constraint shows a larger difference from the attained index to the required index. This shows that five bulkheads does in fact increase the attained index as was expected.

A.2. Parallel Coordinate Plots

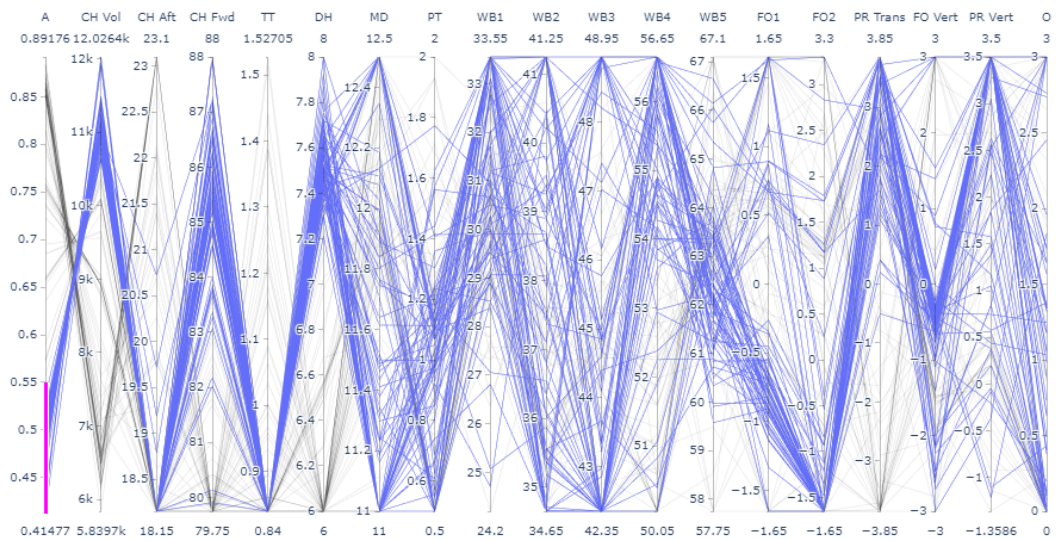
This appendix shows the parallel coordinate plots generated for both the two and five bulkhead designs. For every design, the full parallel coordinate plot is shown, as well as a plot where only the lowest attained index region is highlighted and one for the lowest. Figure A.9a shows the total parallel coordinate plot, where all trend lines can be observed. For clarification, the extremities are shown for the attained index regions in figure A.9b and A.9c. This same procedure is used for the five bulkhead design in figure A.10a, A.10b and A.10c. The iterations of the initial design points are not taken into account in this graph as the pseudo-randomness of the Halton sequence is not able to show any trends between the parameters and the objectives.

The plots show the trends between the objective values and the values of the parameters. The first plot of the two designs gives the full plot where not much can be concluded from except that the height of the tanktop is always at its minimum and the height of the main deck and pumproom are always at is their maximum. The next two plots show the trends for both extremities of the Pareto front, i.e. the maximum and minimum region of the attained index and cargo hold volume. Here, the trends observed from all other methods can be confirmed. The lower the attained index, the more the longitudinal cargo hold bulkheads move outward. Also, the higher the attained index becomes, the more variation in the position of the water ballast tanks is observed.

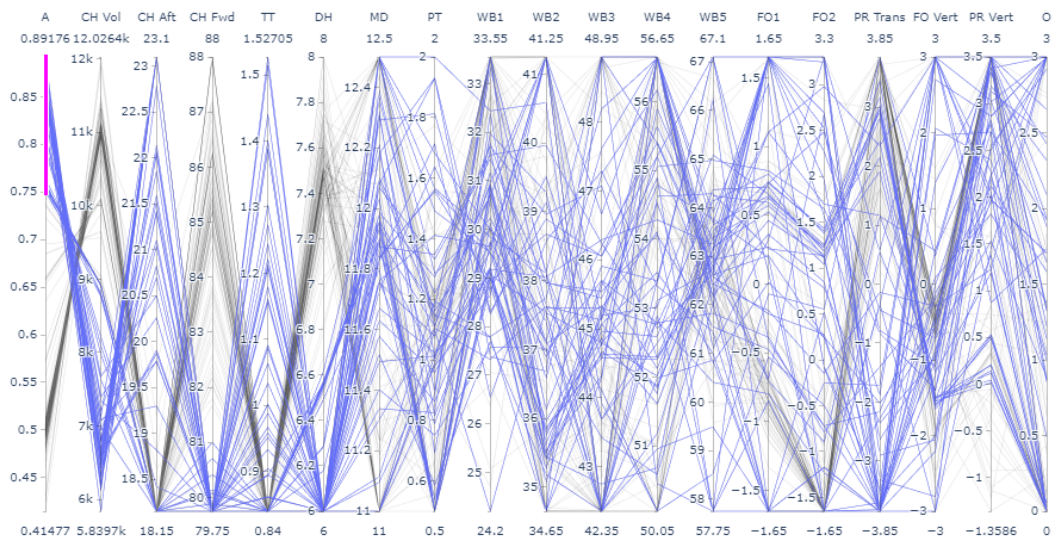
These parallel coordinate plots show the same behaviour as the Pareto front plots from chapter 5.2 with some explainable differences. For instance the tanktop is not always at its minimum height. The reason this is not observed in the Pareto front is because the height of the tanktop greatly influences the cargo hold volume, even more than it influences the attained index. This means that all designs that do not have the lowest possible tanktop height are dominated by designs that do have this feature.



(a) Pareto front for 200 iterations and two WB BH.

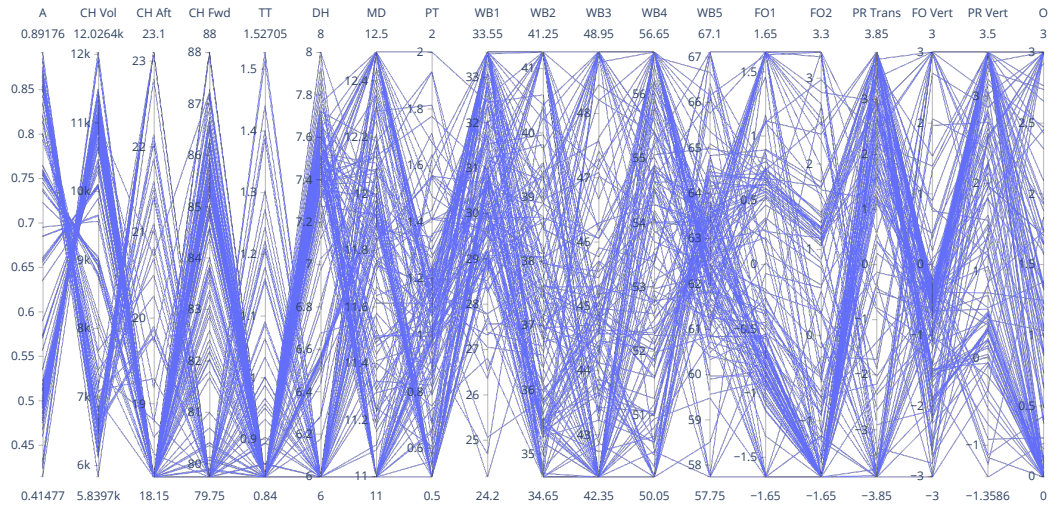


(b) Parallel coordinate plot for 200 iterations and two WB BH showing the highest attained index region.

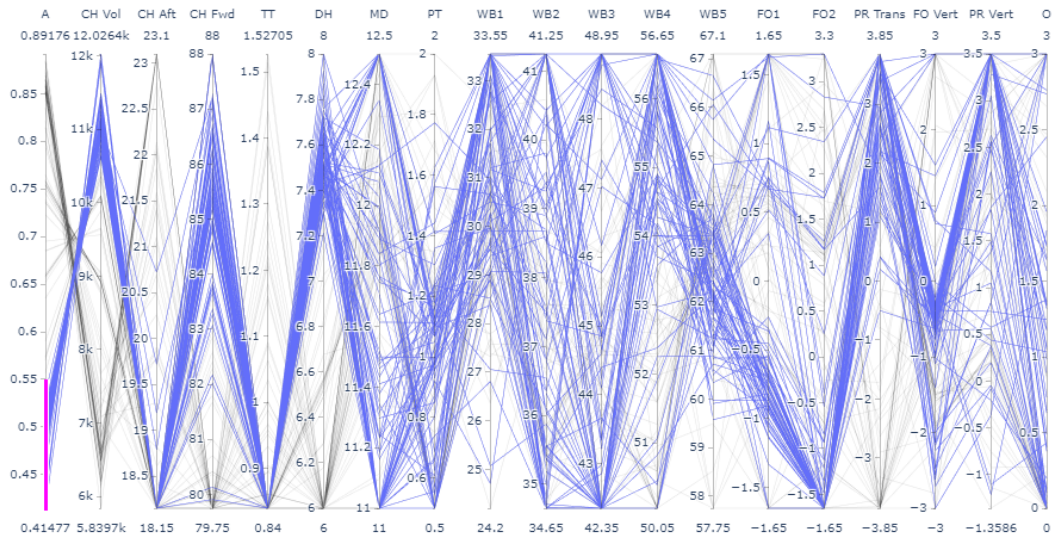


(c) Parallel coordinate plot for 200 iterations and two WB BH showing the lowest attained index region.

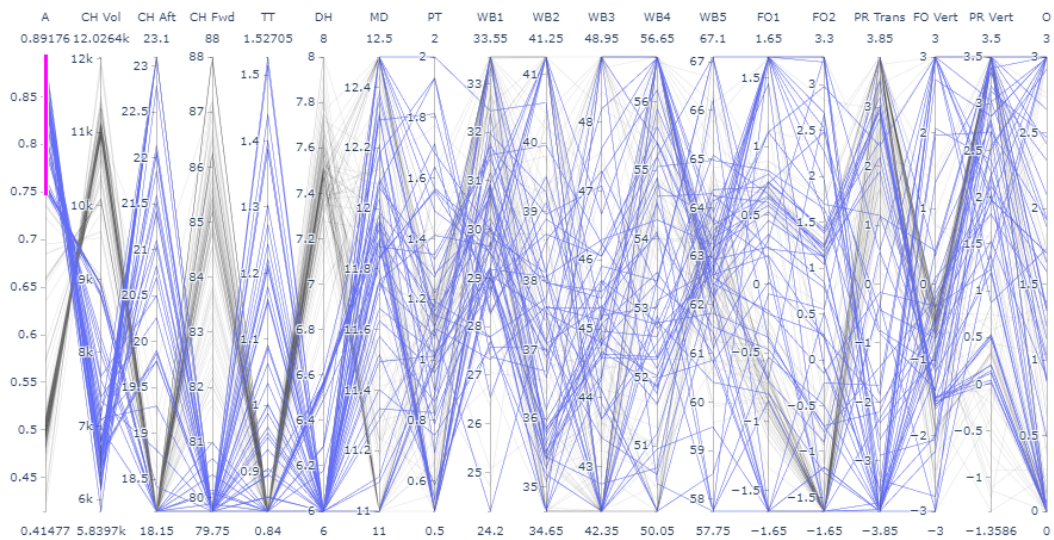
Figure A.9: These figures show the parallel coordinate plots for the two WB BH design.



(a) Pareto front for 200 iterations and five WB BH



(b) Parallel coordinate plot for 200 iterations and five WB BH showing the highest attained index region



(c) Parallel coordinate plot for 200 iterations and five WB BH showing the lowest attained index region

Figure A.10: These figures show the parallel coordinate plots for the five WB BH design.

B

Single-Objective Optimisation Results

In figure B.1 below, the converged layout for a minimum cargo hold volume of $8500m^3$ is shown that is being compared to two experiments. Namely the addition of the cargo hold cutout and a change in permeability for the pump room and FO tanks.

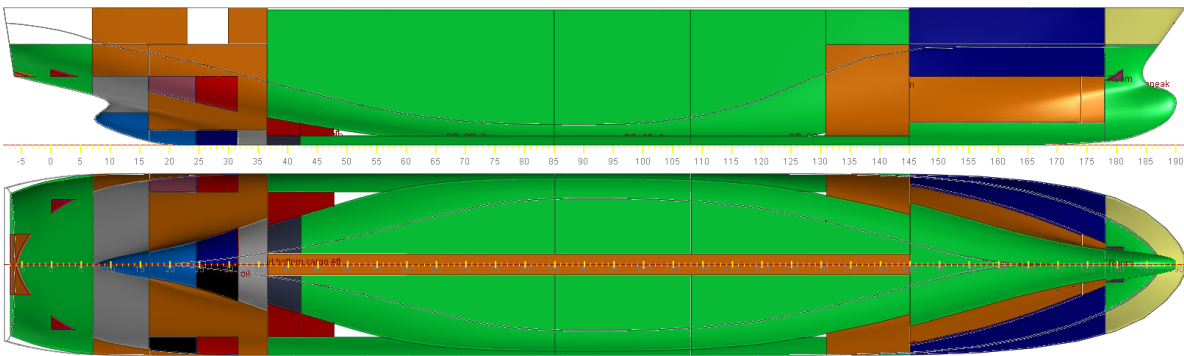


Figure B.1: Converged layout for a minimum cargo hold volume of $8500m^3$ and maximum attained index.

B.0.1. Cargo Hold Cutout

This section aims to provide evidence for the claims made in section 5.3.4. First the total layout of the converged model is shown in figure B.2 is shown.

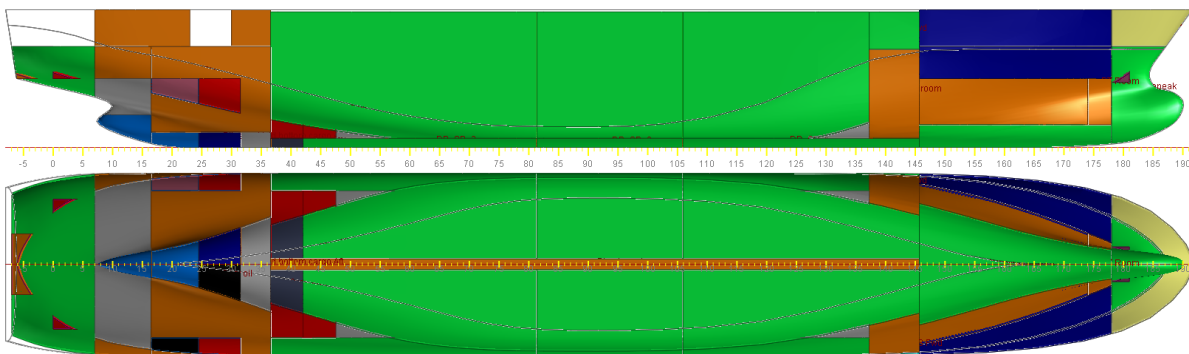


Figure B.2: Converged layout for a minimum cargo hold volume of $8500m^3$, a maximum attained index and fitted with the cargo hold cutouts

Although the difference is small between the two bulkhead distances, the location of the pump room bulkhead shifts towards the forward section when the cargo hold cutout is used.

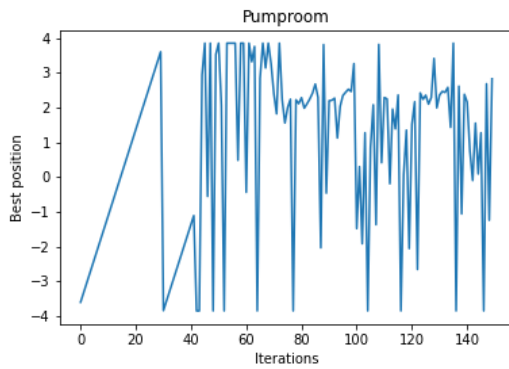


Figure B.3: Pump room bulkhead location without cargo hold cutout

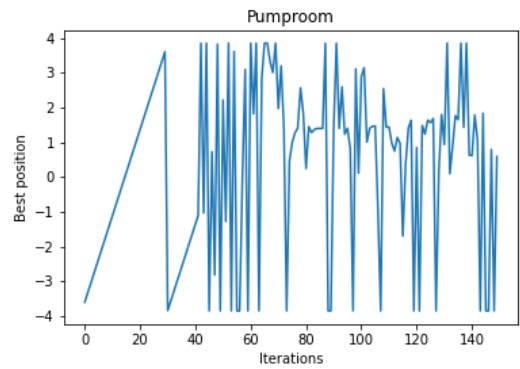


Figure B.4: Pump room bulkhead location with cargo hold cutout

B.0.2. Change in Permeability

This section aims to provide evidence for the claims made in section 5.3.5. First the layout of the converged model is shown in figure B.5

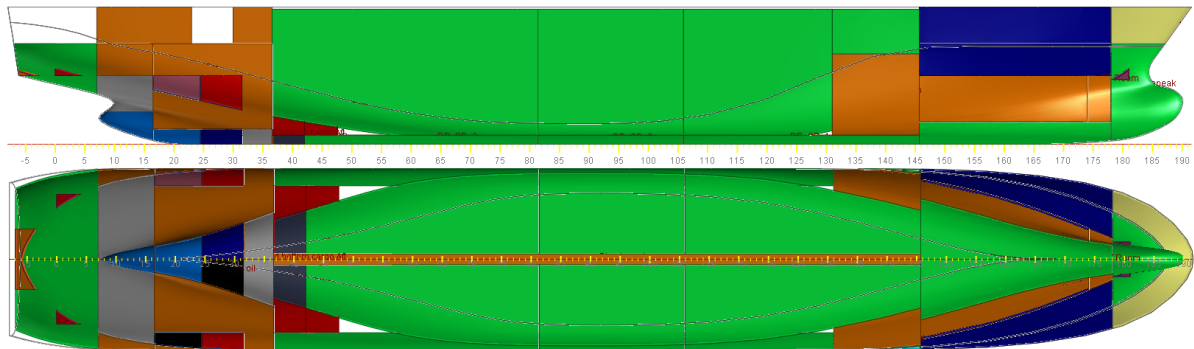


Figure B.5: Converged layout for a minimum cargo hold volume of $8500m^3$, a maximum attained index and a change in permeability for the pump room and FO tanks.

Figures B.6 and B.7 show the volumes of the pump room when between the single optimisation with the standard permeability's and the change in permeability described in table 5.8. What can be seen is that after 100 iterations, the pump room volume for the design with a higher pump room permeability trends upwards instead of downwards. This shows that a slight difference in trend is present that causes the difference in design between the two designs.

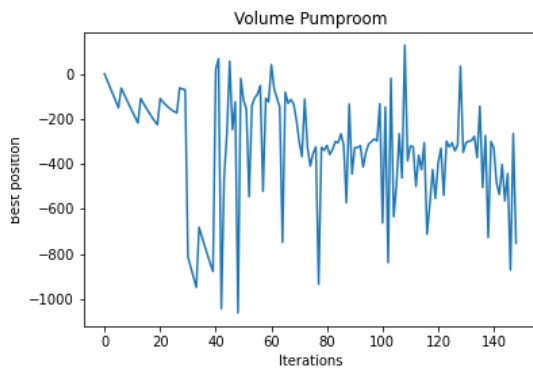


Figure B.6: Pump room volume without change in permeability

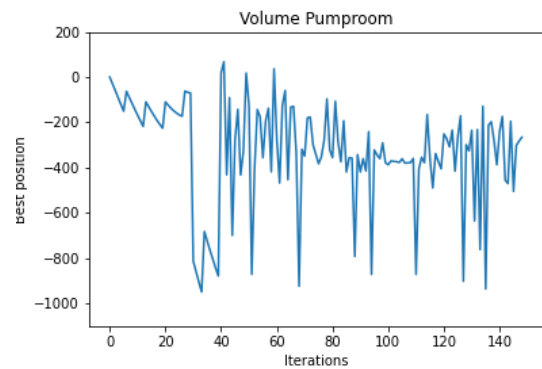
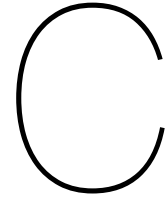


Figure B.7: Pump room volume with change in permeability



Sensitivity Analysis Results

C.1. Morris Method Results

In this appendix, the Morris method results are listed and further elaborated upon. The tables contain the following output:

- μ = The elementary effect;
- μ^* = The absolute of the mean elementary effect;
- σ = The standard deviation of the elementary effect;
- μ_{conf}^* = The bootstrapped confidence interval.

The bootstrap confidence interval of 95% is used which should be smaller than 10% of the total elementary effect of the most influential parameter.

$$10 > \frac{100 \times \mu_{conf}^*}{\mu} \quad (4.15 \text{ revisited})$$

x3 has the highest elementary effect for all three experiments. The total percentage of the confidence interval w.r.t. the elementary effect for 20 trajectories is:

$$\frac{100 \times 0.024995}{0.291914} = 8.56\% \quad (C.1)$$

In tables C.1, C.2 and C.2, the results of the Morris method experiments are presented, used to determine the number of trajectories for this case study.

Table C.1: Results Morris method for N=20 trajectories

Table C.2: Results Morris method for N=60 trajectories

	μ	μ^*	σ	μ_{conf}^*	μ	μ^*	σ	μ_{conf}^*
CH Aft	0.054431	0.054894	0.035388	0.013631	0.036001	0.037703	0.036154	0.006893
CH Fwd	-0.129298	0.129298	0.053849	0.023975	-0.146548	0.146548	0.052278	0.010444
TT	-0.016759	0.026703	0.029106	0.008634	-0.019554	0.030803	0.033936	0.004357
DH	-0.291914	0.291914	0.057119	0.024995	-0.276219	0.276219	0.066244	0.013250
MD	0.011518	0.011686	0.017089	0.007871	0.008492	0.008681	0.011908	0.002298
PT	0.000079	0.003314	0.003992	0.000754	0.000554	0.004193	0.006753	0.001015
WB1	0.014753	0.022498	0.030988	0.010849	0.006950	0.018447	0.025733	0.003735
WB2	-0.000954	0.014950	0.021799	0.006395	-0.011260	0.020814	0.026061	0.003502
WB3	0.000002	0.000002	0.000007	0.000003	0.004297	0.009487	0.013136	0.002070
WB4	0.000142	0.001250	0.001791	0.000532	0.000566	0.001126	0.001863	0.000322
WB5	-0.009105	0.010885	0.012475	0.004633	-0.005865	0.012112	0.015164	0.001945
FO1 T.	-0.030335	0.032602	0.028190	0.011389	-0.045733	0.047307	0.042496	0.008440
FO2 T.	0.011932	0.015578	0.016701	0.005487	0.006098	0.016771	0.019416	0.002261
PR	0.092658	0.092658	0.045288	0.020251	0.071889	0.072942	0.050878	0.008392
FO V.	0.020954	0.023114	0.030357	0.011045	0.027621	0.028299	0.029103	0.005844
PR V.	0.003307	0.003866	0.007247	0.003033	0.002568	0.002714	0.008356	0.001590

Table C.3: Results Morris method for N=100 trajectories

	μ	μ^*	σ	μ_{conf}^*
CH Aft	0.036001	0.037703	0.036154	0.006893
CH Fwd	-0.146548	0.146548	0.052278	0.010444
TT	-0.019554	0.030803	0.033936	0.004357
DH	-0.276219	0.276219	0.066244	0.013250
MD	0.008492	0.008681	0.011908	0.002298
PT	0.000554	0.004193	0.006753	0.001015
WB1	0.006950	0.018447	0.025733	0.003735
WB2	-0.011260	0.020814	0.026061	0.003502
WB3	0.004297	0.009487	0.013136	0.002070
WB4	0.000566	0.001126	0.001863	0.000322
WB5	-0.005865	0.012112	0.015164	0.001945
FO1 Trans.	-0.045733	0.047307	0.042496	0.008440
FO2 Trans.	0.006098	0.016771	0.019416	0.002261
PR	0.071889	0.072942	0.050878	0.008392
FO Vert.	0.027621	0.028299	0.029103	0.005844
PR Vert.	0.002568	0.002714	0.008356	0.001590

x3 has the highest elementary effect. The total percentage of the confidence interval w.r.t. the elementary effect is:

$$\frac{100 \times 0.013250}{0.276219} = 4.80\% \tag{C.2}$$

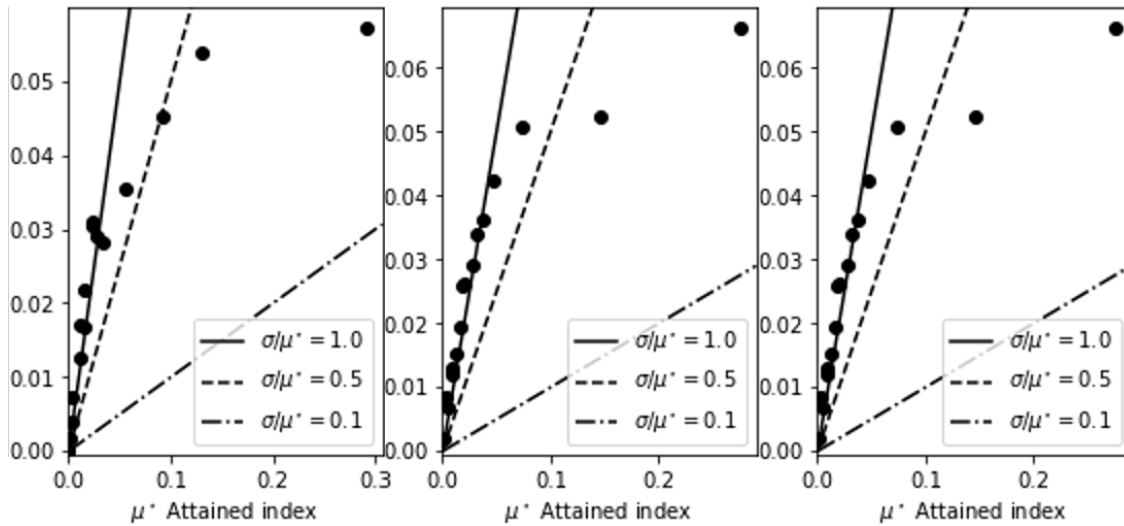


Figure C.1: Classification of the Morris method results

Table C.4 shows the Morris indices for the final Morris simulation used in chapter 5.4.1.

Table C.4: Results Morris method for N=20 trajectories for five water ballast bulkheads

	μ	μ^*	σ	μ_{conf}^*
CH Aft	0.031212	0.036696	0.039450	0.013233
CH Fwd	-0.184930	0.184930	0.059779	0.023453
TT	-0.022348	0.032944	0.036965	0.011857
DH	-0.293161	0.293161	0.060564	0.023827
MD	0.006532	0.006931	0.012839	0.005909
PT	-0.000562	0.002255	0.003411	0.001000
WB1	0.003952	0.008929	0.010830	0.003260
WB2	-0.003429	0.007992	0.010518	0.003144
WB3	-0.000212	0.010460	0.014442	0.004159
WB4	-0.002211	0.011755	0.016215	0.004662
WB5	0.017990	0.020893	0.022956	0.008470
FO1 Trans.	-0.000286	0.000423	0.000877	0.000320
FO2 Trans.	-0.007033	0.008834	0.010184	0.003792
PR	-0.042437	0.044369	0.041059	0.017735
FO Vert.	0.003759	0.013277	0.015147	0.003182
PR Vert.	0.086869	0.086869	0.050267	0.023364
O	0.002531	0.002968	0.011281	0.005177

C.2. Correlation Matrix

In this section, the correlation matrices for three situations are given, namely the correlation matrix for:

- An initial sampling size of 200 iterations LHS;
- The optimiser results of the SAMO-COBRA optimiser.

The correlation matrix of the sampling method only, was computed by the use of Latin Hypercube sampling. This method is described in chapter 3.5.2 and is an efficient pseudo random sampling method. The reason Halton sampling was not used in this case is that the method changes the last parameter only once over its entire range with a relatively small step size. Although it encompasses the entire parameter space, this makes it unfit to be used for the correlation matrix, as the correlation between the attained index and a parameter becomes more clear the more its changed. What can be seen is that the correlation between the parameters is uniformly spread over the matrix and close to zero. This is due to the parameters not influencing each other, as their value is determined only by the LHS method. They do influence the attained index and cargo hold volume without any bias like was found in the optimisation algorithm.

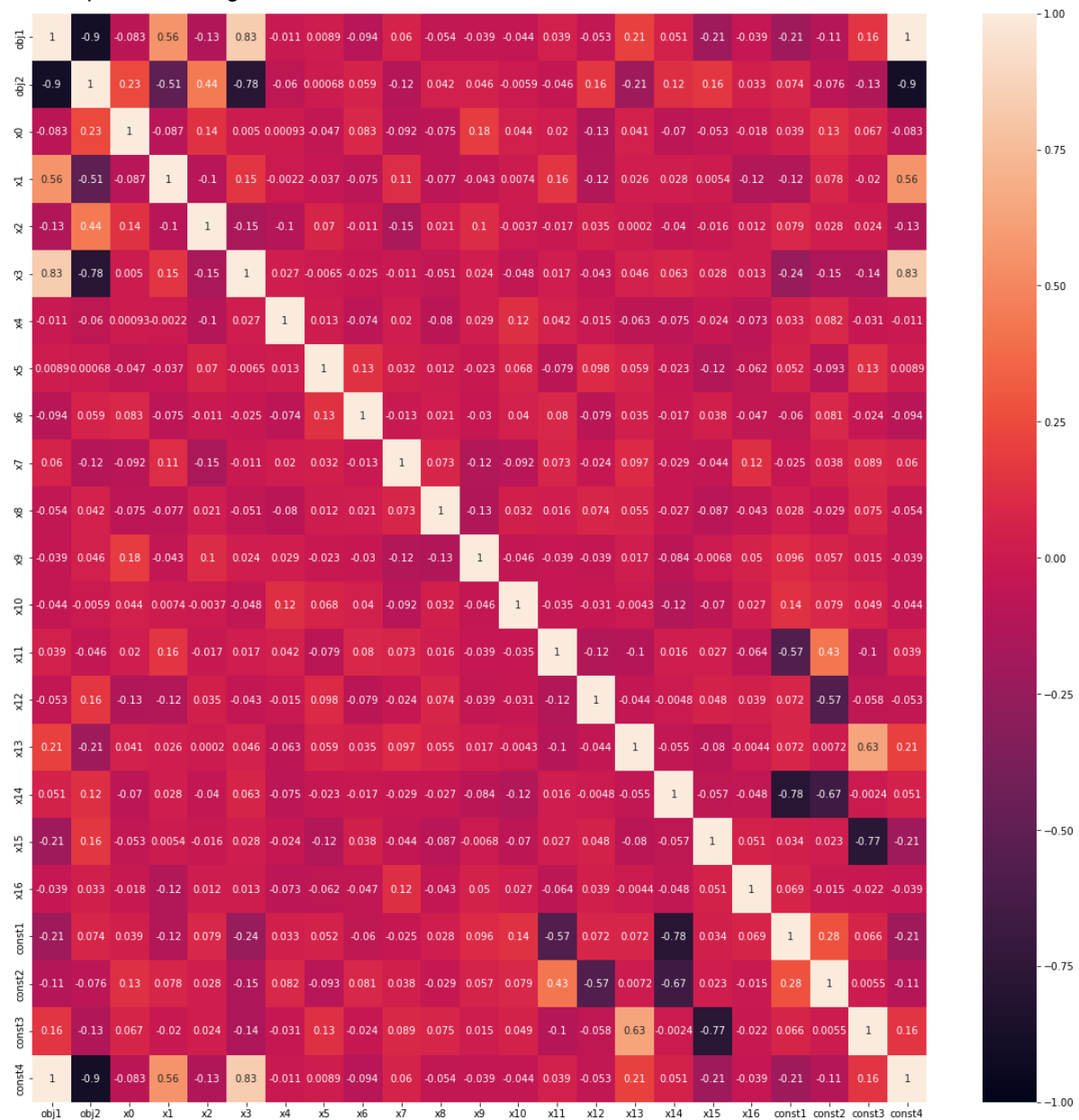


Figure C.2: Correlation matrix for only the initial design points for all parameters

The correlation matrix for the optimisation stage shows the correlation based on the optimiser after the 3*d initial sampling points. The downside of this, is that the optimiser already has a certain bias for some parameters being in their right locations. However, if no initial sampling points were used, the first iterations would be similar to a random sampling method. Leaving the correlation matrix to show the same results as figure 5.45. The combined correlation matrix from these two matrices is shown in figure 5.46 in section 5.4.2.

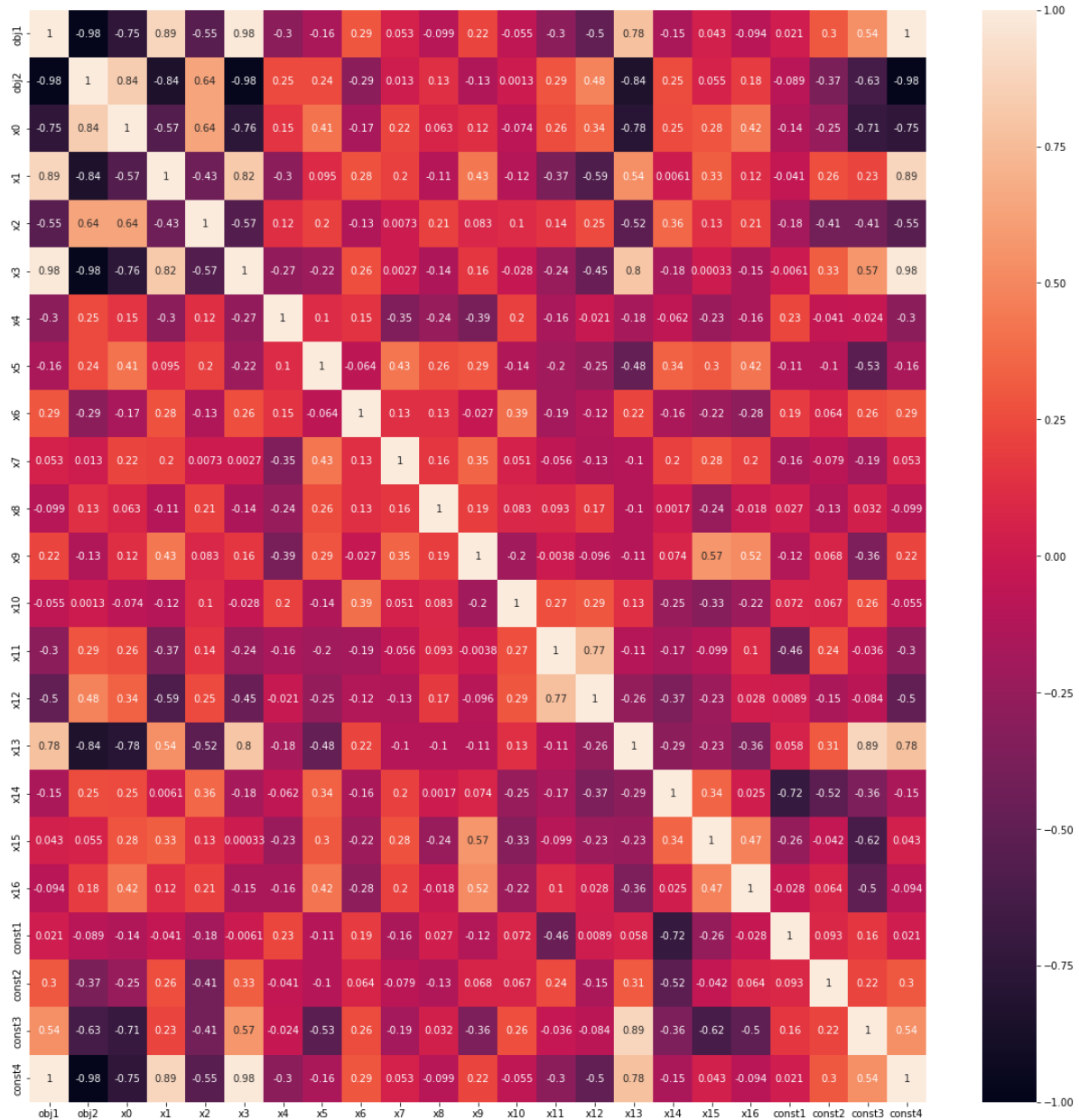
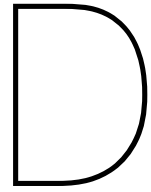


Figure C.3: Correlation matrix for 200 iterations and all parameters



Interview Design Process Implementation

INTERVIEW DESIGN PROCES IMPLEMENTATION

Subject: Design Process Implementation proposed PDS framework for C-Job

Participants: Alexander van den Ing & Bas Milatz

Date: 07-08-2022

Interview notes:

Question: How much time is required to come up with a design that satisfies the damage stability requirements? (A full optimisation with 20 Pareto efficient designs and sensitivity analysis requires approximately 3-4 days to set up and produce results).

Answer: For small, simple ships one can make it quite good (with respecting (web-)frame grid in 3 directions) within 1 day. For large, complex ships you should have a reasonable starting point in about 3-4 days, assuming the modelling is already done.

Question: How many designs do you produce on average as final options for the design?

Answer: 1

Question: How many designs do you consider on average, prior to proposing a final design?

Answer: In an iterative process, eventually two at a time. You make a variation, compare it with the results of the previous design and continue the process with the “winner”. You keep repeating until no significant increase in attained index can be found. If you present multiple designs to a client, it are mostly two, maybe three, but rarely more.

Question: To what degree do you currently use the probabilistic damage stability method as a base of design?

Answer: The method refers to the calculation. You could also replace the word for calculation. It is considered, knowing that low-freeboard-ships cannot deal very well with large compartments and low-GM ships cannot deal very well with asymmetry. When estimating initial main dimensions, you keep this in mind when determining the subdivision of a ship. We also keep in mind that if a ship performs less (in prob.dam.stab.) in one area, you have the possibility to compensate this by above-average-performance in an other area of the ship, to keep the Attained index at the desired level.

Question: To what degree do you think an optimisation algorithm can be fitted in the design process? (As a base of design or only partially)

Answer: Key is to have all constraints (continuous routes, corridor width, compartment dimensions, nr. Of compartments, MARPOL/IGF requirements wrt clear distance from the shell, etc. In the algorithm, to ensure you end with relevant, viable results. Normally this ‘thinking’ is part of the work of the naval architect. Once this is done, it has the potential to save time on the usual trial-and-error process to find the optimum (or at least ‘good enough’) result, where you know the design (set of main dimensions + subdivision) does not have unused margin, which could have been utilized for, for example, making the ship less wide. Personally, I do not expect huge differences in design, but these last percents do have the potential to distinguish your fleet from what the competition is doing. Since everything in a ship is related, you can spark a chain reaction in downsizing and an optimization algorithm can contribute to this.